

EFFECT OF JORUNNAMYCIN A ON CANCER STEM CELLS OF HUMAN LUNG CANCER
H460 CELLS



A Dissertation Submitted in Partial Fulfillment of the Requirements
for the Degree of Doctor of Philosophy in Biomedical Chemistry
Department of Biochemistry and Microbiology
FACULTY OF PHARMACEUTICAL SCIENCES
Chulalongkorn University
Academic Year 2020
Copyright of Chulalongkorn University

ผลของโจรึ้นนามัยชิน เอ ต่อเซลล์ต้นกำเนิดมะเร็งของเซลล์มะเร็งปอดมนุษย์ชนิดเอช 460



วิทยานิพนธ์นี้เป็นส่วนหนึ่งของการศึกษาตามหลักสูตรปริญญาวิทยาศาสตรดุษฎีบัณฑิต

สาขาวิชาชีวเวชเคมี ภาควิชาชีวเคมีและจุลชีววิทยา

คณะเภสัชศาสตร์ จุฬาลงกรณ์มหาวิทยาลัย

ปีการศึกษา 2563

ลิขสิทธิ์ของจุฬาลงกรณ์มหาวิทยาลัย

Thesis Title	EFFECT OF JORUNNAMYCIN A ON CANCER STEM CELLS OF HUMAN LUNG CANCER H460 CELLS
By	Miss Somruethai Sumkhemthong
Field of Study	Biomedical Chemistry
Thesis Advisor	Assistant Professor CHATCHAI CHAOTHAM, Ph.D.

Accepted by the FACULTY OF PHARMACEUTICAL SCIENCES, Chulalongkorn University in Partial Fulfillment of the Requirement for the Doctor of Philosophy

..... Dean of the FACULTY OF
PHARMACEUTICAL SCIENCES
(Assistant Professor RUNGPETCH SAKULBUMRUNGSIL,
Ph.D.)

DISSERTATION COMMITTEE

..... Chairman
(PREEDAKORN CHUNHACHA, Ph.D.)

..... Thesis Advisor
(Assistant Professor CHATCHAI CHAOTHAM, Ph.D.)

..... Examiner
(EAKACHAI PROMPETCHARA, Ph.D.)

..... Examiner
(WANATCHAPORN ARUNMANEE, Ph.D.)

..... Examiner
(KANNIKA KHANTASUP, Ph.D.)

..... External Examiner
(Assistant Professor MONRUEDEE SUKPRASANSAP, Ph.D.)

สมฤทัย สุ่มเข้มทอง : ผลของโจรันนามัยซิน เอ ต่อเซลล์ต้นกำเนิดมะเร็งของเซลล์มะเร็งปอดมนุษย์ชนิดเอช 460. (EFFECT OF JORUNNAMYCIN A ON CANCER STEM CELLS OF HUMAN LUNG CANCER H460 CELLS) อ.ที่ปรึกษาหลัก : ผศ. ภก. ดร. ฉัตรชัย เชาว์ธรรม

เซลล์ต้นกำเนิดมะเร็งที่พบในเนื้องอกมีส่วนสำคัญอย่างยิ่งต่อการรักษาที่ล้มเหลวและส่งผลต่ออัตราการเสียชีวิตของผู้ป่วยมะเร็งปอดที่สูงขึ้น เนื่องจากลักษณะคล้ายกับเซลล์ต้นกำเนิดในการแบ่งตัวแล้วได้เซลล์ที่มีคุณสมบัติเหมือนตัวเองและสามารถเกิดเป็นก้อนมะเร็งขึ้นใหม่ เซลล์ต้นกำเนิดมะเร็งนำไปสู่ปัญหาการดื้อยาและการกลับมาของโรคมะเร็ง งานวิจัยนี้แสดงให้เห็นผลการยับยั้งของโจรันนามัยซิน เอ ซึ่งเป็นสารในกลุ่มบิสเตรราไฮโดรไอโซควิโนลิโนน สกัดแยกได้จากฟองน้ำสีน้ำเงินของไทยสกุลเซสโทสปองเจีย ต่อการเกิดก้อนมะเร็งในสภาวะแขวนลอยและการแบ่งตัวให้ได้เซลล์ที่เหมือนตัวเองในเซลล์ต้นกำเนิดมะเร็งของเซลล์มะเร็งปอดมนุษย์ การลดลงของโปรตีนควบคุมการถอดรหัสพันธุกรรมชนิด Nanog, Oct-4 และ Sox2 ที่ควบคุมความเป็นเซลล์ต้นกำเนิดในเซลล์ต้นกำเนิดมะเร็งปอดเมื่อได้รับโจรันนามัยซิน เอ ที่ความเข้มข้น 0.5 ไมโครโมลาร์ เป็นผลมาจากการกระตุ้น GSK-3 β และการลดลงของ β -catenin ตามลำดับ เป็นที่น่าสนใจว่าเมื่อได้รับโจรันนามัยซิน เอ ที่ความเข้มข้น 0.5 ไมโครโมลาร์เป็นเวลา 24 ชั่วโมง เพิ่มความไวต่อการตายแบบอะพอพโทซิสที่เหนี่ยวนำโดยซิสพลาตินในเซลล์ต้นกำเนิดมะเร็งปอด โดยการเพิ่มขึ้นของโปรตีน p53 และการลดลงของโปรตีน Bcl-2 นอกจากนี้การใช้โจรันนามัยซิน เอ (ความเข้มข้น 0.5 ไมโครโมลาร์) ร่วมกับซิสพลาติน (ความเข้มข้น 25 ไมโครโมลาร์) ยังลดจำนวนเซลล์ที่มีการแสดงออกของ CD133 ในเซลล์ต้นกำเนิดมะเร็งอีกด้วย ดังนั้นข้อมูลกลไกของโจรันนามัยซิน เอ ที่ได้จากงานวิจัยนี้อาจนำไปสู่การพัฒนาสารผลิตภัณฑ์ธรรมชาติทางทะเลเป็นยาเคมีบำบัดที่มุ่งเป้ากำจัดเซลล์ต้นกำเนิดมะเร็งในการรักษามะเร็งปอดได้

สาขาวิชา ชีวเวชเคมี
ปีการศึกษา 2563

ลายมือชื่อนิสิต
ลายมือชื่อ อ.ที่ปรึกษาหลัก

5776143733 : MAJOR BIOMEDICINAL CHEMISTRY

KEYWORD: cancer stem-like cells; cisplatin; lung cancer; jorunnamycin A;
stemness transcription factors

Somruethai Sumkhemthong : EFFECT OF JORUNNAMYCIN A ON CANCER
STEM CELLS OF HUMAN LUNG CANCER H460 CELLS. Advisor: Asst. Prof.
CHATCHAI CHAOTHAM, Ph.D.

It has been recognized that cancer stem-like cells (CSCs) in tumor tissue crucially contribute to therapeutic failure, resulting in a high mortality rate in lung cancer patients. Due to their stem-like features of self-renewal and tumor formation, CSCs can lead to drug resistance and tumor recurrence. Herein, the suppressive effect of jorunnamycin A, a bistetrahydroisoquinolinequinone isolated from Thai blue sponge *Xestospongia* sp., on cancer spheroid initiation and self-renewal in the CSCs of human lung cancer cells is revealed. The depletion of stemness transcription factors, including Nanog, Oct-4, and Sox2 in the lung CSC-enriched population treated with jorunnamycin A (0.5 μM), resulted from the activation of GSK-3 β and the consequent downregulation of β -catenin. Interestingly, pretreatment with jorunnamycin A at 0.5 μM for 24 h considerably sensitized lung CSCs to cisplatin-induced apoptosis, as evidenced by upregulated p53 and decreased Bcl-2 in jorunnamycin A-pretreated CSC-enriched spheroids. Moreover, the combination treatment of jorunnamycin A (0.5 μM) and cisplatin (25 μM) also diminished CD133-overexpressing cells presented in CSC-enriched spheroids. Thus, evidence on the regulatory functions of jorunnamycin A may facilitate the development of this marine-derived compound as a novel chemotherapy agent that targets CSCs in lung cancer treatment.

Field of Study: Biomedical Chemistry

Student's Signature

Academic Year: 2020

Advisor's Signature

ACKNOWLEDGEMENTS

This thesis could not successfully complete without the guidance and the help of several persons who in one way or another contributed and extended their valuable assistance in the preparation and completion of this study.

Firstly, I would like to express sincere gratitude to my thesis advisors, Assistant Professor Chatchai Chaotham, Ph.D. for his invaluable advice, attention, motivation, encouragement, and patience. His kindness is really appreciated. Also, I would like to thank thesis committees; Dr. Preedakorn Chunhacha, Dr. Eakachai Prompetchara, Dr. Wanatchaporn Arunmanee, Dr. Kannika Khantasup and Dr. Monruedee Sukprasansap for their invaluable suggestion. I wish to express my grateful thanks to Assistant Professor Supakarn Chamni, Ph.D. for providing tested compound throughout this study. Additionally, I would like to thank my close friends whose name are not mentioned here for encouragement me to finish this chapter.

I am grateful to Miss Kanokwan Hongtong and Miss Marisa Nuankul for their kind support and help whenever required throughout my Ph.D. study in Department of Biochemistry and Microbiology. I also wish to express my thanks to all lab members at Department of Biochemistry and Microbiology for their friendships, constant support and cooperation.

I also thank to Pharmaceutical Research Instrument Center (P.R.I.C.) for providing scientific instruments for this study.

Finally, I wish to express my infinite thanks to my family and Mr. Suphachok Sengnongban, who always love, understand and support everything in my life.

This work was financially supported by the 90th Anniversary of Chulalongkorn University Fund (Ratchadaphisedksomphot Endowment Fund).

Somruethai Sumkhemthong

TABLE OF CONTENTS

	Page
ABSTRACT (THAI).....	iii
ABSTRACT (ENGLISH).....	iv
ACKNOWLEDGEMENTS	v
TABLE OF CONTENTS	vi
LIST OF TABLES.....	vii
LIST OF FIGURES	xi
LIST OF ABBREVIATIONS	xiv
CHAPTER I INTRODUCTION.....	1
CHAPTER II LITERATURE REVIEWS.....	6
CHAPTER III MATERIALS AND METHODS	25
CHAPTER IV RESULTS	37
CHAPTER V DISCUSSION AND CONCLUSION.....	80
REFERENCES.....	87
APPENDICES.....	104
VITA.....	144

LIST OF TABLES

	Page
Table 1 The half-maximal inhibitory concentration on cell viability (IC ₅₀) and proliferation (IG ₅₀) of jorunnamycin A in human lung cancer and normal lung epithelial cells.....	47
Table 2 Cell viability of human lung cancer H460 cells after treatment with jorunnamycin A (JA) for 24 h.....	104
Table 3 Percent apoptosis of attached H460 cells after 24 h jorunnamycin A (JA) treatment	105
Table 4 Percent growth inhibition of human lung cancer H460 cells over 24-72 h of jorunnamycin A (JA) treatment.....	106
Table 5 Colony number of jorunnamycin A (JA)-treated human lung cancer H460 cells evaluated through limiting dilution assay (LDA) for 14 days	107
Table 6 Relative colony size of jorunnamycin A (JA)-treated CSC-enriched H460 spheroids evaluated by single 3D spheroid formation.....	108
Table 7 Percent CD133-overexpressing cells detected in jorunnamycin A (JA)-treated CSC-enriched spheroids of H460 cells for 3 days via flow cytometry	109
Table 8 Relative mRNA level of stemness transcription factors in CSC-enriched lung cancer H460 cells treated with jorunnamycin A (JA) for 24 h.....	110
Table 9 Relative protein level of CSC self-renewal markers in CSC-enriched lung cancer H460 cells treated with jorunnamycin A (JA) for 24 h.....	110
Table 10 Relative protein level of related up-stream proteins in CSC population of lung cancer H460 cells treated with jorunnamycin A (JA) for 24 h	111
Table 11 Cell viability of human lung cancer H23 cells after treatment with jorunnamycin A (JA) for 24 h.....	112

Table 12 Percent apoptosis of attached H23 cells after 24 h jorunnamycin A (JA) treatment	113
Table 13 Percent growth inhibition of human lung cancer H23 cells over 24-72 h of jorunnamycin A (JA) treatment	114
Table 14 Cell viability of human lung cancer A549 cells after treatment with jorunnamycin A (JA) for 24 h	115
Table 15 Percent apoptosis of attached A549 cells after 24 h jorunnamycin A (JA) treatment	116
Table 16 Percent growth inhibition of human lung cancer A549 cells over 24-72 h of jorunnamycin A (JA) treatment	117
Table 17 Cell viability of human lung epithelial BEAS-2B cells after treatment with jorunnamycin A (JA) for 24 h	118
Table 18 Percent apoptosis of attached BEAS-2B cells after 24 h jorunnamycin A (JA) treatment	119
Table 19 Percent growth inhibition of human lung epithelial BEAS-2B cells over 24-72 h of jorunnamycin A (JA) treatment	120
Table 20 Colony number of jorunnamycin A (JA)-treated human lung cancer H23 cells evaluated through limiting dilution assay (LDA) for 14 days	121
Table 21 Relative colony size of jorunnamycin A (JA)-treated CSC-enriched H23 spheroids evaluated by single 3D spheroid formation	122
Table 22 Percent CD133-overexpressing cells detected in jorunnamycin A (JA)-treated CSC-enriched spheroids of H23 cells for 3 days via flow cytometry	123
Table 23 Colony number of jorunnamycin A (JA)-treated human lung cancer A549 cells evaluated through limiting dilution assay (LDA) for 14 days	124
Table 24 Relative colony size of jorunnamycin A (JA)-treated CSC-enriched A549 spheroids evaluated by single 3D spheroid formation	125

Table 25 Percent CD133-overexpressing cells detected in jorunnamycin A (JA)-treated CSC-enriched spheroids of A549 cells for 3 days via flow cytometry.....	126
Table 26 Relative mRNA level of stemness transcription factors in CSC-enriched lung cancer H23 cells treated with jorunnamycin A (JA) for 24 h.....	127
Table 27 Relative mRNA level of stemness transcription factors in CSC-enriched lung cancer A549 cells treated with jorunnamycin A (JA) for 24 h.....	127
Table 28 Relative protein level of related up-stream proteins in CSC population of lung cancer H23 cells treated with jorunnamycin A (JA) for 24 h.....	128
Table 29 Relative protein level of related up-stream proteins in CSC population of lung cancer A549 cells treated with jorunnamycin A (JA) for 24 h.....	128
Table 30 Colony number of jorunnamycin A (JA)-treated human lung epithelial BEAS-2B cells evaluated through limiting dilution assay (LDA) for 14 days	129
Table 31 Relative colony size of jorunnamycin A (JA)-treated stem cell-enriched BEAS-2B spheroid evaluated by single 3D spheroid formation	130
Table 32 Percent CD133-overexpressing cells detected in jorunnamycin A (JA)-treated BEAS-2B spheroids for 3 days via flow cytometry	131
Table 33 Flow cytometry analysis for ROS measurement in jorunnamycin A (JA)-treated CSC-enriched H460 spheroids for 1-9 h	131
Table 34 Colony number of human lung cancer H460 cells after treatment with jorunnamycin A (JA) for 14 days with or without N-acetyl cysteine (NAC) pretreatment	132
Table 35 Relative colony size of CSC-enriched H460 spheroids after treatment with jorunnamycin A (JA) for 0-7 days with or without N-acetyl cysteine (NAC) pretreatment	133
Table 36 Relative protein level of related autophagy proteins in CSC population of lung cancer H460 cells treated with 0.5 μ M jorunnamycin A (JA) for 0-12 h	134

Table 37 Colony number of human lung cancer H460 cells after treatment with jorunnamycin A (JA) for 14 days with or without wortmannin pretreatment.....	135
Table 38 Relative colony size of CSC-enriched H460 spheroids after treatment with jorunnamycin A (JA) for 0-7 days with or without wortmannin pretreatment	136
Table 39 Cell viability of attached H460 cells after treatment with cisplatin for 24 h with or without pretreatment with jorunnamycin A (JA).....	137
Table 40 Percent apoptosis of attached H460 cells after treatment with cisplatin for 24 h with or without pretreatment with jorunnamycin A (JA)	137
Table 41 Relative colony size of CSC-enriched H460 spheroids after treatment with cisplatin for 0-7 days with or without jorunnamycin A (JA) pretreatment	138
Table 42 Percent CD133-overexpressing cells detected in jorunnamycin A (JA)-pretreated CSC-enriched spheroids of H460 cells after incubation with cisplatin for 3 days via flow cytometry.....	139
Table 43 Mode of cell death detected in jorunnamycin A (JA)-pretreated CSC-enriched spheroids of H460 cells for 24 h prior to 24 h of cisplatin treatment via flow cytometry.....	140
Table 44 Relative colony size of CSC-enriched H23 spheroids after treatment with cisplatin for 0-7 days with or without jorunnamycin A (JA) pretreatment	141
Table 45 Relative colony size of CSC-enriched A549 spheroids after treatment with cisplatin for 0-7 days with or without jorunnamycin A (JA) pretreatment	142
Table 46 Relative protein level of apoptosis-related proteins in CSC-enriched H460 spheroids treated with jorunnamycin A (JA) for 24 h	143

LIST OF FIGURES

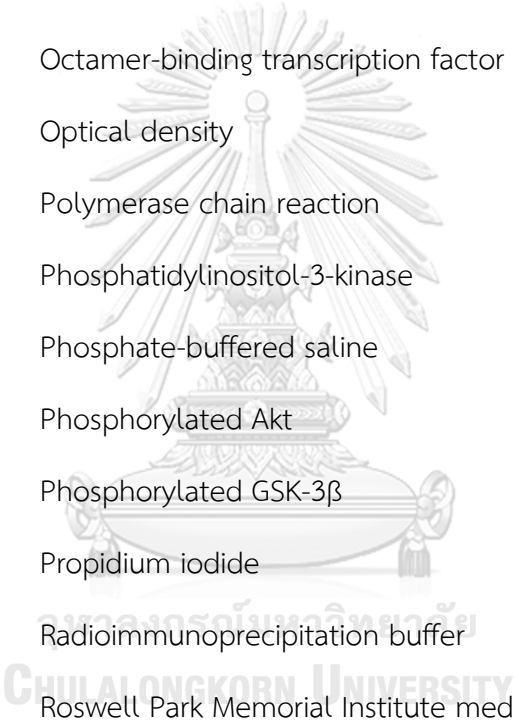
	Page
Figure 2.1 Estimated death rate in distinct cancer types in 2020.....	6
Figure 2.2 Histological classification of lung cancer.....	7
Figure 2.3 Illustration of the non-small lung cancer (NSCLC) staging.....	8
Figure 2.4 Cancer stem-like cells characteristics.....	12
Figure 2.5 PI3K/Akt/ β -catenin signaling pathway for activation of stemness gene transcription in CSCs.....	14
Figure 2.6 Cellular ROS production and homeostasis.....	15
Figure 2.7 ROS level in maintenance of CSCs stemness.....	16
Figure 2.8 Machinery of autophagy pathway.....	17
Figure 2.9 Responsibility of autophagy in CSCs.....	18
Figure 2.10 Machinery of intrinsic and extrinsic apoptosis pathway.....	20
Figure 2.11 Chemical structure of cisplatin.....	22
Figure 2.12 DNA damage induced by cisplatin.....	23
Figure 2.13 Chemical structure of jorunnamycin A.....	24
Figure 3.1 Conceptual framework.....	32
Figure 3.2 Experimental Design.....	33
Figure 4.1 Cytotoxicity of jorunnamycin A in human lung cancer H460 cells.....	38
Figure 4.2 The inhibitory effect of jorunnamycin A on CSCs of lung cancer H460 cells.....	40
Figure 4.3 The suppressing effect of jorunnamycin A on CSCs of H460 lung cancer cells.....	41

Figure 4.4 Jorunnamycin A restrained CD133-overexpressing cells in CSCs of H460 lung cancer cells.....	42
Figure 4.5 Jorunnamycin A downregulates stemness transcription factors and related proteins in CSC-enriched lung cancer H460 cells.....	44
Figure 4.6 Jorunnamycin A-induced cytotoxicity in human lung cancer H23 cells.....	48
Figure 4.7 Cytotoxicity activity of jorunnamycin A in human lung cancer A549 cells.....	50
Figure 4.8 Cytotoxicity of jorunnamycin A in human lung epithelial BEAS-2B cells.....	52
Figure 4.9 Jorunnamycin A suppresses stem-like phenotypes of lung cancer H23 cells.....	55
Figure 4.10 Suppressive effect of jorunnamycin A on stem-like phenotypes of lung cancer A549 cells.....	57
Figure 4.11 Jorunnamycin A downregulates stemness transcription factors and related proteins in various lung CSCs.....	59
Figure 4.12 No alteration of stemness phenotypes in human lung epithelial cells cultured with jorunnamycin A.....	61
Figure 4.13 The relative ROS level in CSC-enriched H460 spheroids incubated with jorunnamycin A (JA) for 1-9 h was assessed vis flow cytometry using DCFH ₂ -DA probe.....	63
Figure 4.14 ROS effect in spheroid-initiating capability of jorunnamycin A observed in human lung cancer H460 cells.....	64
Figure 4.15 ROS modulating effect of jorunnamycin A in CSC-enriched H460 spheroid.....	66
Figure 4.16 The alteration of autophagy-related proteins in jorunnamycin A-treated CSC-enriched spheroid.....	67

Figure 4.17 Autophagic effect of jorunnamycin A on tumor-initiating cell observed in human lung cancer H460 cells.....	69
Figure 4.18 Autophagy inducing effect of jorunnamycin A in CSC-enriched H460 spheroids.....	70
Figure 4.19 The sensitizing effect of jorunnamycin A in cisplatin-induced apoptosis in lung cancer H460 cells.....	72
Figure 4.20 Sensitization of CSC-enriched lung cancer cells to cisplatin-induced apoptosis by jorunnamycin A.....	75
Figure 4.21 Cisplatin sensitizing effect of jorunnamycin A in various lung CSCs.....	77
Figure 4.22 Alteration of apoptosis-related proteins in jorunnamycin A-treated lung CSCs.....	78
Figure 5.1 Jorunnamycin A potential benefits in cancer treatment.....	85
Figure 5.2 Schematic representation of jorunnamycin A-mediated suppression of CSC phenotype and sensitization of CSC-enriched lung cancer cells to cisplatin-induced apoptosis.....	86

LIST OF ABBREVIATIONS

3D	=	Three-dimension
μM	=	Micromolar
β -catenin	=	Beta-catenin
Akt	=	Protein kinase B
ANOVA	=	Analysis of variance
BAX	=	Bcl-2-associated X
BCA	=	Bicinchoninic acid
Bcl-2	=	B-cell lymphoma 2
BSA	=	Bovine serum albumin
CD133	=	Prominin-1
CSCs	=	Cancer stem-like cells
DMEM	=	Dulbecco's modified Eagle's medium
DMSO	=	Dimethyl sulfoxide
EDTA	=	Ethylenediaminetetraacetic acid
EMT	=	Epithelial-to-mesenchymal transition
FBS	=	Fetal bovine serum
FITC	=	Fluorescein isothiocyanate
GAPDH	=	Glyceraldehyde-3 phosphate dehydrogenase
GSK-3 β	=	Glycogen synthase kinase-3 β
h	=	Hour
HRP	=	Horseradish peroxidase
JA	=	Jorunnamycin A
LC3	=	Microtubule-associated protein light chain 3



LDA	=	Limiting dilution assay
Mcl-1	=	Myeloid cell leukemia 1
mM	=	Millimolar
MTT	=	3-(4,5-Dimethylthiazol-2-yl)-2,5-diphenyltetrazolium bromide
NAC	=	N-Acetylcysteine
nm	=	Nanometer
nM	=	Nanomolar
Oct-4	=	Octamer-binding transcription factor 4
OD	=	Optical density
PCR	=	Polymerase chain reaction
PI3K	=	Phosphatidylinositol-3-kinase
PBS	=	Phosphate-buffered saline
p-Akt	=	Phosphorylated Akt
p-GSK-3 β	=	Phosphorylated GSK-3 β
PI	=	Propidium iodide
RIPA	=	Radioimmunoprecipitation buffer
RPMI	=	Roswell Park Memorial Institute medium
Rpm	=	Revolutions per minute
RT-PCR	=	Reverse transcription polymerase chain reaction
RT-qPCR	=	Reverse transcription quantitative real-time PCR
SD	=	Standard deviation
SDS-PAGE	=	Sodium dodecyl sulfate polyacrylamide gel electrophoresis
Sox2	=	(Sex determining region Y)-box 2
TBST	=	Tris-buffered saline with Tween 20

CHAPTER I INTRODUCTION

Lung cancer has been identified as the highest cancer-related death among all cancers. Approximately, there was 1.8 million deaths from lung cancer worldwide in 2020 [1]. Lung cancer patients reportedly show low five-year survival rate (19%) for all stage diagnosis [2]. Although lung cancer patients complete full treatment, they occasionally present low drug response and tumor relapse due to violent characteristics and heterogeneity of lung cancer cells [3, 4]. Heterogeneous population is found in tumor tissue. Generally, tumor mass composes mostly with chemo/radiosensitive cells which could be eliminated by conventional therapy. Whereas, small population of cancer stem-like cells (CSCs) is chemo-resistant and exhibit explicit growth capability, leading to recurrence of tumor pathology [5]. Notably, CSCs or tumor initiating cells possess unique stem cell-like properties of self-renewal and differentiation. Moreover, they have aberrant signaling maintaining proliferation and immortality [6, 7]. According to their specific features, CSCs play a critical role on drug resistance, tumor progression and treatment failure [8]. Thus, CSC-targeted therapy could be a promising strategy for novel lung cancer treatments [9].

Accumulating clinical data demonstrate that CSCs have been presented in tumor specimen obtained from patients with non-small cell lung cancer (NSCLC) [10-12]. Distinguishing markers such as CD133, CD44, ALDH1A1 and ABCG2 are used to classify lung CSCs [7]. High expression of CD133 associates with poor prognosis and short lifespan in NSCLC patients [13]. In addition, Oct4, Sox2, and Nanog are transcription factors that modulate stemness in both normal and cancer stem cells including in lung cancer [14, 15]. Not only patients' specimen but also human lung cancer cell lines express these CSCs protein markers [16]. Intriguingly, treatment with available chemotherapeutic drug, cisplatin enriched CSC population in lung cancer cells [17].

The regulatory mechanism of Akt-dependent pathway on CSC properties has been continuously reported [18-20]. In NSCLC, Akt signaling pathway is commonly stimulated and acts as a key mediator to promote survival, proliferation and migration [21]. Emerging evidence suggests that Akt is an upstream machinery of Oct4 to mediate

CSC phenotypes [18]. Phosphorylated-Akt (p-Akt) prolongs stability of Oct4 by prevention of protein degradation after adding phosphate group to Oct4 (p-Oct4). Consequently, p-Oct4 translocates into nucleus and collaborates with Sox2 to promote Nanog stemness gene transcription [22]. On the contrary, *in vitro* and *in vivo* studies showed that inhibition of Akt and Oct4 potently diminished cancer cells proliferation and CSC tumorigenicity [23]. Therefore, targeting on Akt pathway may be benefit for suppression and eradication of CSCs [24].

Several studies indicated that autophagy promotes survival and drug resistance in CSCs [25-27]. Autophagy is an intracellular catabolic process that reserves novel bioenergetics from lysosomal degradation of cytoplasmic components [28]. Expression of Beclin-1, LC3-I/II, SQSTM1/p62 protein is widely used as autophagy protein markers [29]. Akt regulates autophagy mechanism through Beclin-1 phosphorylation [30]. Recent study demonstrated that increment of autophagy in CSCs through activating Akt signaling pathway bring about chemotherapeutic resistance [31]. Autophagy-mediated cell survival mechanism facilitates CSCs tolerance to conventional therapies [32]. Thus, autophagy inhibition in CSCs might be overcome tumor recurrence and drug resistance [31, 33]. Nevertheless, role of autophagy on modulation of CSCs is still controversial.

The important role of reactive oxygen species (ROS) has been also pointed out on CSC phenotypes [34, 35]. ROS not only mediate cellular redox status but also involve in regulation of intracellular activities including proliferation, division and migration [36]. CSCs contain low cellular ROS level due to gain high antioxidant defending system in order to protect oxidative stress caused by exogenous stimuli [35]. ROS-modulating agents are found to dramatically eliminate CSCs and inhibit tumor growth in both *in vitro* and *in vivo* models [37]. Recent study indicated that ROS inactivated Akt pathway consequence with suppression of cell proliferation and induction of cell death in CSCs [38]. Hence, the alteration of cellular ROS level might disturb self-renewal and differentiation capacities of CSCs [38, 39].

Augmenting studies reveal the potential of Thai natural marine products as biological resource for anticancer agents [40-42]. Jorunnamycin A, a

bistetrahydroisoquinolinequinone isolated from Thai blue sponge *Xestospongia* sp. is the one of renieramycin M derivatives that previously reported about anticancer and antimetastatic activity. Renieramycin M treatment demonstrated apoptosis inducing effect in non-small cell lung cancer H460 cells by induction of p53 and down regulation of anti-apoptotic proteins. Additionally, renieramycin M inhibited migration and invasion in lung cancer cells [43]. Renieramycin M was also found to diminish observable characteristics of lung CSCs [44], yet this investigation lacked of mechanism details. Recent study revealed that jorunnamycin A promoted detachment-induced cell death, inhibited epithelial to mesenchymal transition (EMT) and attenuated anchorage-independent growth in human lung cancer cells [45]. However, the effect of jorunnamycin A on CSC regulation has not yet been clarified.

This study aims to investigate the effect of jorunnamycin A on CSC phenotypes as well as relating underlying mechanisms. Although the potential in enhancing chemotherapeutic treatment of natural products from marine organism was noticed, no information about the activity of jorunnamycin A on cisplatin-treated lung cancer H460 cells has been addressed. Herein, chemo-sensitizing activity of jorunnamycin A in cisplatin-treated lung cancer cells will also be evaluated. The findings from this study could serve as a guide for novel treatment for human lung cancer to prevent chemotherapeutic resistance and provide important insights to facilitate further development of jorunnamycin A for CSC-targeted approaches.

Research Questions

1. Does jorunnamycin A affect CSC phenotypes in human lung cancer cells?
2. What are the possible regulatory pathways relating to the activity of jorunnamycin A on CSCs in human lung cancer cells?
3. Does jorunnamycin A sensitize lung CSCs to cisplatin-induced cell death?
4. Does jorunnamycin A diminish cisplatin-induced CSCs in human lung cancer cells?

Objectives

1. To evaluate the effect of jorunnamycin A on CSC phenotypes in human non-small cell lung cancer H460 cells.
2. To investigate the underlying mechanisms of jorunnamycin in CSCs of human non-small cell lung cancer H460 cells.
3. To evaluate the chemo-sensitizing effect of jorunnamycin A in cisplatin-induced apoptosis cell death in CSCs of human non-small cell lung cancer H460 cells.

Hypothesis

Jorunnamycin A enhances anticancer effect of cisplatin via alteration of CSC phenotypes in CSCs of human non-small cell lung cancer H460 cells.

Benefit of this study

1. This study would provide the scientific evidence for the effect of jorunnamycin A on CSC phenotypes in human non-small cell lung cancer H460 cells.
2. This study would provide the information of the intracellular mechanism of jorunnamycin A in modulating CSCs and chemotherapeutic response in CSCs of human non-small cell lung cancer H460 cells.
3. This study would initiate the development of jorunnamycin A as CSC-targeted therapy.

4. This study would benefit the development of jorunnamycin A as the combination therapy with conventional chemotherapeutic drugs for enhancing therapeutic response.



CHAPTER II LITERATURE REVIEWS

1. Lung cancer

Due to aggressive features and high prevalence rate, lung cancer accounts for most of the cancer deaths worldwide [46]. Although various treatment regimens have been developed, the five-year survival rate of lung cancer patients in all diagnosed stages has not remarkably improved [47]. The most common risk factor for lung carcinoma is individual cigarette smoking, moreover passive smoke inhalation, infection and genetic susceptibility are also harmful factors [48]. Although, the control tobacco policy and effective regimen have been developed for over the past decade, lung cancer still illustrates the highest mortality in cancer patients worldwide (Fig. 2.1).

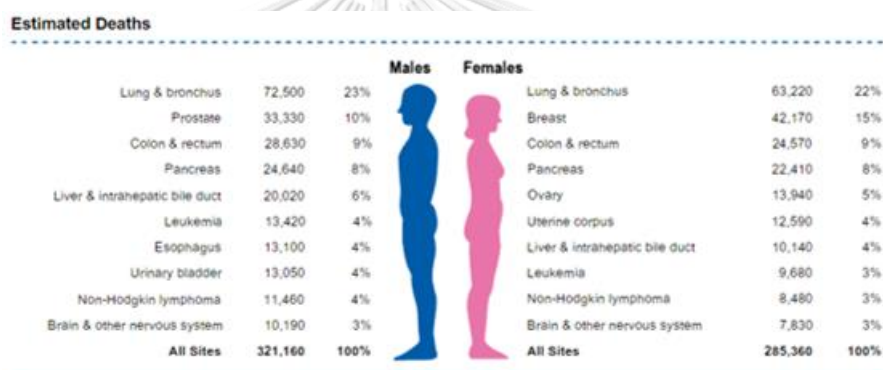


Figure 2.1 Estimated death rate in distinct cancer types in 2020 [47]

Lung cancer is classified into two main histological groups including small cell lung carcinoma (SCLC) and non-small cell lung carcinoma (NSCLC) with approximately 15% and 85% of all lung cancer cases, respectively [49].

The pulmonary neuroendocrine cells in pulmonary airway are the origins of small cell lung carcinoma (SCLC) [50] which exhibits smaller cells and more rapidly growth and spread to second organ than NSCLC [51]. Untreated SCLC is life-threatening among all type of lung cancers. Despite, treated-SCLC patients, five-years of survival rate are remaining only 6% [52].

Non-small cell lung carcinoma (NSCLC) type is mostly found in lung cancers. They are categorized into three subtypes including adenocarcinoma, squamous cell carcinoma and large cell lung carcinoma (Fig. 2.2).

- Adenocarcinoma (ADC) is the most common type of lung cancer with approximately 40% which is derived from epithelial of alveolar cells. This common type is usually developed in both of smokers and nonsmokers.
- Squamous-cell carcinoma (SCC) accounts for 30% of lung cancer which presented from squamous cells of airway epithelial cells in bronchi. It is caused by cigarette smoking.
- Large cell carcinoma (LCC) comprises 15% of all lung cancers cases which are related with smoking. This type can originate in any part of the lung such as central part of the lungs, chest wall. Due to quickly growth and spread properties, it is also found in distant organs as well [53, 54].

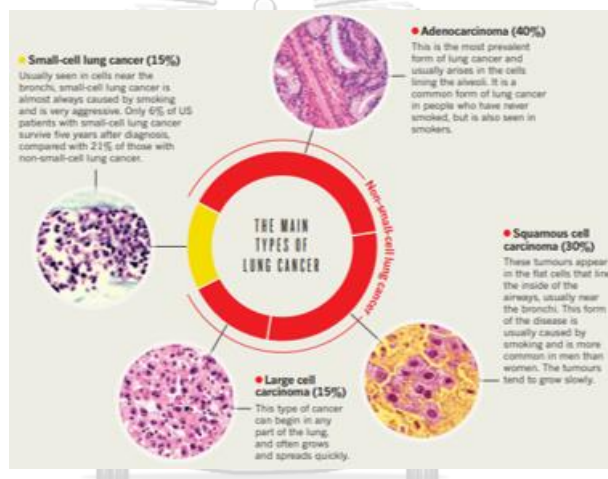


Figure 2.2 Histological classification of lung cancer [54]

Stages of lung cancer

To start treatment of lung cancer, assessment of stage classification is an essential procedure in patients who has been diagnosed with lung cancer. Stages of lung malignant are divided by two major types of lung cancer [55, 56].

1. Small cell lung cancer staging

Small cell lung cancer (SCLC) is classified into two stages, limited and extensive stage by clinical staging of SCLC [55].

1.1 Limited stage of SCLC: tumor is restrained in one part of lung or nearby lymph nodes.

1.2 Extensive stage of SCLC: tumor spread to other part of lung, other lymph nodes and reach to distance organs [51].

2. Non-small lung cancer staging

Non-small lung cancer (NSCLC) is categorized into four major classes by TMN classification for staging of NSCLC 8th edition[56].

2.1 Stage I: cancer is located only in the lung and it does not spread to lymph nodes

2.2 Stage II: cancer is in the lung and nearby lymph nodes

2.3 Stage III: cancer is also found in the lung and lymph nodes in the middle of the chest. This stage is an advance stage which is divided into two subtypes.

2.3.1 Stage IIIA: Cancer invades only to lymph nodes on the same side of the chest where the cancer starts growing.

2.3.2 Stage IIIB: Cancer invades to the lymph nodes on the opposite side of the chest.

2.4 Stage IV: Cancer spread to both lungs or to another part of body such as liver, bone and brain (Fig. 2.3).

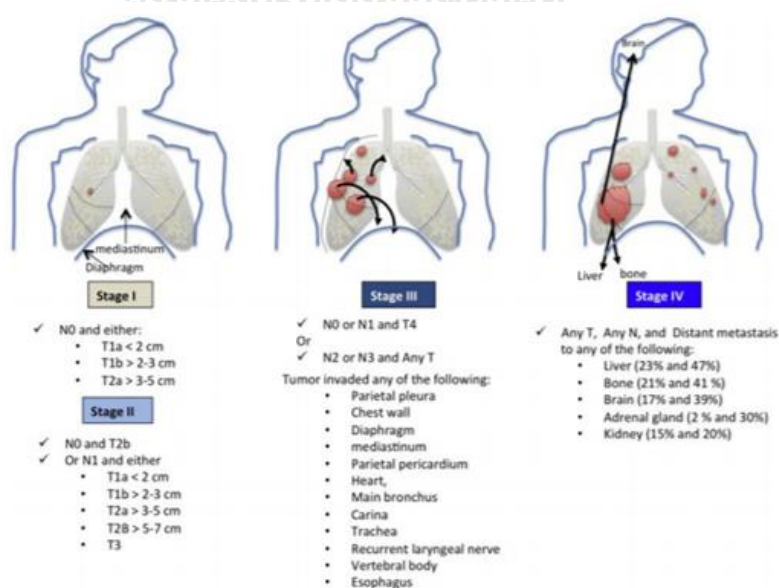


Figure 2.3 Illustration of the non-small lung cancer (NSCLC) staging [51]

Although small cell lung cancer displays rapid metastasis [51], High prevalence is indicated in non-small cell lung cancer (~85%). Moreover, chemotherapeutics resistance has been recognized as a major cause of low 5-years survival rates in non-small cell lung cancer patients [57]. For that reason, researching in non-small cell lung cancer therapy is challenged.

Current treatment options for non-small cell lung carcinoma

1. Surgery

Surgery is used to remove the tumor in lung cancer patients who are diagnosed stage I, II, and IIIA and are able to tolerate surgery [53]. Surgical treatment goals are aimed to decrease morbidity and mortality rate in early-stage patients [58]. Survival rate at five years after resection is approximately 60%–80% for stage I NSCLC and 30%–50% for stage II NSCLC patient. However, surgical resection cannot be used in patients who have metastasis stage [59].

2. Radiotherapy

Radiotherapy is recommended in early-stage NSCLC patients who have small nodule in the lung without spreading to lymph nodes and cannot receive surgical resection. Radiation eradicates cancer cells via using high-energy beams to damage DNA within cancer cells in a certain area. Survival rate at three years after radiation accounts 55.8% [53]. Moreover, radiotherapy is applied to eliminate tumor after and surgery in early-stage NSCLC patients and usually collaborate with chemotherapy in advance-stage NSCLC patients [60].

3. Chemotherapy

New diagnosis NSCLC patients represent nearly 40% in advanced stage. The treatment goal of these patients is to delay progression of disease and improve survival. Chemotherapy has been the first-line therapy in NSCLC advanced stage. Chemotherapy implies to use chemical drugs to treat any disease including cancer. The chemotherapeutic drugs are mostly administrated via intravenous (IV) then are absorbed and distributed

throughout the body and kill cancer cells that metastasized far away from primary tumor to secondary organ. According to their activity, chemotherapy is considered a systematic treatment [53]. The American Society of Clinical Oncology suggested regimen for treatment stage IV NSCLC patient is a combination of a platinum (cisplatin or carboplatin) plus paclitaxel, gemcitabine, docetaxel, vinorelbine, irinotecan, or pemetrexed [61]. Accumulate randomized clinical trials studying revealed median overall survival for NSCLC patients who are treated with that regimen was approximately 8–10 months [62-64]. Although chemotherapy exhibits effectiveness, it can cause some side effects such as nausea, vomiting, hair loss, cardiovascular toxicity and nephrotoxicity depend on each agent [65].

4. Targeted therapy

Targeted therapy refers to use the drugs or other substances which are specific to cancer cells and cause less harmful to normal cells. Although targeted therapy causes fewer side effects than chemotherapeutic, it has high costs [66]. Currently, there are several targeted treatment pathways for lung cancer including EGFR, PI3K/AKT/mTOR, RAS–MAPK, and NTRK/ROS1 pathways. Recent study shows clinical benefits and replacing chemotherapy by targeted therapy as the first line treatment such as EGFR inhibitors erlotinib, gefitinib, PI3K/AKT/mTOR inhibitors everolimus, and NTRK/ROS1 inhibitors entrectinib [67].

5. Immunotherapy

Immunotherapy is considered a new drug group for treatment NSCLC patients with efficiency and improve the quality of life. This drug group worked by increase immune response to recognize cancer cells [68]. According to programmed death 1 (PD-1) displays antitumor activity in advanced NSCLC, high level of programmed death ligand 1 (PD-L1) expression was found in NSCLC patients approximately up to 28%. For example, pembrolizumab, a humanized monoclonal antibody was developed to against PD-1 with increased activity in tumors that express

programmed death ligand 1 (PD-L1) and was significantly prolonged progression-free period and life span in NSCLC patients [69]. Meanwhile, cancer immunotherapy has made remarkable progress in the last decade, but there are persisting limitations such as the low percentage of responders, side effects, and cost effectiveness [70, 71]. At this point, there is a continued need to develop effective CSC-targeted therapy that could thus improve the current standard of care.

Three types of lung cancer cells were used in this study, including H460, H23 and A549, which respectively represent large cell carcinoma, adenocarcinoma and lung carcinoma. Lung cancer H23 cells are adenocarcinoma which are detected in the early stage in which cancer cells does not invade deeper in lung tissue. Although H460 and A549 share the same type of disease, carcinoma, they are in the different stage of cancer. Lung carcinoma A549 cells are also found in stage I of lung cancer where no metastasis nearby lymph nodes is presented. Meanwhile large cell carcinoma H460 cells are presented in a malignant pleural effusion, the fluid around the lung. Thus, H460 cells exhibit in advanced stage or metastasis in stage IV and serve as aggressive behavior of lung cancer cells [72].

2. Cancer stem-like cells (CSCs)

Tumor heterogeneity presents a major challenge, as proven by subpopulations of cancer stem-like cells (CSCs), which possess the stemness features of self-renewal and differentiation and promote drug resistance, metastasis, tumorigenicity, and cancer relapse [5-9, 73].

Cancer stem-like cells (CSCs) characteristics

Basis characteristics of CSCs have been summarized including initiation of new tumor, expression of specific markers which benefit for identification, capacity to transplant generation after generation and resistance to conventional chemotherapy and radiotherapy (Fig. 2.4) [74].

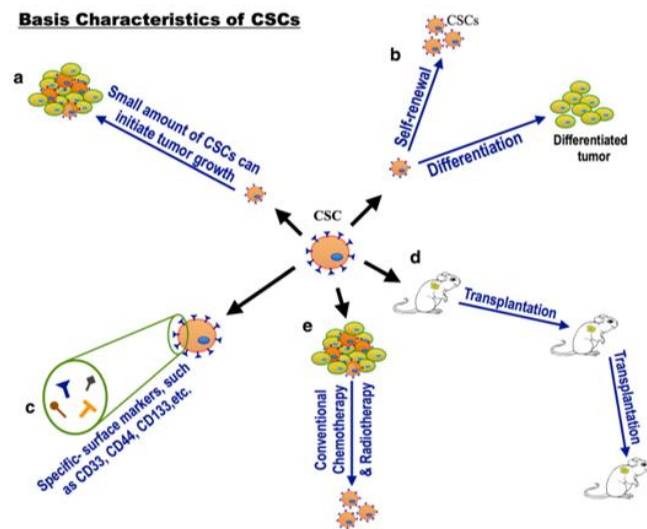


Figure 2.4 Cancer stem-like cells characteristics [74]

Distinct methodologies are used to isolate CSCs such as expression of specific cell surface markers, side population assay by Hoechst 33342 staining and sphere-formation assay [75]. To identify CSCs, specific surface protein markers were used to distinguish CSCs from non-CSCs. Lung cancer stem cells are classified by distinct biomarkers including cell surface glycoprotein, CD133 and transcription factors, Oct4, Nanog and Sox2 [7, 14, 15]. Due to tumor initiating capability of CSCs, limiting dilution assay (LDA) is utilized to verify the amount of tumor initiating cell in cancer population *in vitro* and *in vivo* [76]. Moreover, the ability of those cancer stem cells to replicate themselves known as self-renewal is successfully determined by three-dimensional (3D) spheroid formation [77-79].

CSCs are found in both patient tumor specimen and lung cancer cell lines [10, 16]. Clinical specimens from lung cancer patients have been found to highly express CD133 (Prominin-1), a recognized CSC protein marker in various cancers [10-12]. The upregulation of CD133 has allowed CSC tracking and isolation [16]. The CD133^{high} cancer subpopulation demonstrates self-renewal and tumorigenicity in both *in vitro* and *in vivo* experiments [80, 81]. Furthermore, the CSC phenotype is linked to poor clinical outcomes and therapeutic resistance. The phenotype is correlated with the overexpression of stemness-regulating transcription factors Oct-4 (Octamer-binding transcription factor 4), Sox2 ((Sex determining region Y)-box 2), and Nanog [82].

The collaboration of Oct-4 and Sox2 subsequent with Nanog stemness gene transcription regulated survival and self-renewal activity in CSCs [22, 83]. Sox2 also promote tumor development and maintain pluripotency in lung cancer[84] while, Nanog regulate the self-renewal and proliferation of CSCs [85]. Interestingly, high expression of Oct4 is associated with cisplatin treatment in lung CSCs [17, 85]. Furthermore, the induction of CSC properties and the enhancement of malignancy in lung adenocarcinoma require the co-expression of Oct-4 and Nanog [86]. Several studies have reported the reduction of self-renewal activity and tumor formation in lung cancer was caused by the depletion of these stemness transcription factors [19, 78, 79, 87]. These stemness transcription factors not only maintain stem-like phenotype but also regulate chemotherapeutic resistance in CSCs [88, 89]. Evidence study has been reported the elevation of Sox2 promoted drug resistance while downregulation of SOX2 contributed susceptibility to chemotherapeutics agent [90]. Moreover, lowering Oct4 expression enables sensitivity to cisplatin treatment in lung CSCs [11].

The regulatory role of the PI3K (phosphatidylinositol-3-kinase)/Akt (protein kinase B)/ β -catenin pathway in modulating the CSC phenotype is a point of interest [91]. The expression of self-renewal transcription factors in lung CSCs is mediated by Akt, an up-stream signaling molecule [19, 78, 79]. After phosphorylation by activated Akt (p-Akt), GSK-3 β (glycogen synthase kinase-3 β) will release β -catenin from the degradation complex. Sequestered β -catenin then translocates into the nucleus to stimulate the transcription of target genes, including Nanog and Oct-4 [92]. The suppression of Akt and p-GSK-3 β has been remarkably noted to suppress CSCs in lung cancer [78].

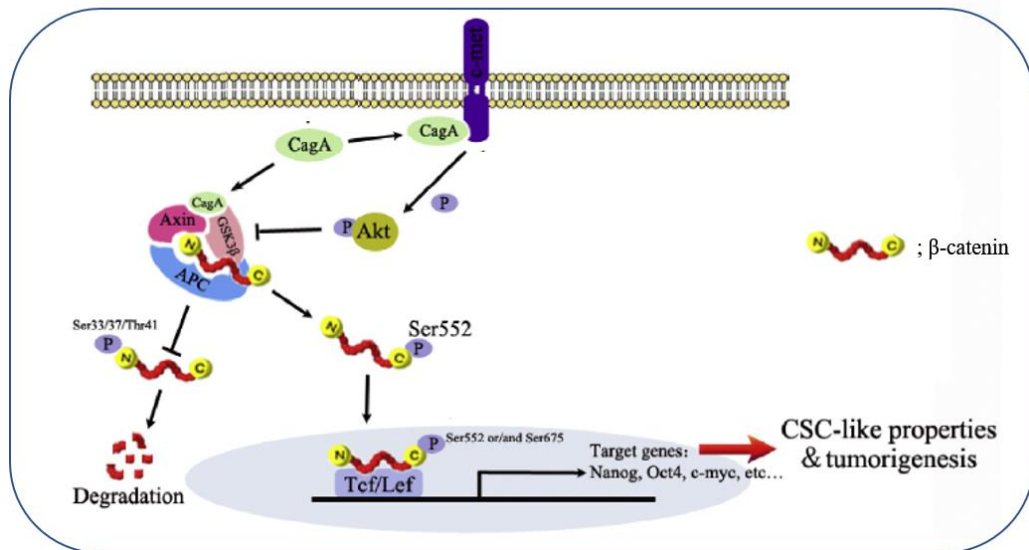


Figure 2.5 PI3K/Akt/ β -catenin signaling pathway for activation of stemness gene transcription in CSCs (Modified from [92])

3. Reactive oxygen species (ROS)

Reactive oxygen species (ROS) are free radicals derived from oxygen molecule which contain one or two unpaired electrons such as hydrogen peroxide (H_2O_2), superoxide anion ($O_2^{\cdot-}$) and hydroxyl radical ($\cdot OH$). These oxygen molecules are responsive to activate chemical reaction cascade [36]. Several factors can induced ROS generation for example, ultraviolet (UV), ionizing radiations, pollutants, heavy metals and xenobiotics [93]. The ROS are mainly generated in mitochondria which involve in redox balanced and regulation of intracellular activities. In addition, cellular ROS production is linked with endoplasmic reticulum stress (ER stress), unfolded protein response and NADPH oxidase complex in cytoplasm. [94]. The production of oxygen free radicals begins with $O_2^{\cdot-}$ generation in mitochondria matrix then is catalyzed to H_2O_2 by catalytic enzyme, superoxide dismutase (SOD). In one hand, unstable H_2O_2 is converted to water (H_2O) by major ROS-scavenging enzymes such as glutathione peroxidase (GPX), glutathione reductase (GR) and catalase. In the other hand, H_2O_2 rapidly alters to $\cdot OH$, hazardous molecule which impaired lipid, protein and DNA damage (Figure 2.6) [36, 95, 96]. Moreover, these ROS-scavenging enzymes act as an

immense antioxidant to maintain intracellular homeostasis. The modulation of ROS in pro-oncogenic signaling pathway resulting in cancer progression, angiogenesis, and survival has been evidenced [36, 97]. Augmentation of ROS has been recognized in cancer cells as a result of high metabolic activity [97]. Thus, targeting ROS alteration may be the one of strategies in cancer treatment.

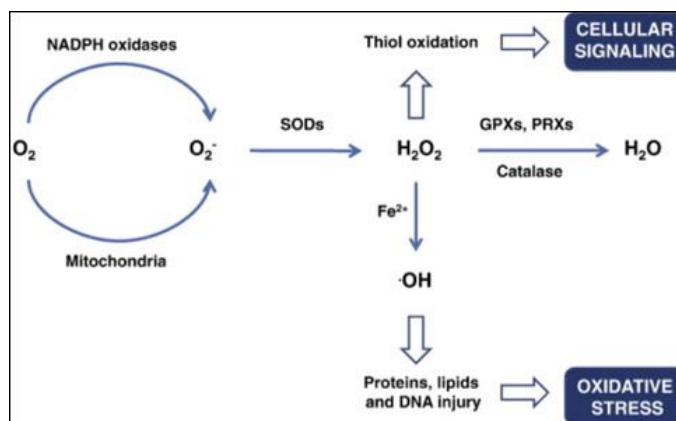


Figure 2.6 Cellular ROS production and homeostasis [96]

Role of ROS in cancer stem-like cells (CSCs)

It should be noted that lower intracellular ROS contents are observed in CSCs compared with non-CSCs due to the elevated expression of free radical scavenging systems [35, 98, 99]. The lowering ROS levels in CSCs not only preserve self-renewal but also maintain stemness properties including quiescence, tumorigenicity and drug resistance which are similar to normal stem cells [100]. Because of ROS scavenging systems raising in CSCs, the pharmacological depletion of ROS scavengers considerably benefited for decrease their clonogenicity and sensitization to radiotherapy [34]. Interestingly, to protect oxidative stress, CSCs gain high antioxidant defending system resulting in low cellular ROS level (Figure 2.7) [35]. Recent studies revealed CSCs are inhibited by superoxide anion ($O_2^{\cdot-}$) [38] whereas hydroxyl radical ($^{\cdot}OH$) promoted lung CSCs phenotypes [39]. Therefore, targeting on ROS modulation may be benefit for eradication of lung CSCs.

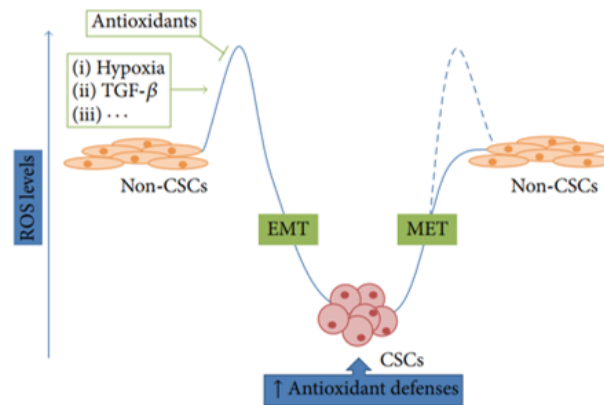


Figure 2.7 ROS level in maintenance of CSCs stemness [35]

4. Autophagy

Autophagy is self-digesting process responsible for both cell survival and cell death mechanism [101]. This catabolism process is also the cell energy supply by degradation of cytoplasmic constituents and organelles in the lysosome resulted in novel nutrition [28]. The recycling and salvage of cellular nutrients are promoted by autophagic degradation which enables cell survival during starvation [102]. Autophagy activated in both under normal and aberrant metabolic condition [103]. Various factors can stimulate autophagy such as nutrient deprivation and energy stress, ER stress, hypoxia, oxidative stress and mitochondrial damage [104]. Autophagy is divided into different three types, macroautophagy, main type of autophagy, mitophagy and chaperone-mediated autophagy which serve different mechanisms and cellular functions [103, 105]. In this study highlight in macroautophagy due to the most prevalent form.

The machinery of autophagy consists of many steps including initiation, nucleation, expansion, fusion and degradation. This procedure initiates with formation of the phagophore assembly site (PAS) then elongates the nucleation of phagophore. Further nucleation engulfs cytosolic proteins and organelles and enclose to form the double-membrane autophagosome in expansion step subsequently, the autolysosome derived from the fusion process between autophagosome and lysosome where contains lysosomal hydrolases to degrade sequestered contents.

Finally, macromolecules are returned to cytoplasm as a nutrient recycling (Figure 2.8). Whereas, microautophagy directly fuse with lysosome and chaperone-mediated autophagy requires heat shock cognate 70 kDa protein (HSC70) chaperone [28]. Distinction protein markers such as Beclin-1, LC3-I/II, SQSTM1/p62 are used as autophagy protein markers. Beclin-1 is recruits for phagophore elongation while LC3-II is converted form conjugation of LC3-I with phosphatidylethanolamine (PE) and p62 exists an autophagy substrate in degradation step [106]. Interestingly, these autophagy monitor proteins have been observed in NSCLC [107, 108].

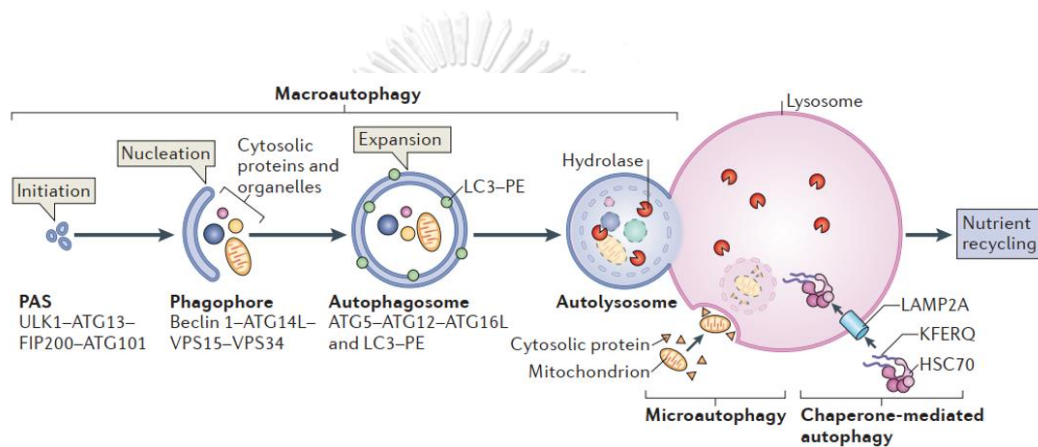


Figure 2.8 Machinery of autophagy pathway [28]

The role of autophagy in both cancer initiation and cancer therapy has been documented [109]. Some evidence suggest that autophagy regulated of many oncogenes and tumor suppressor genes [110, 111], whereas other studies reported that the promotion of tumorigenesis and the development and inhibition of cancer involved with autophagy phenomenon [112-115]. Indeed, inhibition of autophagy has been diminished cancer cell proliferation and increased sensitivity to cisplatin-induced apoptosis in non-small cell lung carcinoma [116]. Thus, alteration on autophagy level may be facilitate lung cancer treatment.

Role of autophagy in cancer stem cells (CSCs)

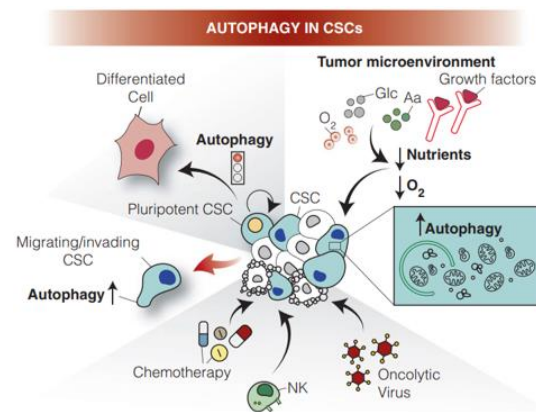


Figure 2.9 Responsibility of autophagy in CSCs [117]

Autophagy is one of the pivotal processes that strongly contributed to maintain stemness and aggressive behavior in CSCs [118]. Roles of autophagy in CSCs have been established. In comparison to adherent cells, tumor spheres displayed an elevation of autophagy level [119] which preserve pluripotency, promotes survival in bad situation of the tumor microenvironment due to hypoxia and limited nutrient conditions. Additionally, migration and invasion of CSCs were facilitated by autophagy along with chemotherapy resistant stimulant and evasion from innate immune cell (Figure 2.9) [117]. Experimental research illustrated the upregulation of autophagy facilitated chemotherapeutics resistance in CSCs via Akt signaling activation [31]. Therefore, inhibition of autophagy is a promising therapeutic approach for cancer treatment. Recently, treatment of CSCs with autophagy inhibition has been shown to increase the efficacy of cisplatin against non-small cell lung carcinoma [33]. However, recent study demonstrated that induction of autophagy contributed to suppress CSCs [120].

5. Apoptosis

Mode of cell death have been classified into three major types containing type apoptosis (type I), autophagy (type II) and necrosis (type III). These following parameters are used to differentiate each programmed cell death including the alteration of morphology, cell surface as well as intracellular marker and the effect to neighboring cells [121]. Apoptosis and autophagy can cause cell death with less damage to nearby tissue, unlike necrosis cell death which has inflammatory response to surrounding cells [122]. Two major apoptosis pathways are included, intrinsic mitochondria-mediated pathway and extrinsic death receptor-induced pathway [123]. During apoptosis, cell shrinkage, chromatin condensation, membrane blebbing, nuclear fragmentation and apoptotic body formation are presented. Subsequently, phagocytic cell removes these debris without destroy enclosing cells. This programmed cell death type I involved with maintenance homeostatic of cell populations during tissues development and aging. Furthermore, it also responds to immune defensive mechanism [124]. The role of apoptosis in disease has been established. Increment of apoptosis is involved in infertility, immunodeficiency, and acute and chronic degenerative diseases whereas excess apoptosis inhibition resulted in autoimmunity and cancer [123, 125]. Thus, stimulating apoptosis signaling pathway is highlighted in anti-cancer research.

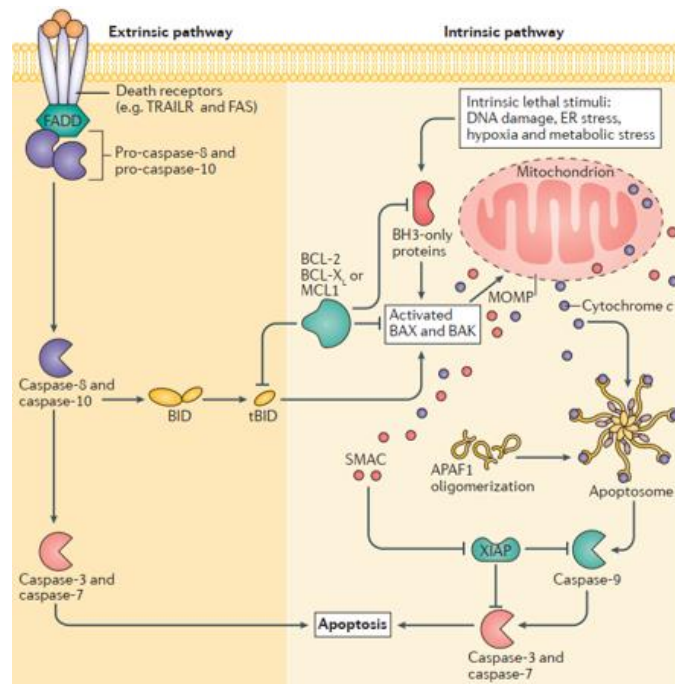


Figure 2.10 Machinery of intrinsic and extrinsic apoptosis pathway [126]

Intrinsic pathway

To respond to several lethal stimuli such as DNA damage, oxidative stress, toxins, and metabolic stress, the mitochondria-mediated apoptosis pathway activation is initiated [127]. Bcl-2 family proteins play a role in the regulation of the intrinsic pathway. The initiation of this process begins with the translocation of pro-apoptotic effector proteins, BAX (Bcl-2 associated X protein) and BAK (Bcl-2 homologous antagonist/killer) to the mitochondrial membrane, where their oligomerization is presented to alter mitochondrial outer membrane permeabilization (MOMP). Subsequently, cytochrome c is leaked into the cytosol and collaborates with Apaf-1 (apoptosis protease activating factor 1) to form the apoptosome, which activates caspase-9. Finally, active caspase-9 stimulates apoptosis cell death via triggering caspase-3 and caspase-7 enzymatic cascade. In addition, anti-apoptotic BCL-2 family proteins such as Bcl-2 (B-cell lymphoma 2), Bcl-XL (B-cell lymphoma-extra-large) and Mcl-1 (myeloid cell leukemia 1) can inhibit these processes (Figure 2.10) [126]. Noticeably, available chemotherapeutic drugs and natural compounds have been reported to trigger the intrinsic apoptosis pathway in various cancers. For example, cisplatin and actinomycin D

promotes lung cancer apoptosis through modulation of anti-apoptosis proteins, Bcl-2 and Mcl-1 [128, 129].

Extrinsic pathway

The extrinsic apoptosis pathway involves with the activation of caspases cascade via signaling form binding of their cognate ligand with death receptors such as tumor necrosis factor (TNF)-related apoptosis-inducing ligand (TRAIL) receptor (TRAILR) and FAS. After binding with death receptors at cell membrane surface, adaptor proteins such as FAS-associated death domain protein (FADD) mediate dimerization of initiator caspases (pro-caspase-8 and pro-caspase-10). Then the effector caspase-3 and caspase-7 are activated by active form of caspase-8 and caspase-10 leading to apoptosis (Figure 2.10) [126]. The tumor necrosis factor (TNF)-related apoptosis-inducing ligand (TRAIL) has been facilitated chemotherapeutic drug in sensitization apoptosis cell death through the expression of death receptor 5 (DR5) by combination treatment [130]. However, the suppression of death receptor stimulating apoptosis is mediated by an anti-apoptotic regulator, c-FLIP (cellular-FLICE inhibitory protein) which inhibits FADD-mediated caspase-8 activation [131]. Moreover, the involvement of c-FLIP overexpression with failure in cisplatin-induced apoptosis was reported [132].

One of CSC-characteristics is ability to conventional chemotherapeutic resistance [74]. Dysregulation of apoptosis were detected in CSCs which were contributed to drug resistance [133, 134]. Prior study indicated that increase expression of anti-apoptosis protein, Bcl-2 augmented chemoresistance ability and tumorigenicity *in vitro* and *in vivo* of lung CSCs [80]. Currently, the development of Bcl-2 inhibitors against CSCs have been proceeded in preclinical and clinical studies [127, 135, 136]. Beside the alteration of Bcl-2 affects apoptosis signaling, mutation of tumor suppressor protein, p53 is interested. Emerging evidence demonstrated that activation of self-renewal of cisplatin-resistant lung CSCs was provoked by p53 mutation [137]. In addition, mutant p53 proteins have been reported to be the cancer protectors [138]. Cellular functions were interfered leading to augmentation of cell survival and aberration of DNA repair machinery on account of p53 mutation [139]. Thus, regulation on Bcl-2 or p53 protein may provide benefit in cancer therapy. Interestingly, several

studies informed that p53 was regulated by nanog. This stemness transcription factor reduces expression of p53 in CSCs [16, 80, 140]. Recent study illustrated the potential of marine-derived natural compound in terms of induction of p53-dependent apoptosis and sensitizing cisplatin-mediated cell death in the lung cancer cells [141]. Hence, induction on apoptosis signaling in CSCs reveals a potential strategy to overcome CSCs.

6. Cisplatin

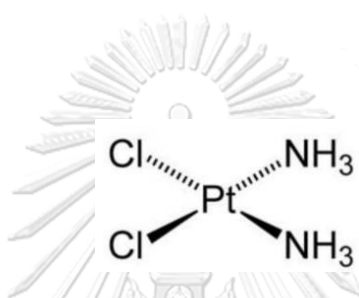


Figure 2.11 Chemical structure of cisplatin [142]

Chemotherapeutic is the first regimen for treatment advanced stage non-small cell lung cancer to increase survival rate, improve life quality and control of disease progression. Moreover, post-surgical chemotherapeutic is used to eliminate remaining cancer cells and relapse prevention [53]. Cisplatin or *cis*-diamminedichloroplatinum (II) (CDDP) is belonging of platinum-based chemotherapy agents which is a drug of choice in lung cancer treatment [142, 143]. Mechanism of this platinum-containing drug reportedly induced apoptosis cell death in cancer cells via interfering with DNA repair mechanisms by adducts with purine bases on the DNA. Intra-strand DNA adducts and inter-strand crosslinks are two major DNA injury approximately 90% and 5%, respectively (Figure 2.12) [144].

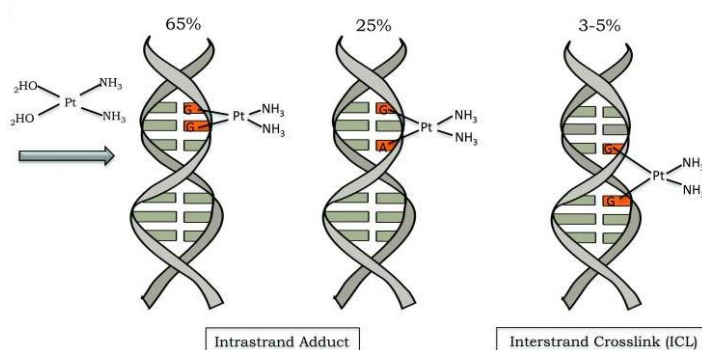


Figure 2.12 DNA damage induced by cisplatin [144]

Experimental evidence suggested that cisplatin induced apoptosis in non-small cell lung cancer via up-regulation of tumor suppressor p53 and pro-apoptosis protein, BAX [128]. While, overexpression of Mcl-1, anti-apoptosis protein facilitated cisplatin-resistant in non-small cell lung cancer cells [145]. In addition, Bcl-2 inhibitor has been reported as a potential utility for chemotherapeutic resistance [146]. Although cisplatin-based chemotherapy remains the first-line drug for lung cancer treatment, eventual therapeutic failure and selection of multidrug resistant CSC subpopulations are major issues [147-149].

7. Jorunnamycin A

Jorunnamycin A, a bistetrahydroisoquinolinequinone that has been extracted from Thai blue sponge *Xestospongia* sp. for this study, is also found in the Thai nudibranch *Jorunna funebris* [40]. This natural marine product is similar to ecteinascidin 743 [150] and to renieramycin M, with the key difference being the side chain at the C-22 position (Figure 2.13), as renieramycin M possesses an angeloyl ester while jorunnamycin A has an alcohol side chain instead. In the tetrahydroisoquinoline family, ecteinascidin 743 (ET-743, Yondelis™, Trabectedin) is the first marine anticancer drug which is approved in the European Union for the treatment of patients with soft tissue sarcoma [151]. Its mechanism of action has shown as DNA-interacting agent with covalent binding to the DNA minor groove resulting in block cell cycle progression, interference with cell division and inhibition of DNA repairing [152]. Renieramycin M has been previously reported to induce apoptosis through p53 activation subsequently

down-regulated anti-apoptotic Mcl-1 and Bcl-2 proteins in human non-small cell lung cancer cells [43]. Jorunnamycin A is the one of renieramycin M's derivatives which is prepared from renieramycin M with 45–54% yield through three-step procedure namely, hydrogenation, hydride reduction, and air oxidation. Different side chain at C-22 position leads to dissimilar effect. The hydroxyl group at this position of jorunnamycin A shows better activity on cancer cells than renieramycin M because IC_{50} of jorunnamycin A is lower than IC_{50} of renieramycin M evidenced with the lower IC_{50} of jorunnamycin A in both colon carcinoma and breast cancer cells compared renieramycin M [41]. Jorunnamycin A and renieramycin M derivatives have exhibited potent cytotoxicity against human lung cancer cells [42, 153, 154]. A recent study revealed the inhibitory effect of renieramycin M on CSC features of lung cancer cells; however, its regulatory mechanism has never been investigated [34]. Interestingly, jorunnamycin A was found to promote detachment-induced cell death and to inhibit epithelial-to-mesenchymal transition (EMT) and anchorage-independent growth in human lung cancers [45]. This study aimed to investigate the suppressive activity of jorunnamycin A on stem-like phenotypes of CSCs from human lung cancer cells and its underlying mechanisms. The findings may facilitate the development of this marine-derived compound as a novel chemotherapy for targeting CSCs in lung cancer treatment, which could also serve as an adjuvant that improves the current standard of care.

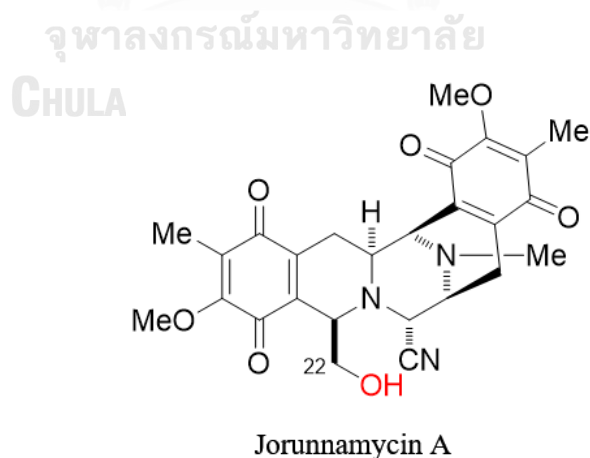


Figure 2.13 Chemical structure of jorunnamycin A. The hydroxyl group marked in red at C-22 ester side chain is the point of difference between jorunnamycin A and renieramycin M, another promising anticancer compound.

CHAPTER III MATERIALS AND METHODS

Materials

1. Chemicals and Reagents

Jorunnamycin A (JA) extracted from *Xestospongia* sp. was kindly provided by Asst. Prof. Supakarn Chamni, Ph.D., Department of Pharmacognosy and Pharmaceutical Botany, Faculty of Pharmaceutical Sciences, Chulalongkorn University. Reagents for cell culture including Roswell Park Memorial Institute (RPMI) 1640 medium, Modified Eagle Medium (DMEM), fetal bovine serum (FBS), phosphate buffered saline (PBS); pH 7.4, 0.25% trypsin contains 0.53 mM EDTA, L-glutamine and penicillin/streptomycin solution were obtained from Gibco (Gaithersburg, MA, USA). Chemical reagents including cisplatin, Hoechst33342, propidium iodide (PI), 2,7-dichlorouorescein diacetate (DCFH₂-DA) and N-acetylcysteine (NAC), ethylenediaminetetraacetic acid (EDTA), crystal violet solution (1% w/v), and formaldehyde solution (37% w/v) were purchased from Sigma Chemical, Inc. (St. Louis, MO, USA). Dimethyl sulfoxide (DMSO) and bovine serum albumin (BSA) were obtained from EMD Millipore corporation (Billerica, MA, USA). Annexin V/FITC-conjugated apoptosis detection kit and 3-(4,5-dimethylthiazol-2-yl)-2,5-diphenyltetrazolium bromide (MTT) were respectively procured from ImmunoTools (Friesoythe, Lower Saxony, Germany) and Life Technologies (Eugene, OR, USA). Primary antibody of Nanog, Oct4, Sox2, β -catenin, Akt, p-Akt (Ser473), GSK-3 β , p-GSK-3 β (Ser9), Bcl-2, Mcl-1, BAX, p-53, GAPDH, peroxidase-labeled specific secondary antibodies and Alexa Fluor 488-conjugated secondary antibody were obtained from Cell Signaling Technology, Inc. (Denver, MA, USA). CD133 specific antibody for stem cell protein marker was provided by US Biological life sciences (Salem, MA, USA). Pierce™ Bicinchoninic acid (BCA) protein assay kit and SuperSignal™ West Pico PLUS Chemiluminescent Substrate sourced from Thermo Scientific (Rockford, IL, USA).

2. Cell culture

Human lung cancer cells (H460, H23 and A549) and human lung epithelial BEAS-2B cells were obtained from the American Type Culture Collection (ATCC, Manassas, VA, USA). RPMI 1640 medium supplemented with 2 mmol/L L-glutamine, 10% (v/v) FBS

and 100 units/mL of penicillin/streptomycin was used for the culture of H460 and H23 cells. Meanwhile A549 cells and BEAS-2B cells were cultured in DMEM contained with 2 mmol/L L-glutamine, 10% (v/v) FBS and 100 units/mL of penicillin/streptomycin. All cells were maintained in an incubator supplied with 5% CO₂ at 37°C until reaching approximately 80 to 90% confluence before further use in experiments.

Methods

1. Preparation for jorunnamycin A (JA)

For culture with lung cancer cells, jorunnamycin A was primarily dissolved in DMSO then diluted to desired concentrations in culture medium. The final concentration of DMSO in culture medium was less than 0.5% (v/v).

2. Determination of Half-Maximal Inhibitory Concentration on Cell Viability (IC₅₀) and Growth (IG₅₀)

Cell viability was evaluated by MTT assay, which measures cellular capacity to reduce 3-(4,5-dimethylthiazol-2-yl)-2,5-diphenyltetrazolium bromide to purple formazan crystal by mitochondria dehydrogenase enzymes. After treatment with jorunnamycin A for 24 h, the cells, which were seeded at a density of 1 × 10⁴ cells/well in a 96-well plate, were then incubated with 0.4 mg/mL of MTT solution for 4 h at 37°C away from light. MTT solution was then discarded and DMSO was added to dissolve the purple formazan crystals. The absorbance was determined by a microplate reader (Perkin Elmer, Waltham, MA, USA) at 570 nm. Percentage cell viability, which was calculated from the absorbance ratio of treatment to non-treated control cells, was used for determination of half-maximal inhibitory concentration (IC₅₀).

$$\text{Cell viability (\%)} = \frac{A570_{\text{treatment}}}{A570_{\text{control}}} \times 100$$

Antiproliferative effect of jorunnamycin A was assessed through crystal violet assay. Cells were seeded at a density of 2 × 10³ cells/well in a 96-well plate and

treated with nontoxic concentrations (0–0.5 μM) of jorunnamycin A for 72 h. At the indicated time point, the cells were washed with deionized water and fixed with 1% (w/v) formaldehyde for 30 min. Then, they were immersed in 0.05% (w/v) crystal violet solution for 30 min. After washing twice with deionized water and left air-dried, methanol (200 μL /well) was added to dissolve the crystal violet-stained biomass. The optical density (OD) was measured at 570 nm using a microplate reader (Perkin Elmer, Waltham, MA, USA). Percentage growth inhibition, which was represented after subtracting with OD of untreated control cells, was used for determination of half-maximal growth inhibitory concentration (IG_{50}).

$$\text{Growth inhibition (\%)} = \frac{A570_{\text{control}} - A570_{\text{treatment}}}{A570_{\text{control}}} \times 100$$

3. Nuclear staining assay

Mode of cell death was detected via nuclear staining assay of Hoechst33342 and propidium iodide (PI). After incubation with specific treatment, cells were costained with 10 μM of the Hoechst33342 and 5 $\mu\text{g}/\text{mL}$ PI for 30 min at 37°C. The observation under fluorescence microscope (Olympus IX51 with DP70, Olympus, Japan) demonstrates apoptosis cells stained with bright blue fluorescence of Hoechst33342 which presented chromatin condensation and/or fragmented nuclei. Meanwhile PI positive necrosis cells were visualized as red fluorescence.

4. Limiting dilution assay

Limiting dilution assay (LDA) is used to measure the frequency of tumor initiating cells in cancer population [76]. Human lung cancer cells were seeded into a 96-well ultralow attachment plate in the gradually decreasing numbers from 200 to 1 cells/well in 200 μL of culture medium containing 1% (v/v) FBS with or without jorunnamycin A at nontoxic concentrations. After 14 days, the morphology and number of forming cancer colonies were observed under an inverted microscope (Nikon Ts2, Nikon, Japan).

5. Single three-dimensional (3D) spheroid formation

The enrichment of CSC subpopulation in cancer cells was successfully performed through three-dimensional (3D) spheroid formation [77]. Briefly, human lung cancer cells (2.5×10^3 cells/well) were maintained in culture medium supplemented with 1% (v/v) FBS under anchorage-independent condition in 24-well ultralow attachment plate. After 7 days, the obtained primary CSC-enriched spheroids were resuspended into single cell using 1 mM EDTA and seeded again into a 24-well ultralow attached plate (2.5×10^3 cells/well). Secondary CSC-enriched spheroids were cultured for another 14 days before performing further experiments.

To determine the inhibitory effect on self-renewal [155], a single secondary CSC-enriched spheroid was isolated and treated with jorunnamycin A (0-0.5 μ M). The alteration of spheroids after 0-7 days of jorunnamycin A treatment was observed under an inverted microscope (Nikon Ts2, Nikon, Japan) and presented as a relative value to spheroid size at day 0.

6. Determination of CD133-overexpressing cells in CSC-enriched spheroids via flow cytometry

Expression of CD133, a lung cancer stem cell marker, was evaluated by flow cytometry. After treatment for 3 days, jorunnamycin A-treated CSC-enriched secondary spheroids were collected and prepared into single cell suspension in PBS, pH 7.4. The cells were incubated with 0.5% (w/v) BSA in PBS for 30 min at 4°C before probing with anti-CD133 antibody (US Biological life sciences, Salem, MA, USA: Cat no. 521102; Dilution 1:200) for 1 h at 4°C. After washing the cell pellets with PBS, Alexa Fluor 488-conjugated secondary antibody (Cell Signaling Technology, Inc., Denver, MA, USA: Cat no. #4412S; Dilution 1:1,000) was added and incubated for 30 min at 4°C protected from light. Fluorescence intensity was determined by flow cytometry (EMD Millipore, Billerica, MA, USA) using a 488 nm excitation beam and detection wavelength at 519 nm. Mean fluorescence intensity was quantified by guavaSoft version 3.2 software (EMD Millipore, Billerica, MA, USA).

7. Flow cytometry analysis of annexin V-FITC/PI

Quantification of cell death in CSC-enriched spheroids was determined via flow cytometry analysis of annexin V-FITC/PI. After indicated treatment, CSC-enriched

secondary spheroids were collected and prepared into a single cell suspension in PBS, pH 7.4. Annexin V-FITC/PI staining was performed according to the manufacturer's instructions. Briefly, cell pellets were collected and resuspended in 90 μ L of binding buffer. The cell suspensions were stained with 5 μ L of annexin V-FITC (1 μ g/mL) and 5 μ L of PI (2.5 μ g/mL) for 20 min in the dark place. After adding of 400 μ L of binding buffer, the cell samples were placed on ice for immediate analysis via a Guava easyCyte™ 5HT benchtop flow cytometer (EMD Millipore, Billerica, MA, USA) using guavaSoft version 3.2 software.

8. Reverse transcription quantitative real-time PCR (RT-qPCR)

Total mRNA was extracted from jorunnamycin A-treated CSC-enriched spheroids by using RevertAid First Strand cDNA Synthesis Kit (Thermo Scientific, Madison, WI, USA) according to the supplier's protocol. Quantification of obtained cDNA was conducted by Thermo Scientific NanoDrop One microvolume UV-Vis Spectrophotometers (Thermo Scientific, Madison, WI, USA) at 260 nm. Primers specific to Nanog, Oct-4, Sox2 and glyceraldehyde-3phosphate dehydrogenase (GAPDH) were as follows:

Nanog Forward: 5'-ACCAGTCCCAAAGGCAAACA-3'

Reverse: 5'-TCTGCTGGAGGCTGAGGTAT-3'

Oct-4 Forward: 5'-AAGCGATCAAGCAGCGACTA-3'

Reverse: 5'-GAGACAGGGGGAAAGGCTTC-3'

Sox2 Forward: 5'-ACATGAACGGCTGGAGCAA-3'

Reverse: 5'-GTAGGACATGCTGTAGGTGGG-3'

GAPDH Forward: 5'-GACCACAGTCCATGCCATCA-3'

Reverse: 5'-CCGTTCAGCTCAGGGATGAC-3'

Expression levels of transcription factor genes (Nanog, Oct-4 and Sox2) and housekeeping gene (GAPDH) in the CSC-enriched spheroids were analyzed by RT-qPCR using the CFX 96 Real-time PCR system (Bio-Rad, Hercules, CA, USA). One-step RT-qPCR reaction was carried using 50 ng of total cDNA using Luna Universal qPCR Master Mix

(Bio-Rad, Hercules, CA, USA) with final volume of 20 μ L per reaction. The initial denaturation step was performed at 95°C for 3 min, followed by 40 cycles of denaturation at 95°C for 5 sec and primer annealing at 57°C for 30 sec. The relative mRNA expression levels of the target genes were calculated using the comparative C_q values. The PCR products were normalized with the GAPDH gene as an internal control.

9. Western blot analysis

After treatment, CSC-enriched H460 spheroids were harvested and incubated in a RIPA lysis buffer (Merck, DM, Germany) containing 20 mM Tris-HCl (pH 7.5), 150 mM sodium chloride, 1 mM disodium EDTA, 1 mM EGTA, 1% NP-40, 1% sodium deoxycholate, 2.5 mM sodium pyrophosphate, 1 mM β -glycerophosphate, 1 mM sodium orthovanadate, 1 μ g/mL leupeptin and protease inhibitor cocktail (Sigma-Aldrich, St. Louis, MO, USA) for 40 min at 4°C. The cell lysates were centrifuged at 12,000 rpm (4°C) for 15 min, then the supernatants were collected. Total protein contents were determined using BCA protein assay kit. An equal amount of protein of each sample was denatured by heating at 95°C for 5 min with sample loading buffer and subsequently loaded onto a 10% SDS-PAGE. After separation, proteins were transferred onto 0.45 μ M nitrocellulose membranes (Bio-Rad, Hercules, CA, USA). The transferred membranes were blocked for 1 h in 5% nonfat dry milk in TBST (25 mM Tris-HCl pH 7.5, 125 mM NaCl, and 0.05% Tween 20) and incubated with the appropriate primary antibodies at 4°C overnight. Then, the membranes were washed with TBST (5 min \times 3 times) and incubated with horseradish peroxidase-labeled isotype-specific secondary antibodies for 2 h at room temperature. Primary antibody of SQSTM1/p62 (Cat no. #8025; Dilution 1:1000), Beclin-1 (Cat no. #3495; Dilution 1:1000), LC3-I/II (Cat no. #12741; Dilution 1:1000), Oct-4 (Cat no. #2750S; Dilution 1:1000), Sox2 (Cat no. #3579S; Dilution 1:1000), Nanog (Cat no. #4903S; Dilution 1:2000), β -catenin (Cat no. #8480S; Dilution 1:1000), Akt (Cat no. #4691S; Dilution 1:1000), p-Akt (Ser473, Cat no. #4060S; Dilution 1:2000), GSK-3 β (Cat no. #12456S; Dilution 1:1000), p-GSK-3 β (Ser9, Cat no. #5558S; Dilution 1:1000), p53 (Cat no. #2527; Dilution 1:1000), Mcl-1 (Cat no. #94296S; Dilution 1:1000), Bcl-2 (Cat no. #4223S; Dilution 1:1000), BAX (Cat no. #5023S; Dilution 1:1000), GAPDH (Cat no. #5174S; Dilution 1:1000), and peroxidase-labeled specific secondary antibodies (Cat no. #7074S; Dilution 1:2000) for

Western blot analysis were purchased from Cell Signaling Technology, Inc. (Denver, MA, USA). The immune complexes were detected by enhancement with chemiluminescence substrate and quantified by analyst/PC densitometric software (Bio-Rad, Hercules, CA, USA).

10. Drug sensitivity assay

Drug sensitivity assay was evaluated by pretreatment of lung cancer H460 cells with noncytotoxic concentration of jorunnamycin A prior to expose with cisplatin. Briefly, H460 cells were placed in 96-well plate at density of 1×10^4 cells/well overnight and were treated with jorunnamycin A at 0.5 μM for 24 h. Then, the pretreated cells were exposed with 25 μM cisplatin and further incubate at 37°C for 24 h. Cell viability and mode of cell death were determined by MTT colorimetric assay and nuclear staining assay, respectively.

11. Statistical analysis

All data were presented as means \pm standard deviation (SD) from three independent experiments. The differences among the groups were evaluated by one-way analysis of variance (ANOVA), followed by Tukey HSD post-hoc test using SPSS version 22 (IBM Corp., Armonk, NY, USA). Statistical significance was defined as $p < 0.05$ for all tests.

Conceptual framework

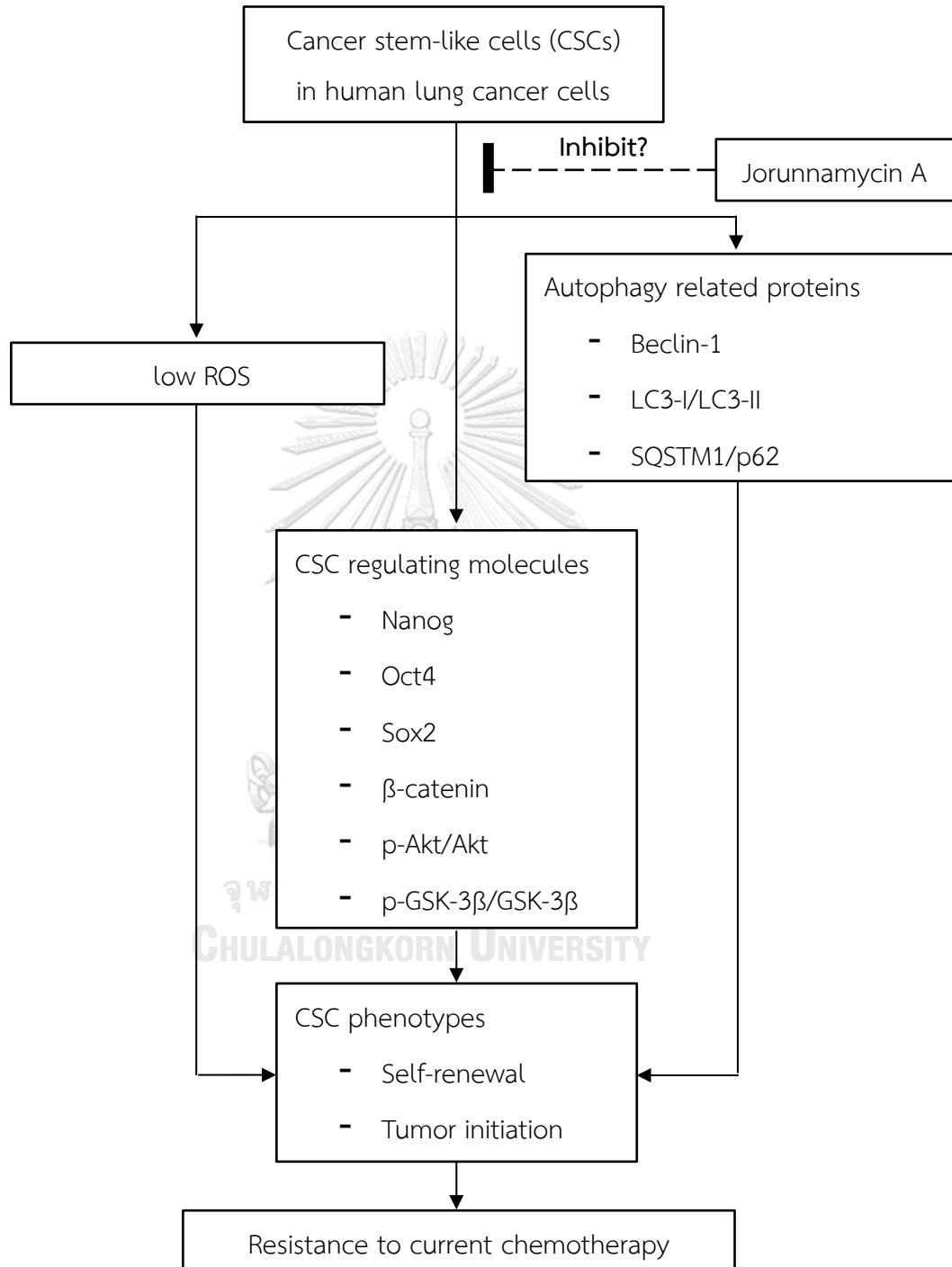


Figure 3.1 Conceptual framework

Experimental design

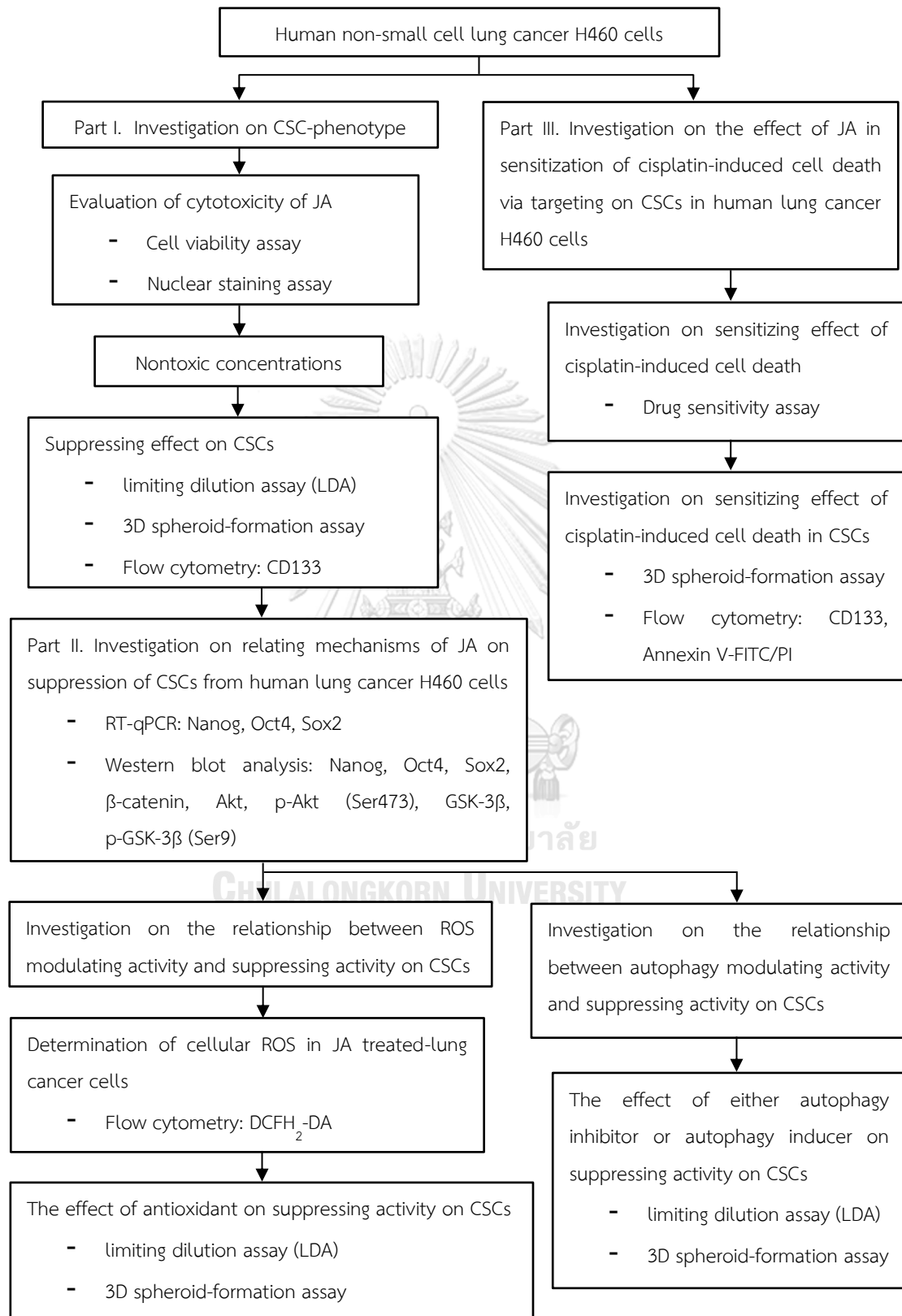


Figure 3.2 Experimental Design

Experimental Design

1. Investigation on the effect of jorunnamycin A on CSC phenotype in human lung cancer H460 cells

1.1 Investigation on cytotoxicity of jorunnamycin A in human lung cancer cells

The cytotoxic effects of jorunnamycin A (0-5 μM for 24 h) in human lung cancer H460 cells in attachment condition was firstly characterized. Cell viability and mode of cell death were determined by MTT colorimetric assay and nuclear staining assay, respectively. Apoptosis induction was scored by the cells with bright blue fluorescence of Hoechst33342. Non-toxic concentrations of jorunnamycin A which cause no significant effect on cell viability at 24 h were used in further experiments.

1.2 Investigation on suppressing effect of jorunnamycin A on CSCs in human lung cancer cells

The effect of jorunnamycin A on CSCs in lung cancer cells was evaluated through single three-dimensional (3D) spheroid-formation assay. Flow cytometry was performed to determine the alteration of CD133, a cell-surface protein marker in secondary spheroid of H460 lung cancer cells treated with jorunnamycin A (0.1-0.5 μM) for 3 days. Furthermore, the frequency of tumor-initiating cells in cancer population cultured with 0.05-0.5 μM jorunnamycin A was determined by limiting dilution assay (LDA). Numbers of formed colonies in jorunnamycin A-treated cells were counted and compared to untreated control. The experiments on suppressive effect of jorunnamycin A on CSCs were also carried out in lung cancer H23 and A549 cells to confirm the effect of jorunnamycin A on other lung cancer cells. On the other hand, the safety profile of jorunnamycin A on stemness features of normal lung stem cells was clarified in human lung epithelial BEAS-2B cells.

2. Investigation on relating mechanisms of jorunnamycin A on suppression of CSCs from human lung cancer cells

Reverse transcription quantitative real-time PCR (RT-qPCR) was used to detect the expression levels of transcription factor genes (Nanog, Oct-4 and Sox2) and housekeeping gene (GAPDH) in jorunnamycin A treated-CSC enriched spheroids at non-toxic concentration for 24 h. Western blot analysis was performed to evaluate the level of key proteins in upstream signaling pathway including β -catenin, Akt, p-Akt (Ser473), GSK-3 β and p-GSK-3 β (Ser9). The investigation on relating mechanisms of jorunnamycin A were also carried out in CSCs from human lung cancer H23 and A549 cells.

3. Investigation on the relationship between ROS modulating activity and CSC suppressive effect of jorunnamycin A in H460 lung cancer cells

The modulation on cellular ROS level was evaluated in lung cancer cells incubated with jorunnamycin A at non-toxic concentrations for 0 – 9 h by flow cytometry using fluorescence probe, DCFH₂-DA. To evaluate the relationship between ROS modulating activity and CSC suppressive effect of jorunnamycin A in lung cancer H460 cells, secondary CSC-enriched spheroids were pretreated with antioxidant (N-acetyl cysteine) for 30 minutes before exposed with 0.5 μ M jorunnamycin A, then size of spheroid formation was observed by inverted microscope at day 0-7. Furthermore, LDA assay was also performed in jorunnamycin A cultured-H460 cells pretreated with N-acetyl cysteine.

4. The effect of autophagy modulated by jorunnamycin A on CSC phenotype in lung cancer H460 cells

The effect of jorunnamycin A on mediating autophagy in CSC population was investigated through single three-dimensional (3D) spheroid formation assay and LDA assay. CSC-enriched lung cancer cells were incubated either autophagy inhibitor (0.5 μ M wortmannin) or autophagy inducer (100 nM rapamycin) for 30 minutes prior treatment with 0.5 μ M jorunnamycin A for 24 h, then size of spheroid formation was detected by inverted microscope at day 0-7. The frequency of tumor initiating-cells in cancer population was evaluated

by LDA assay in jorunnamycin A cultured-H460 cells pretreated either with autophagy inhibitor or autophagy inducer.

5. Investigation on the effect of jorunnamycin A in sensitization of cisplatin-induced cell death via targeting on CSCs in human lung cancer H460 cells

5.1 Investigation on drug sensitizing activity of jorunnamycin A in cisplatin-induced cell death in human lung cancer H460 cells

The effect of jorunnamycin A on susceptibility of human lung cancer H460 cells to chemotherapeutic agent was evaluated by drug sensitivity assay in human lung cancer H460 cells.

5.2 Investigation on the effect of jorunnamycin A on CSC suppression in cisplatin-treated human lung cancer H460 cells

To investigate whether drug sensitizing effect of jorunnamycin A mediates through CSC suppression, H460 cells were subjected to the single three-dimensional (3D) spheroid formation assay then were pretreated with 0.5 μM jorunnamycin A for 24 following with 25 μM cisplatin. The alteration of spheroids after 0-7 days of the indicated treatment was observed under an inverted microscope.

Secondary CSC-enriched spheroids were treated with 0.5 μM jorunnamycin A for 24 h prior treatment with 25 μM cisplatin for 72 h. The reduction of %CD133^{high} population and alteration on apoptosis induction of CSC-enriched spheroids treated with jorunnamycin A and cisplatin were determined by flow cytometry analysis of CD133-overexpressing cells and annexin V-FITC/PI, respectively. The underlying mechanisms involved in the chemosensitizing activity of jorunnamycin A in CSCs of human lung cancer cells were performed by western blot analysis.

CHAPTER IV RESULTS

1. Cytotoxicity of jorunnamycin A in H460 human lung cancer cells

1.1 Effect of JA on viability of human lung cancer H460 cells

To evaluate the effect on CSCs, cytotoxic profile of jorunnamycin A in human lung cancer cells was first determined through MTT viability assay. After treatment for 24 h, jorunnamycin A at 1-5 μM decreased viability in lung cancer H460 cells, while there was no significant alteration of %cell viability at lower concentrations of 0.05-0.5 μM (Figure 4.1A). Costaining of Hoechst33342 and propidium iodide (PI) revealed apoptosis with no necrosis in H460 cells incubated with 1-5 μM jorunnamycin A for 24 h (Figure 4.1C). However, the augmentation of %apoptosis was not significantly noted in the cells treated with 0.05-0.5 μM jorunnamycin A compared with non-treated control cells (Figure 4.1B). Therefore, jorunnamycin A at nontoxic concentration range between 0.05-0.5 μM was chosen for further investigations.

Antiproliferative effect of jorunnamycin A in human lung cancer cells was additionally examined. Treatment with jorunnamycin A at 0.1-0.5 μM for 72 h significantly reduced proliferation in lung cancer H460 cells compared with untreated control cells (Figure 4.1D). Notably, the reduction of %cell proliferation was promptly observed in the cells treated with 0.5 μM jorunnamycin A for 48 h.

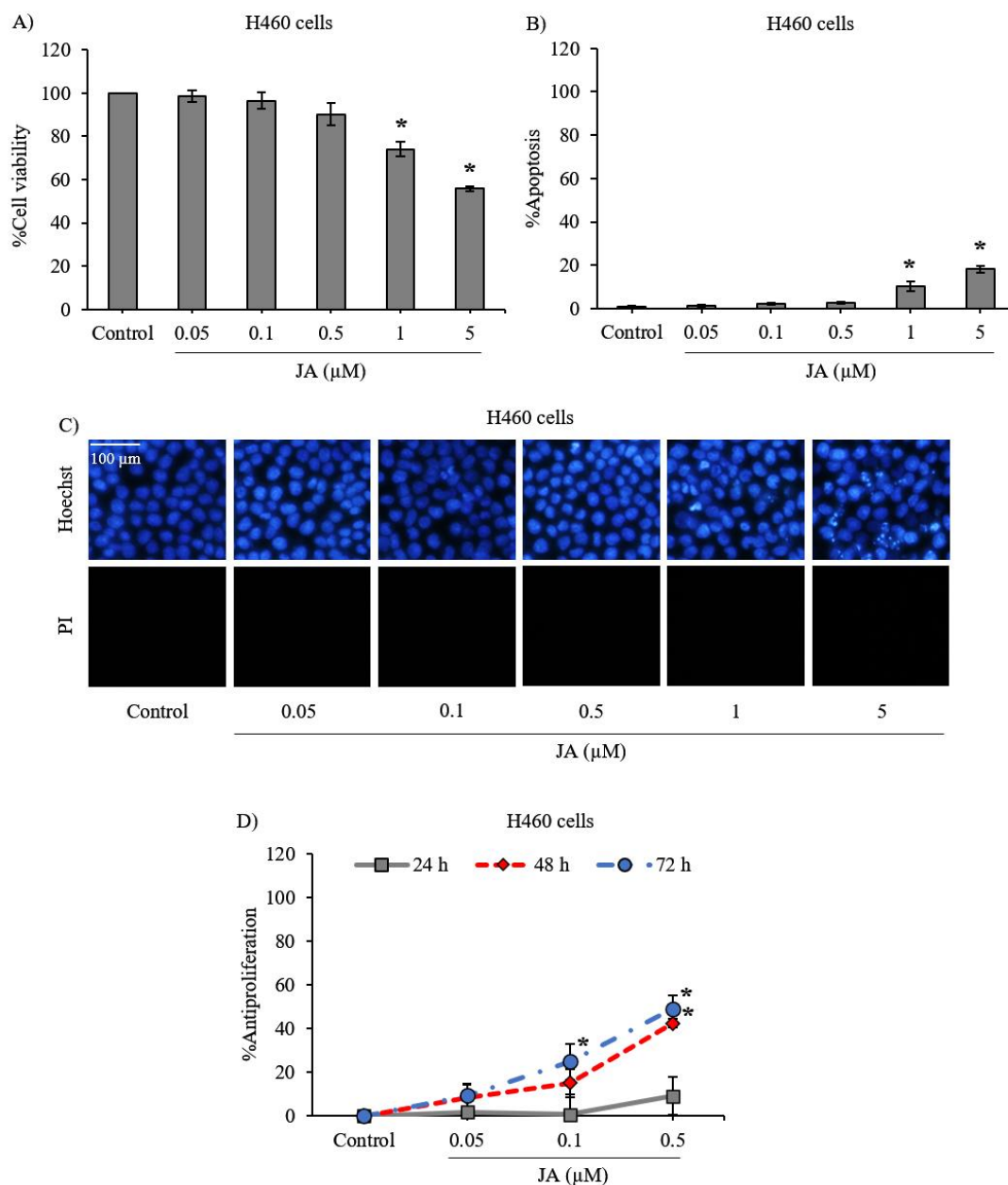


Figure 4.1 Cytotoxicity of jorunnamycin A in human lung cancer H460 cells. (A) MTT assay revealed the significant reduction of cell viability in lung cancer H460 cells after treatment with 1-5 μM of jorunnamycin A (JA) for 24 h. (B) The augmentation of %apoptosis was shown in H460 cells treated with 1 and 5 μM of JA. (C) Costaining with Hoechst33342/propidium iodide (PI) demonstrated that no necrosis cell death was detected in H460 cells at all treatment concentrations of JA for 24 h. (D) The antiproliferative effect of JA treatment (0.1-0.5 μM) in human lung cancer H460 cells revealed the significant inhibition at 72 h time point. The %apoptosis (B) was analyzed

in H460 cells co-stained with Hoechst33342/PI (C). Data represent means \pm SD of three independent experiments. * $p < 0.05$ versus non-treated control.

1.2 Jorunnamycin A diminishes cancer spheroid-initiating cells in lung cancer H460 cells

As H460 has been reported to not only being composed of a high number of CSCs but also having aggressive self-renewal property and in vivo tumorigenicity [19, 78, 79, 156], the effect of jorunnamycin A targeting on the CSC subpopulation was primarily evaluated in human lung cancer H460 cells. To clarify the inhibitory effect of jorunnamycin A on CSCs, a limiting dilution assay (LDA) was used to quantify the frequency of tumor-initiating cells in cancer populations. After culture for 14 days under detachment condition and deprivation of nutrients and growth factors in LDA, the formation of cancer spheroids mostly resulted from CSCs that possessed aggressive features and tumor-initiating activity [157]. As demonstrated in Figure 4.2A, the formation of cancer spheroids in LDA at day 14 was evident in human lung cancer H460 cells. It should be noted that H460 cells at different cell densities (1–200 cells/well in ultra-low attachment 96 well-plate) strongly showed spheroid-forming activity, which suggests the CSC phenotype. Intriguingly, jorunnamycin A at nontoxic concentrations (0.05–0.5 μM) significantly diminished colony formation in H460 cells at all cell densities used. To confirm anticancer activity, cisplatin, a recommended chemotherapy agent for lung cancer treatment, was used at toxic concentration as a positive control in this study. Both jorunnamycin A (0.5 μM) and cisplatin (25 μM) comparably reduced colony number in lung cancer H460 cells (Figure 4.2B). These results suggest that jorunnamycin A could diminish the frequency of cancer spheroid-initiating cells in the CSC subpopulation of human lung cancer cells.

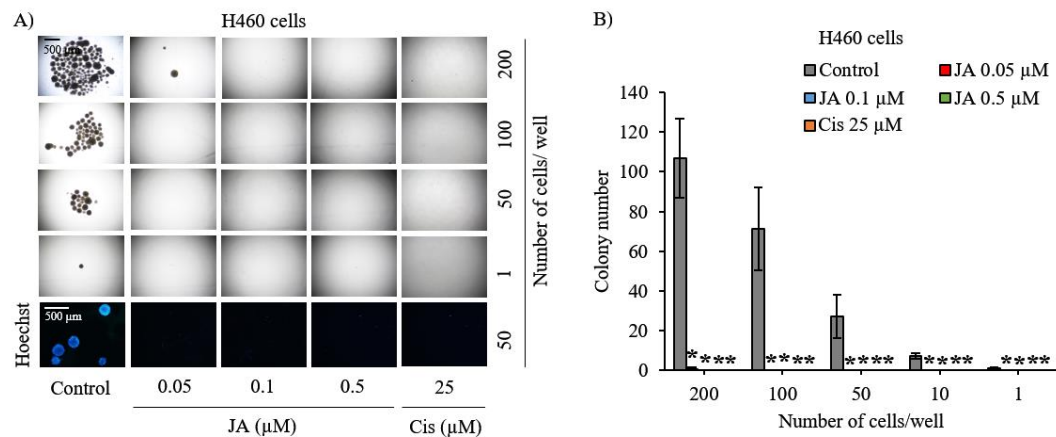


Figure 4.2 The inhibitory effect of jorunnamycin A on CSCs of lung cancer H460 cells. (A) Jorunnamycin A (JA) at 0.05–0.5 μM inhibited cancer spheroid-initiating capability of human lung cancer H460 cells, as evidenced by the suppression of cancer colony generation in the limiting dilution assay (LDA). At day 14 of treatment, spheroid images were captured by optical microscopy (4 \times), while bright blue fluorescence of Hoechst33342 was taken by fluorescence microscopy (10 \times). (B) The number of forming colonies at all cell densities was decreased in all nontoxic concentrations (0.05–0.5 μM) of JA. Cisplatin (Cis) at 25 μM was used as a positive control. The colony number (B) was analyzed in cancer colonies (A). Data represent means \pm SD of three independent experiments. * $p < 0.05$ versus non-treated control.

1.3 Suppressive effect of jorunnamycin A in CSC-enriched lung cancer cells

Successful assays for determining treatment effects on H460 CSCs involve with the enrichment of the CSC subpopulation and investigation of the stemness traits of self-renewal and differentiation in CSC-enriched spheroids cultured under detachment condition [78]. The formation of CSC-enriched spheroids derived from lung cancer H460 cells was assessed after culture with 0–0.5 μM jorunnamycin A from days 0–7. Figure 4.3A depicts the anchorage-independent growth of CSC-enriched H460 spheroids after culture for 7 days. Although the incubation with either jorunnamycin A (0.05–0.5 μM) or cisplatin (25 μM) obviously suppressed the enlargement of CSC spheroids, no apoptosis was visibly revealed in Hoechst33342 staining. Importantly, the relative

spheroid size was significantly reduced in jorunnamycin A-treated CSC spheroids in time- and dose-dependent manner (Figure 4.3B).

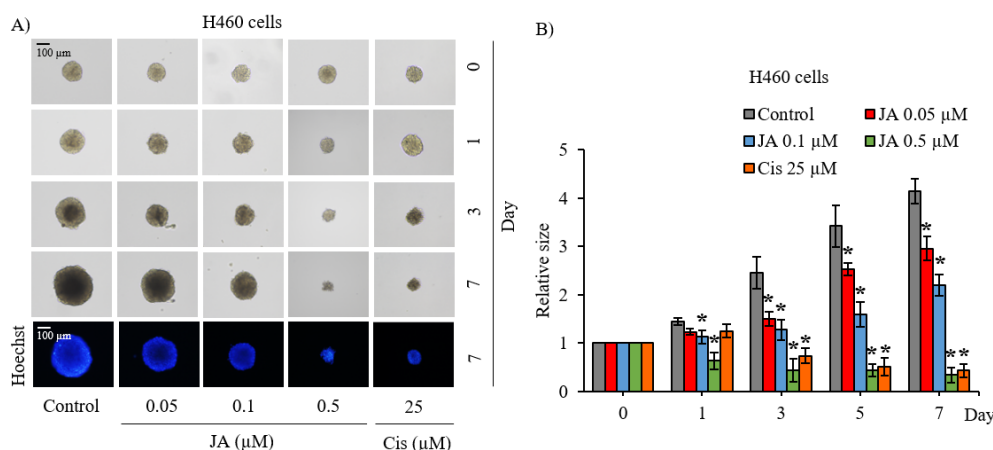


Figure 4.3 The suppressing effect of jorunnamycin A on CSCs of H460 lung cancer cells. (A) Suppressive effect of Jorunnamycin A (JA) in CSC-enriched lung cancer cells was evaluated by single 3D CSC spheroid formation. At day 7 of treatment, all single 3D CSCs were visualized by optical microscopy (10×) and images reflecting the bright blue fluorescence of Hoechst33342 were taken by fluorescence microscopy (10×). (B) JA exhibited a significant reduction of relative size of CSC-enriched spheroid from days 1 – 7. The relative size (B) was analyzed in CSC-enriched spheroids (A). Data represent means ± SD of three independent experiments. * $p < 0.05$ versus non-treated control.

As CD133 is a selective marker for lung CSCs [149], the detection of CD133 in CSC-enriched H460 spheroids was performed to further assess the self-renewal trait. Thus, the alteration of the CD133^{low} and CD133^{high} subpopulations in CSC-enriched spheroids after 3 days treatment was evaluated via flow cytometry, and the results are presented in dot plots (Figure 4.4A). Figure 4.4B reveals that approximately 80% of the cells containing H460 spheroids were CD133-overexpressing cells, which confirms the CSC-enrichment of spheroids. Both jorunnamycin A (0.1–0.5 μM) and cisplatin (25 μM) treatment significantly decreased the CD133^{high} population compared with the

untreated CSC spheroids. The treatments also evidently increased the %CD133low population in CSC-enriched H460 spheroids.

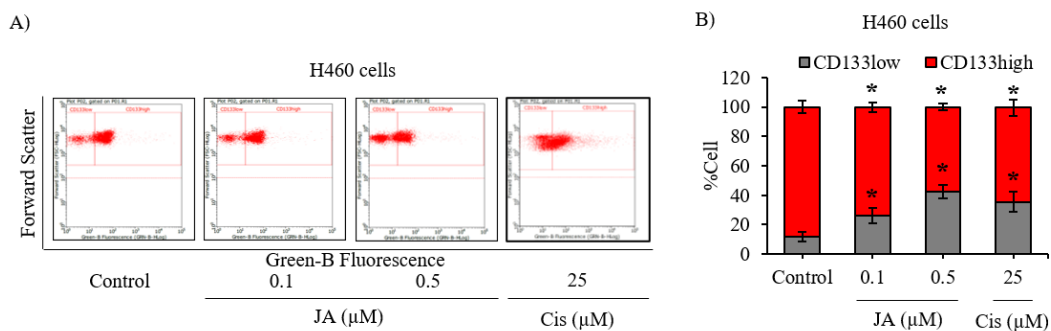


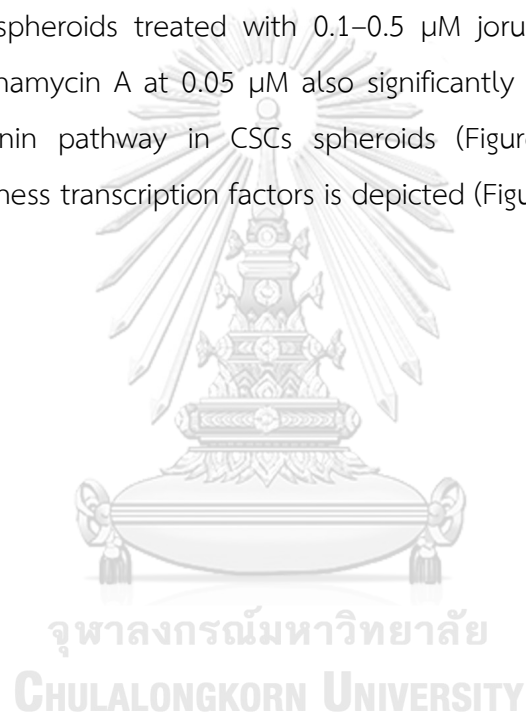
Figure 4.4 Jorunnamycin A restrained CD133-overexpressing cells in CSCs of H460 lung cancer cells. (A) Flow cytometry analysis of CD133 expression confirmed the alteration of CD133high population after treatment with JA (0.1–0.5 μM) for 3 days. (B) The proportion of CD133high cells in JA-treated population was lower compared with non-treated control. Cisplatin (Cis) at 25 μM was used as a positive control. The %cell demonstrated in (B) was calculated from dot plots presented in (A). Data represent means \pm SD of three independent experiments. * $p < 0.05$ versus non-treated control.

1.4 Jorunnamycin A downregulates stemness transcription factors and related proteins in CSC-enriched spheroids

The modulation on transcription factors involved in the stemness phenotype was further elucidated in the CSC-enriched lung cancer cells cultured with jorunnamycin A. The mRNA level of Nanog, Oct-4, and Sox2 determined by reverse transcription quantitative real-time PCR (RT-qPCR) is indicated in Figure 4.5A. Jorunnamycin A at 0.1–0.5 μM dramatically downregulated mRNA level of Nanog, Oct-4, and Sox2 in CSC H460 spheroids promptly at 24 h of treatment. The dose-dependent decrease in the protein level of Nanog and Oct-4 detected via Western blot analysis was also observed in the CSC-enriched spheroids cultured with jorunnamycin A for 24 h (Figure 4.5B). However, the significant reduction of Sox2 protein level was only observed in CSC H460 spheroids in response to treatment with 0.5 μM jorunnamycin

A (Figure 4.5C). It is worth noting that the alteration of these stemness transcription factors correlated with the lower relative spheroid size observed at day 1 after jorunnamycin A treatment, compared with the nontreated control.

Because the PI3K/Akt/ β -catenin pathway has been reported to be an up-stream signal regulating CSC phenotype [91], CSC-enriched H460 spheroids were treated with jorunnamycin A (0–0.5 μ M) for 24 h to evaluate the expression level of p-Akt, Akt, p-GSK-3 β , GSK-3 β , and β -catenin by Western blotting. The reduced level of p-Akt/Akt coinciding with the downregulation of p-GSK-3 β /GSK-3 β and β -catenin was clearly observed in the spheroids treated with 0.1–0.5 μ M jorunnamycin A (Figure 4.5D). Surprisingly, jorunnamycin A at 0.05 μ M also significantly decreased signaling in the Akt/GSK-3 β / β -catenin pathway in CSCs spheroids (Figure 4.5E), though a minor alteration of stemness transcription factors is depicted (Figure 4.5A).



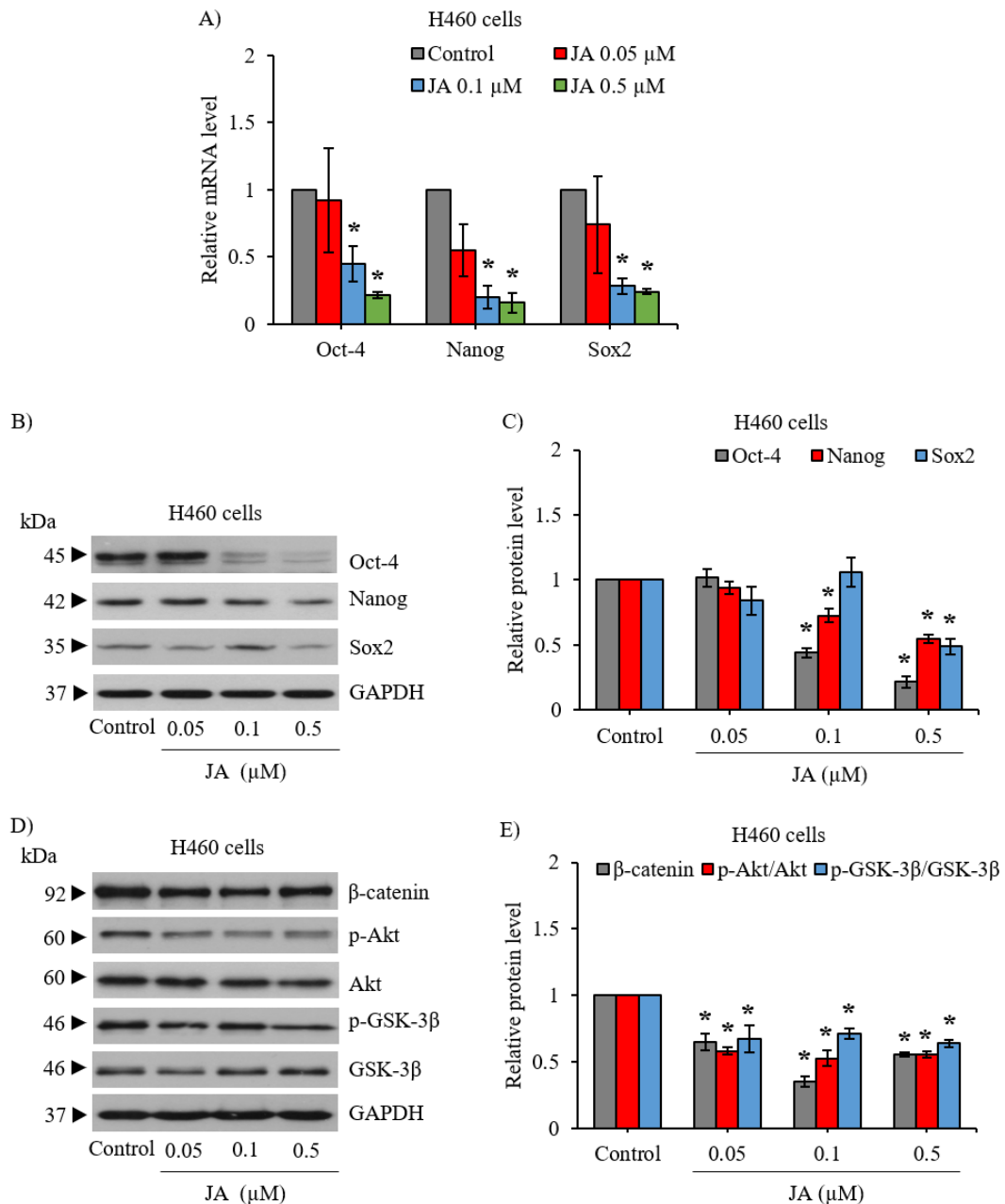


Figure 4.5 Jorunnamycin A downregulates stemness transcription factors and related proteins in CSC-enriched lung cancer H460 cells. The alteration of CSC self-renewal markers, Nanog, Oct-4, and Sox2, was determined in jorunnamycin A (JA)-treated CSC-enriched spheroids using (A) real-time RT-PCR and (B, C) Western blot analysis. GAPDH acted as an internal control. (D) Western blot analysis also revealed the downregulation of related up-stream proteins in CSC population of lung cancer H460 cells treated with JA for 24 h. (E) Noticeably, there was significant decrease of p-Akt/Akt, p-GSK-3 β /GSK-3 β , and β -catenin in JA-treated CSC-enriched spheroids. The relative

protein level indicated in (C, E) was respectively analyzed from chemiluminescent signal detected in Western blotting presented in (B, D). Data represent means \pm SD of three independent experiments. * $p < 0.05$ versus non-treated control.



2. Cytotoxicity and inhibitory effect of jorunnamycin A in CSCs of various lung cancer cells

2.1 Effect of jorunnamycin A on viability of various human lung cancer cells

Besides cytotoxicity of jorunnamycin A in human lung cancer H460 cells (p53 and KRas wild type), the anticancer activity of jorunnamycin A was further established in others human lung cancer cells, including H23 (p53 and KRas mutant), and A549 (KRas mutant). The determination of non-toxic concentrations of jorunnamycin A in attached H23 and A549 cell lines for 24h-incubation period is depicted in Figure 4.6 and 4.7, respectively. MTT assay revealed non-toxic concentrations in lung cancer H23 and A549 cells were up to 0.5 μM jorunnamycin A (Figure 4.6A and 4.7A) likewise non-toxic doses were used for H460 experiments. Using Costaining with Hoechst33342/propidium iodide (PI), the bright blue fluorescence of Hoechst33342 representing apoptosis cells in lung cancer H23 and A549 cells are respectively shown in Figures 4.6C and 4.7C while, necrosis cells (red fluorescence of propidium iodide; PI) were not detected. Correspondence with Figure 4.6B and 4.7B, jorunnamycin A at 1-5 μM offered significant increased %apoptosis in lung cancer H23 and A549 cells in a similar obtained result in H460 cells. Therefore, 0.05-0.5 μM jorunnamycin A were used to carry out further investigations for these cell lines.

Antiproliferative effect of jorunnamycin A in human lung cancer H23 and A549 cells were additionally extended. Although the antiproliferation percentage was reduced by 0.5 μM jorunnamycin A at 72 h of incubation time in both lung cancer cells, the reduction of %cell proliferation was early observed in H23 cells treated with 0.1 μM jorunnamycin A for 48 h (Figure 4.6D and 4.7D).

In addition, the effect of jorunnamycin A was observed in normal lung epithelial BEAS-2B cells. Figure 4.8 details cytotoxicity profile of jorunnamycin A in BEAS-2B cells in terms of %cell viability (Figure 4.8A), %apoptosis (Figure 4.8B), nuclear staining (Figure 4.8C) and %antiproliferation (Figure 4.8D). These results revealed non-toxic concentrations of jorunnamycin A were 0.05-0.5 μM . Although jorunnamycin A at 1-5 μM for 24 h slightly decreased %cell viability in BEAS-2B cells, %apoptosis was

significantly detected in BEAS-2B cells treated with 5 μM jorunnamycin A. Furthermore, treatment with 0.5 μM jorunnamycin A slightly increase %antiproliferation in in BEAS-2B cells for 48 and 72 h.

Herein, the half-maximal concentration that reduced 50% cell viability (IC_{50}) and inhibited 50% growth (IG_{50}) of jorunnamycin A in both lung cancer (H460, H23, and A549) and bronchial epithelial cells (BEAS-2B) was also determined and is presented in Table 1. Notably, the selective anticancer activity of jorunnamycin A was evidenced with higher IC_{50} and IG_{50} value in BEAS-2B cells compared with various lung cancer cells.

Table 1 The half-maximal inhibitory concentration on cell viability (IC_{50}) and proliferation (IG_{50}) of jorunnamycin A in human lung cancer and normal lung epithelial cells.

Cell type	IC_{50} (μM)	IG_{50} (μM)
H460	8.3 ± 2.6	0.27 ± 0.04
H23	2.0 ± 0.2	0.12 ± 0.01
A549	3.1 ± 0.3	0.23 ± 0.05
BEAS-2B	14.8 ± 0.6	0.65 ± 0.02

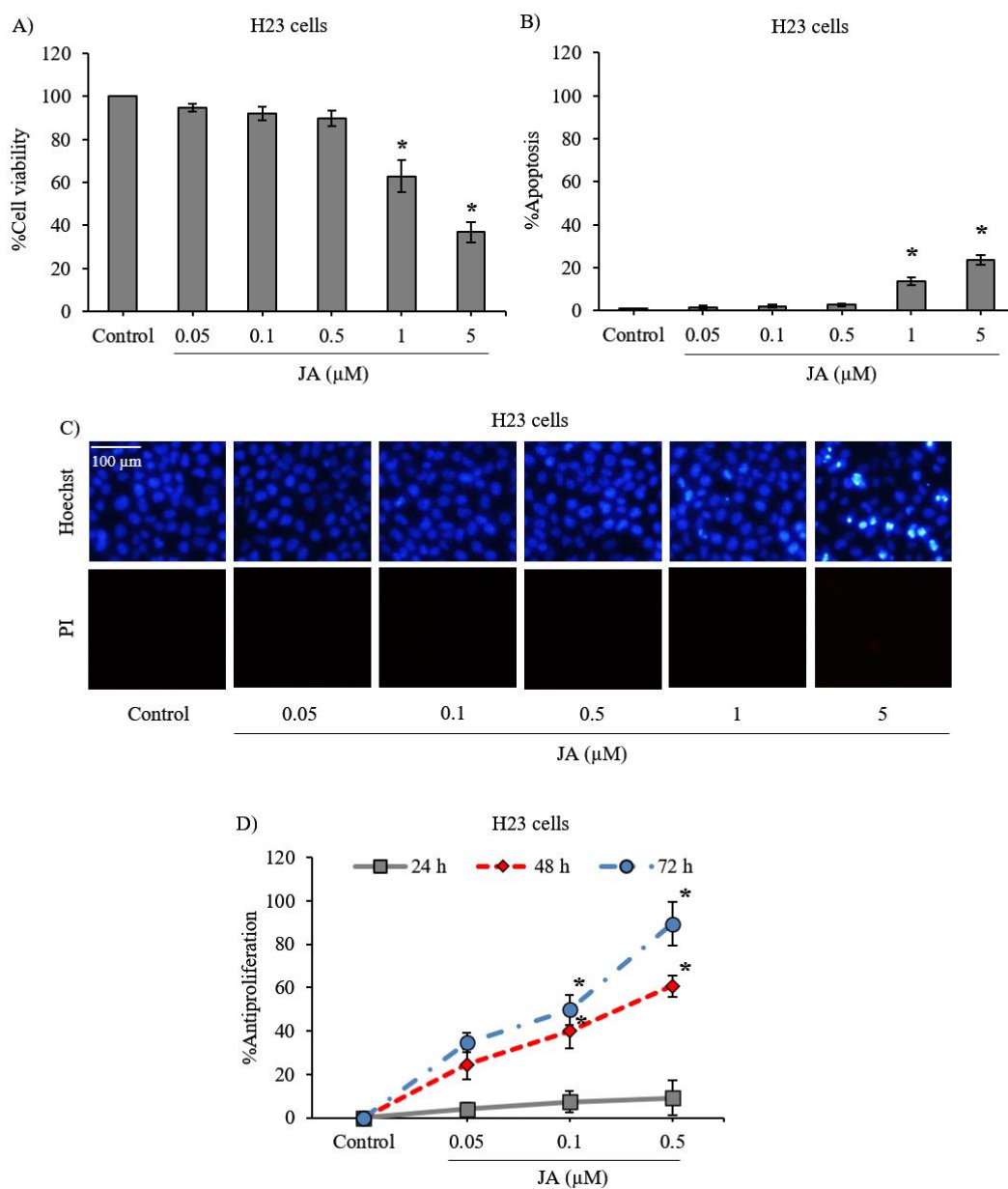


Figure 4.6 Jorunnamycin A-induced cytotoxicity in human lung cancer H23 cells. H23 cells were treated with various concentration of jorunnamycin A (JA) for 24 h. (A) Cell viability was analyzed by MTT assay. The significant reduction of cell viability in lung cancer H23 cells exhibited after treatment with 1-5 μM of JA. (B) Increased percentage of apoptosis was noted after culturing with JA at 1-5 μM . (C) Apoptosis represented by Bright blue fluorescence of Hoechst33342 was observed in H460 cells after treatment with 1-5 μM JA for 24 h, while there was no detectable necrosis (red fluorescence of propidium iodide; PI). (D) The antiproliferative effect of JA treatment (0.1-0.5 μM) in

human lung cancer H23 cells revealed the significant inhibition at 48 and 72 h time point. The %apoptosis (**B**) was analyzed in H23 cells co-stained with Hoechst33342/PI (**C**). Data represent means \pm SD of three independent experiments. * $p < 0.05$ versus non-treated control.



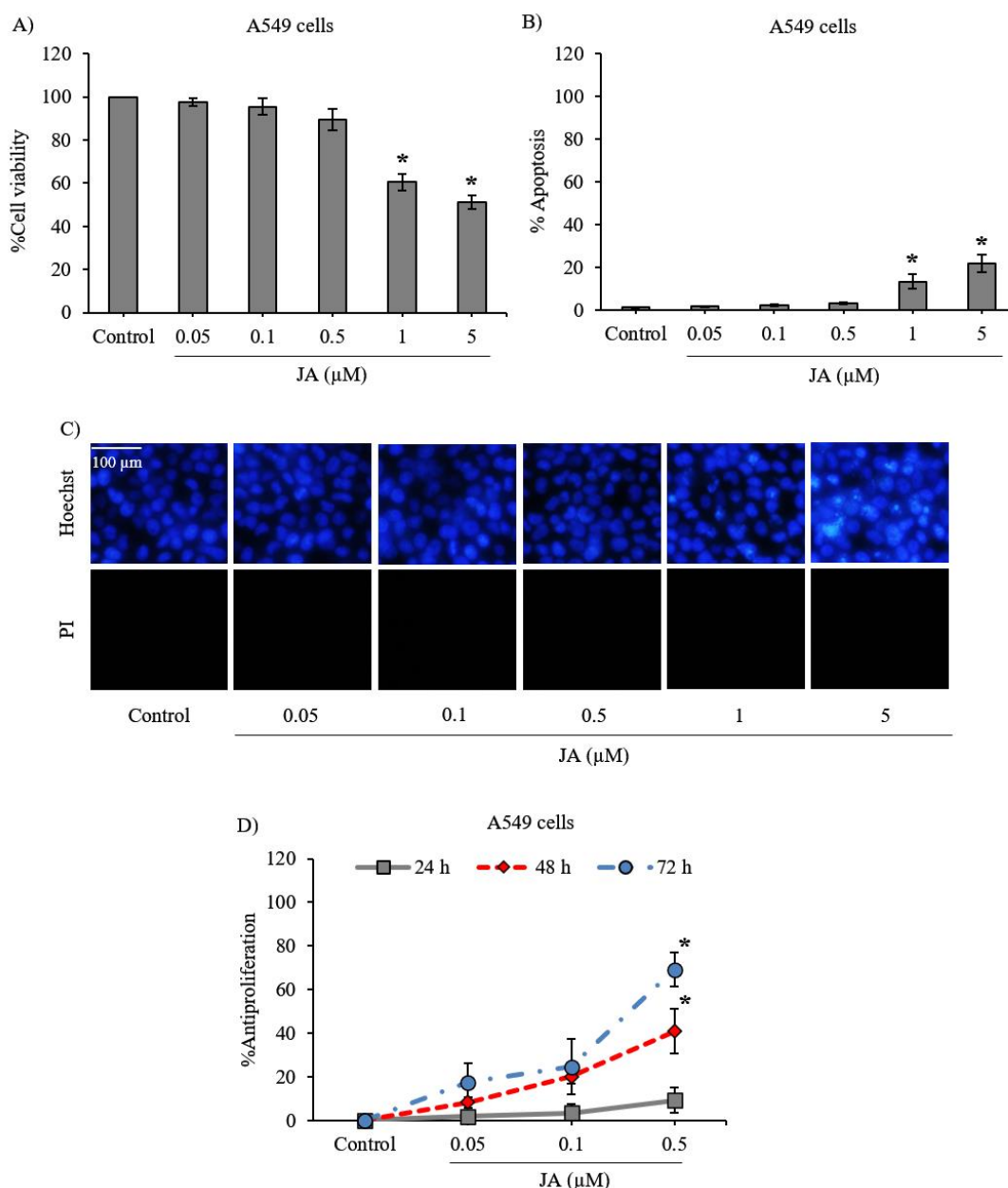


Figure 4.7 Cytotoxicity activity of jorunnamycin A in human lung cancer A549 cells. (A) MTT assay revealed the significant reduction of cell viability in lung cancer A549 cells after treatment with 1-5 μM of jorunnamycin A (JA) for 24 h. (B) JA at 1 and 5 μM significantly increased %apoptosis in A549 cells. (C) Visualization of A549 cells co-stained with Hoechst33342/propidium iodide (PI) was used to demonstrated that no necrosis cell death was detected in A549 cells at all treatment concentrations of JA for 24 h. (D) The antiproliferative effect of JA treatment (0.5 μM) in human lung cancer A549 cells shown the significant inhibition at 48 and 72 h time point. The %apoptosis

(B) was analyzed in A549 cells co-stained with Hoechst33342/PI (C). Data represent means \pm SD of three independent experiments. * $p < 0.05$ versus non-treated control.



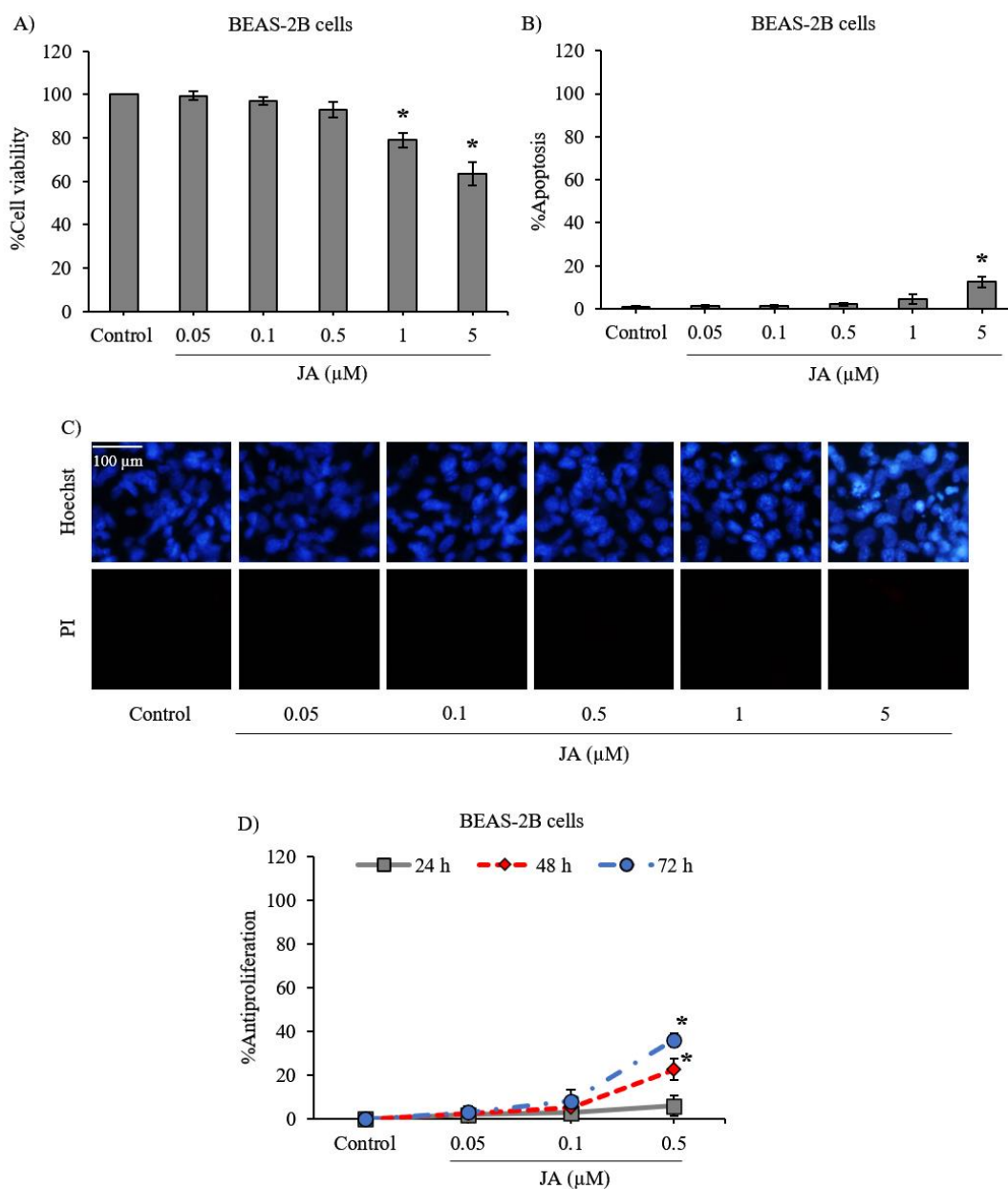


Figure 4.8 Cytotoxicity of jorunnamycin A in human lung epithelial BEAS-2B cells. (A) MTT assay revealed the significant reduction of cell viability in lung epithelial BEAS-2B cells after treatment with 1-5 μM of jorunnamycin A (JA) for 24 h. (B) The augmentation of %apoptosis was shown in BEAS-2B cells treated with 1 and 5 μM of JA. (C) Costaining with Hoechst33342/propidium iodide (PI) demonstrated that no necrosis cell death was detected in BEAS-2B cells at all treatment concentrations of JA for 24 h. (D) The antiproliferative effect of JA treatment (0.5 μM) in human lung cancer H460 cells revealed the significant inhibition at 48 and 72 h time point. The %apoptosis (B) was

analyzed in BEAS-2B cells co-stained with Hoechst33342/PI (C). Data represent means \pm SD of three independent experiments. * $p < 0.05$ versus non-treated control.



2.2 The inhibitory effect of jorunnamycin A in CSCs of various lung cancer cells

The investigation of the inhibitory effect of jorunnamycin A in CSCs was further extended in human lung cancer H23 and A549 cells. Using LDA, the frequency of cancer spheroid-initiating cells in the lung cancer H23 and A549 populations are respectively depicted in Figures 4.9A and 4.10A. The spheroid forming ability appears slightly less pronounced in lung cancer A549 cells, as evidenced by the smaller size of cancer colonies compared with H460 and H23 cells. Figures 4.9B and 4.10B respectively indicate that nontoxic concentrations of jorunnamycin A (0.05–0.5 μM) significantly reduced the number of colonies at all cell densities (1–200 cells/well) in both H23 and A549 cells.

The alteration of anchorage-independent growth of CSC-enriched H23 and A549 spheroids after culture with 0.05–0.5 μM jorunnamycin A for 7 days is depicted in Figures 4.9C and 4.10C, respectively. The reduction of colony size in both H23 and A549 spheroids was promptly observed after incubation of the spheroids with 0.5 μM jorunnamycin A for 1 day (Figures 4.9D and 4.10D). Although anchorage-independent growth of CSC-enriched H23 spheroids was significantly suppressed only at the highest concentration (0.5 μM), jorunnamycin A at all nontoxic concentrations inhibited anchorage-independent growth of CSC-enriched A549 spheroids in a time- and dose-dependent manner, which was similarly observed in H460 cells. Furthermore, Figures 4.9E and 4.10E sequentially demonstrate the alteration of the CD133^{low} and CD133^{high} populations in CSC-enriched spheroids of H23 and A549 cells after culture with jorunnamycin A for 72 h. The CD133^{high} population was significantly reduced by jorunnamycin A at 0.5 μM in both the H23 and A549 spheroids, compared with the untreated CSC spheroids (Figures 4.9F and 4.10F).

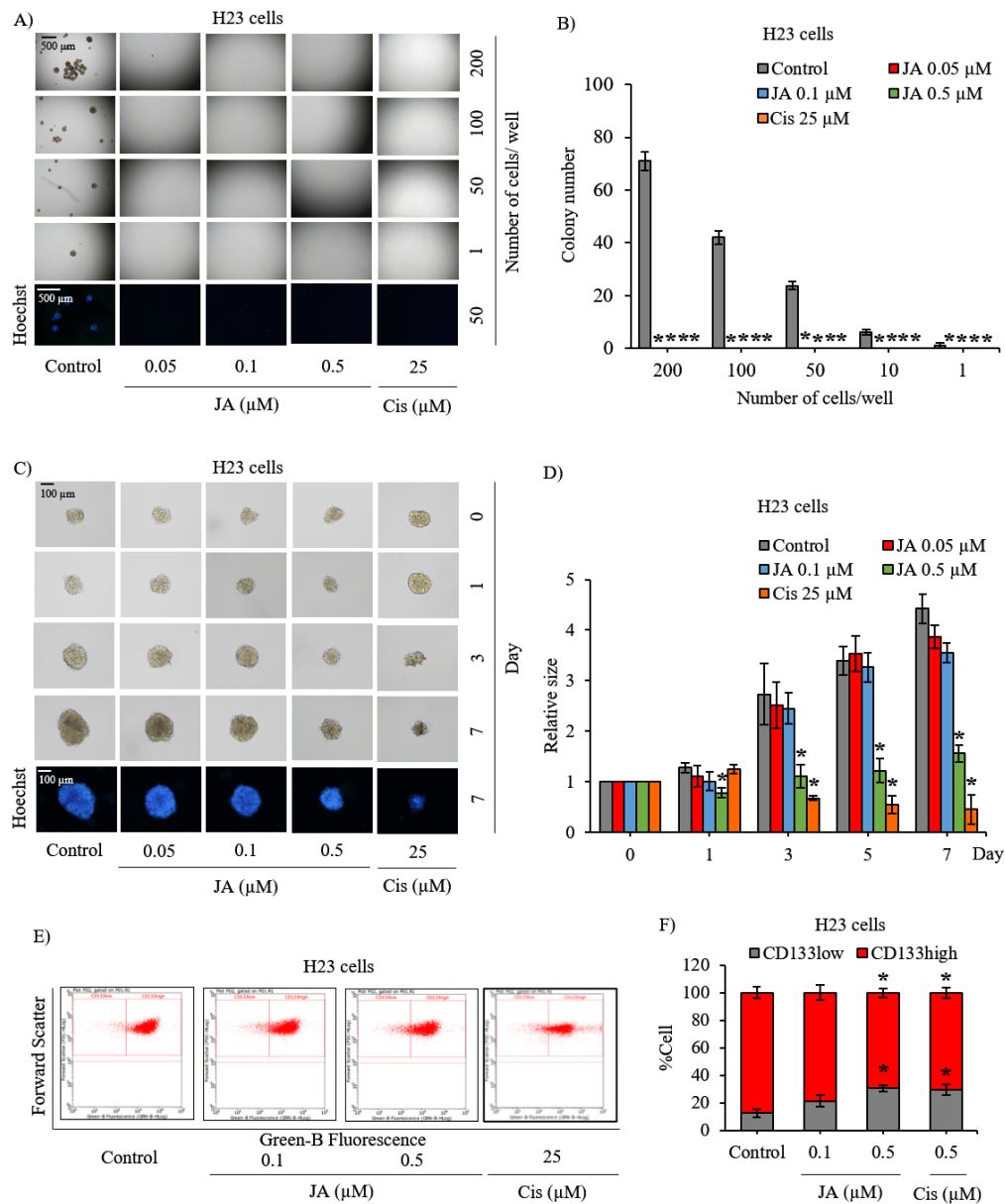


Figure 4.9 Jorunnamycin A suppresses stem-like phenotypes of lung cancer H23 cells. (A) The cancer spheroid-initiating cells of H23 cells were observed through limiting dilution assay (LDA). Jorunnamycin A (JA) inhibited the spheroid-forming capability of human lung cancer H23 cells in LDA for 14 days at all concentrations. At day 14 of treatment, optical microscopy (4x) was used to capture spheroid images, while fluorescence microscopy (10x) was used to visualize blue fluorescence of Hoechst 33342. (B) Decreased colony number was detected in all groups exposed to nontoxic concentrations (0.05–0.5 μM) of JA. (C) Single three-dimensional (3D) CSC spheroid formation was used to distinguish suppressive effect of JA in CSC-enriched

lung cancer cells. At day 7 of treatment, all single 3D CSCs were visualized by optical microscopy (10×), and images depicting bright blue fluorescence of Hoechst 33342 were obtained by fluorescence microscopy (10×). (D) Treatment with JA (0.5 μM) exhibited a significant reduction of the relative size of CSC-enriched spheroids starting from days 1–7. (E, F) Flow cytometry analysis of CD133 expression confirmed the reduction of CD133^{high} population after treatment with JA (0.5 μM) for 3 days. Cisplatin (Cis) at 25 μM was used as a positive control. The colony number (B) and relative size (D) were respectively analyzed from cancer colonies (A) and CSC-enriched spheroids (C). The %cell demonstrated in (F) was calculated from dot plots presented in (E). Data represent means ± SD of three independent experiments. * $p < 0.05$ versus non-treated control.



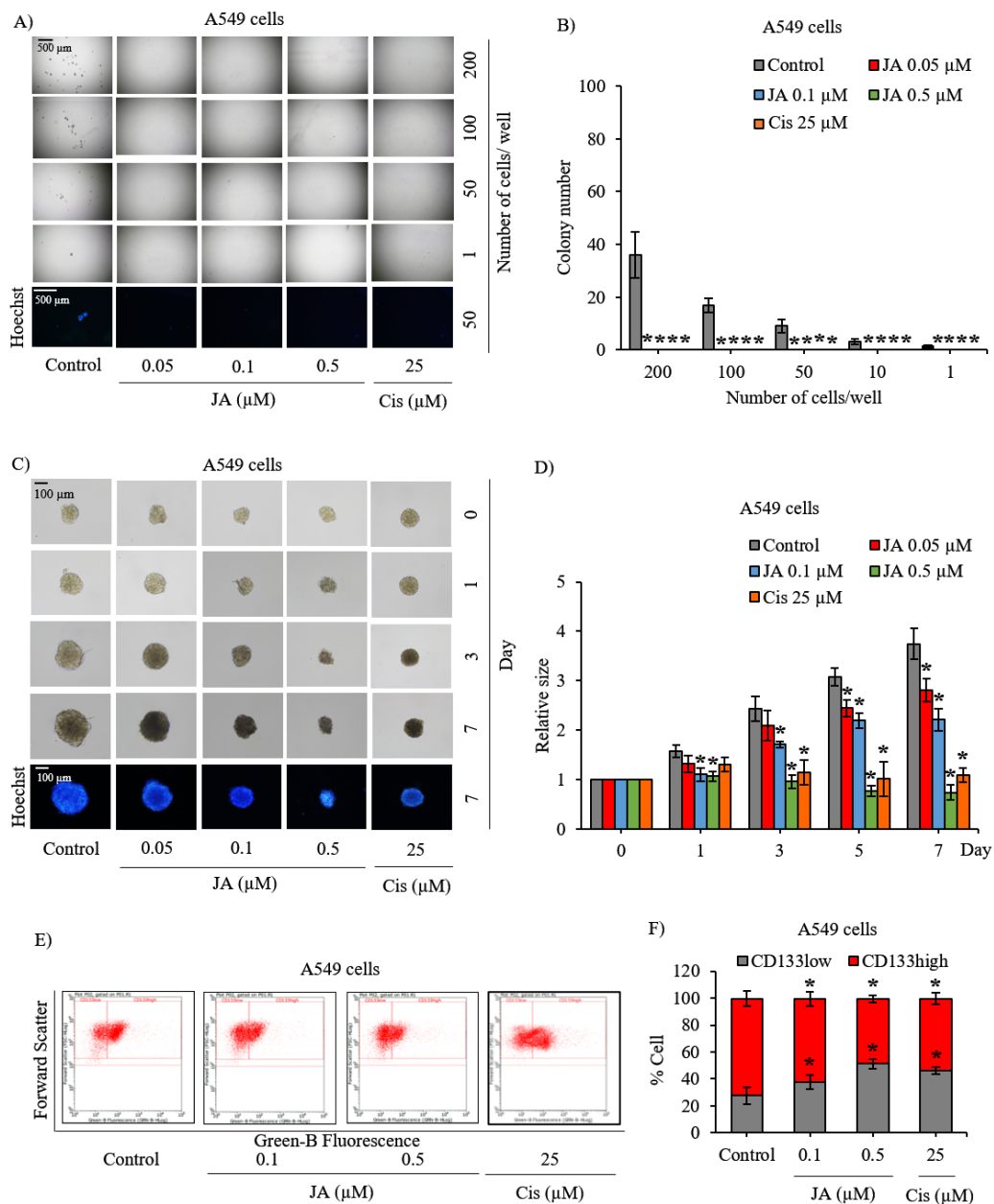


Figure 4.10 Suppressive effect of jorunnamycin A on stem-like phenotypes of lung cancer A549 cells. **(A)** Jorunnamycin A (JA) inhibited capability to generate cancer spheroid of human lung cancer A549 cells in limiting dilution assay (LDA) for 14 days at all concentrations. Optical microscopy (4x) was used to capture spheroid images, while fluorescence microscopy (10x) was used to take images with blue fluorescence from Hoechst33342 staining. **(B)** The number of forming colonies at all cell densities used was decreased in all groups exposed to nontoxic concentrations (0.05–0.5 μM) of JA. **(C)** Suppressive effect of JA in CSC-enriched A549 lung cancer cells was evaluated

by single three dimensional (3D) CSC spheroid formation. The enlargement of CSC spheroids was suppressed by JA (0.05–0.5 μ M). At day 7 of treatment, all single 3D CSCs were photographed by optical microscopy (10 \times) and spheroid images depicting bright blue fluorescence of Hoechst33342 were obtained by fluorescence microscopy (10 \times). (D) Culture with JA (0.1–0.5 μ M) illustrated the significant reduction of relative spheroid size of CSC-enriched lung cancer cells at days 1–7. (E) Flow cytometry analysis of CD133 expression confirmed the reduction of CD133^{high} population after treatment with JA (0.1–0.5 μ M) for 3 days. (F) JA at 0.1–0.5 μ M diminished CD133^{high} population in CSC spheroids compared with untreated control. Cisplatin (Cis) at 25 μ M was used as a positive control. The colony number (B) and relative size (D) were respectively analyzed from cancer colonies (A) and CSC-enriched spheroids (C). The %cell demonstrated in (F) was calculated from dot plots presented in (E). Data represent means \pm SD of three independent experiments. * p < 0.05 versus nontreated control.

Since the stemness factors are known to be transcriptionally activated by Akt/GSK-3 β / β -catenin signal [91, 92] the modulation on stemness transcription factors was further confirmed in CSCs obtained from lung cancer H23 and A549 cells via RT-qPCR. Figure 4.11A, B respectively presents the significant reduction of Nanog, Oct-4, and Sox2 mRNA level in CSC-enriched H23 and A549 spheroids that were cultured with 0.5 μ M jorunnamycin A for 24 h. Interestingly, jorunnamycin A at lower concentrations (0.05–0.1 μ M) dramatically suppressed mRNA expression of these stemness transcription factors in CSC-enriched A549 spheroids. Although the incubation with 0.5 μ M jorunnamycin A for 24 h obviously downregulated the related regulatory proteins, including those of p-GSK-3 β /GSK-3 β and β -catenin, there was no significant alteration of the p-Akt/Akt signal in either H23 (Figure 4.11C, D) or A549 CSC subpopulations (Figure 4.11E, F). The obtained results strongly support the role of jorunnamycin A in modulating CSC phenotypes in human lung cancer cells via the GSK-3 β / β -catenin pathway.

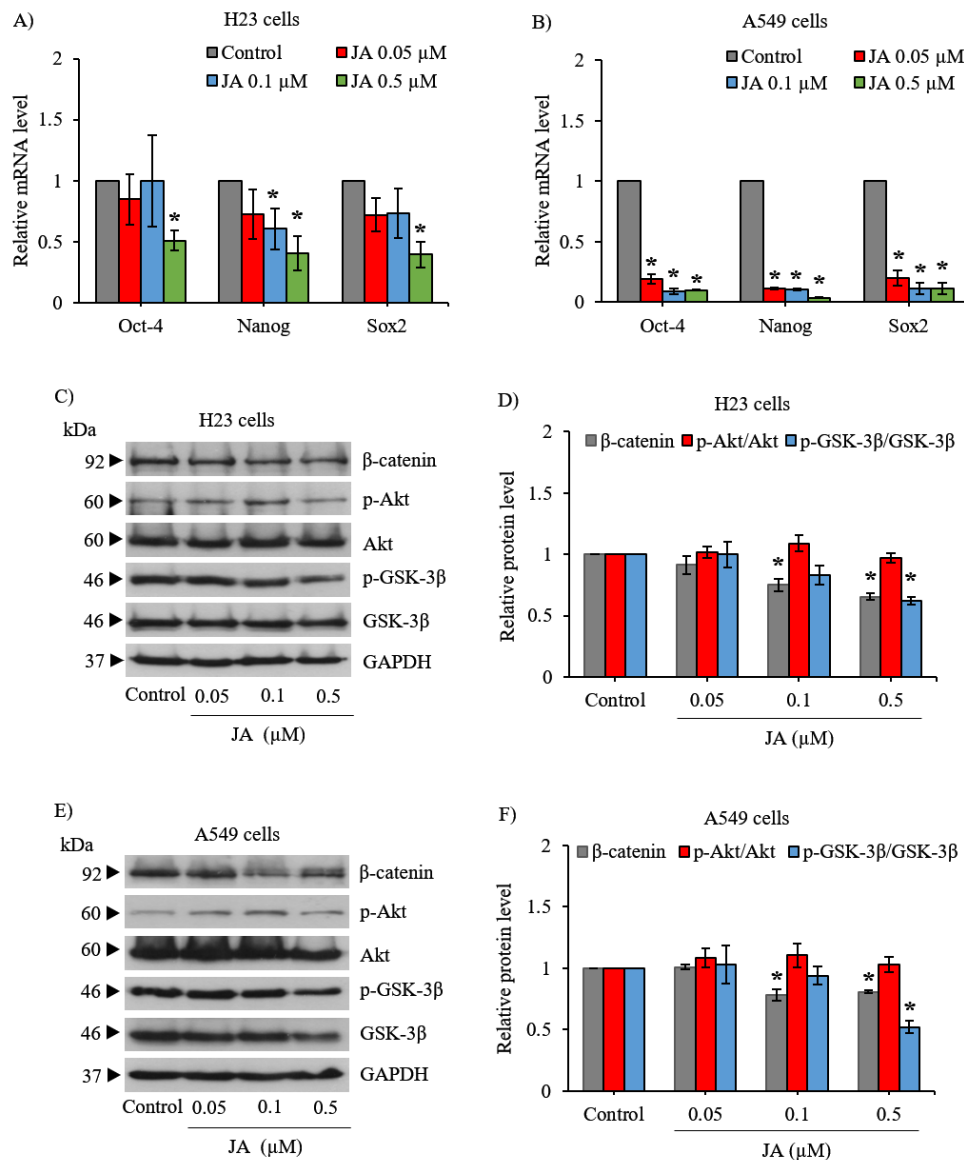


Figure 4.11 Jorunnamycin A downregulates stemness transcription factors and related proteins in various lung CSCs. The diminished mRNA levels of stemness transcription factors, including Nanog, Oct-4, and Sox2, determined by real-time RT-PCR is demonstrated in (A) CSC H23 and (B) CSC A549 spheroids cultured with 0.5 μ M jorunnamycin A (JA) for 24 h. Western blot analysis revealed the downregulation of p-GSK-3 β /GSK-3 β and β -catenin in CSC-enriched population of (C, D) lung cancer H23 and (E, F) A549 cells treated with JA for 24 h. The relative protein level (D, F) was analyzed from chemiluminescent signal detected in Western blotting, as presented in (C, E). Data represent means \pm SD of three independent experiments. * $p < 0.05$ versus non-treated control.

The safety profile of jorunnamycin A on stemness features of normal lung stem cells was clarified in human lung epithelial BEAS-2B cells. Capability to form new colonies of healthy lung stem cells was assessed in LDA, as presented in Figure 4.12A. Despite containing mesenchymal stem cells [158], only a low level of colony formation was observed in BEAS-2B cells at a density of 200 cells/well. Intriguingly, the minor alteration of colony number was noticed in jorunnamycin A-treated and cisplatin-treated human lung epithelial BEAS-2B cells compared with the untreated control (Figure 4.12B). Three-dimensional (3D) spheroid formation was also performed as usual to investigate the self-renewal activity of normal lung stem cells [159]. Surprisingly, no significant alteration of stem cell enriched BEAS-2B spheroids was observed after treatment with jorunnamycin A (0.05–0.5 μM) or 25 μM cisplatin (Figure 4.12C, D).

Since CD133 serves not only as a CSC protein marker but also a mediator of pluripotency in normal stem cells [160], jorunnamycin A-treated BEAS-2B spheroids were assessed for CD133 expression level. Flow cytometry analysis demonstrated that treatment with jorunnamycin A did not alter the %CD133^{high} subpopulation in BEAS-2B spheroids when compared with the control group (Figure 4.12E, F). Indeed, the upregulated expression level of CD133 has been considered as a prognostic marker for lung tumor pathology [161, 162]. Therefore, the present results suggest that jorunnamycin A selectively suppresses CSC phenotypes in various lung cancer cells without alteration of stemness features in healthy lung epithelial cells.

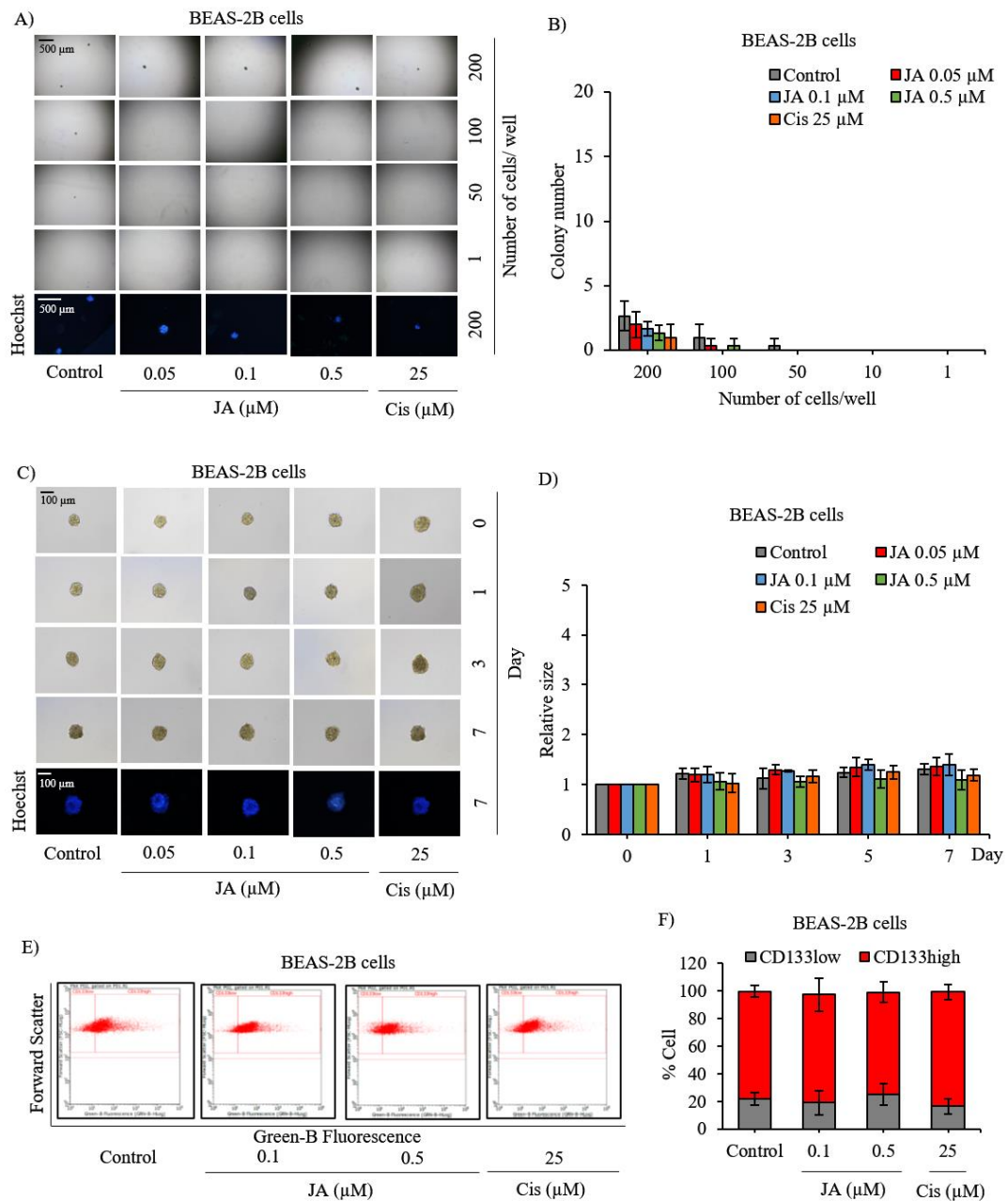
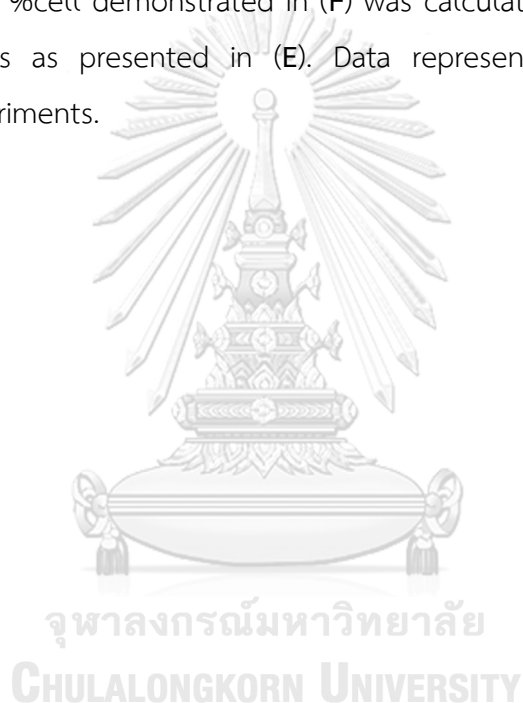


Figure 4.12 No alteration of stemness phenotypes in human lung epithelial cells cultured with jorunnamycin A. (A) Limiting dilution assay (LDA) revealed a low amount of colony formation obtained from normal lung epithelial BEAS-2B cells that were cultured in ultra-low attachment 96-well plate for 14 days. (B) There was no significant difference in the number of colonies generated from BEAS-2B cells incubated with 0.05–0.5 μM jorunnamycin A (JA), compared with untreated cells. Optical microscopy (4x) was used to capture spheroid images, while fluorescence microscopy (10x) was used to take images with blue fluorescence from Hoechst33342 staining. (C) Stemness

features of BEAS-2B cells were also examined in single three-dimensional (3D) spheroid formation. After culture for 7 days, all single 3D spheroids were photographed by optical microscopy (10 \times) and spheroid images depicting bright blue fluorescence of Hoechst33342 were obtained by fluorescence microscopy (10 \times). Neither (D) relative spheroid size nor (E, F) %CD133-overexpressing cells in BEAS-2B spheroids were altered after treatment with JA (0.1–0.5 μ M) when compared with untreated control. Cisplatin (Cis) at 25 μ M was used as a positive control. The colony number (B) and relative size (D) were respectively analyzed from forming colonies (A) and stem cell-enriched spheroids (C). The %cell demonstrated in (F) was calculated from dot plots of flow cytometry analysis as presented in (E). Data represent means \pm SD of three independent experiments.



3. Investigation on the relationship between ROS modulation effect and suppressive activity of jorunnamycin A in CSCs of lung cancer H460 cells

3.1 Jorunnamycin A modulates oxidative stress in CSC-enriched lung cancer cells

The alteration of cellular ROS level in CSCs is a substantial factor for maintenance of stemness in CSCs [35]. Herein, the effect of jorunnamycin A on intracellular ROS level was assessed by flow cytometry using fluorescence DCFH₂-DA probe. To measure cellular oxidative stress, the probe is deacetylated by intracellular esterase to form DCF, which reacts with ROS and generates fluorescence. Figure 4.13A illustrates the value of relative fluorescence obtained from flow cytometry detection. The CSC-enriched H460 spheroids treated with 0.5 μ M jorunnamycin A for 6 and 9 h showed significantly increased relative fluorescence intensity. The resulted demonstrated that jorunnamycin A induced oxidative stress in CSC-enriched lung cancer population.

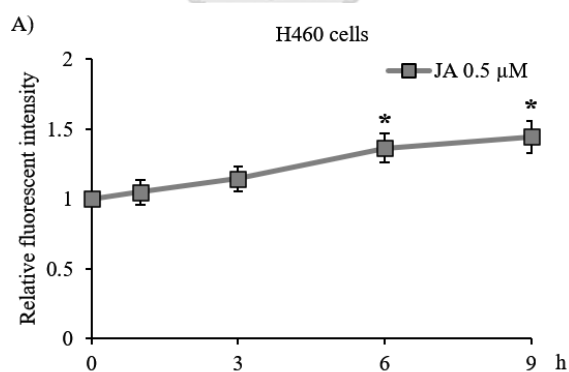


Figure 4.13 The relative ROS level in CSC-enriched H460 spheroids incubated with jorunnamycin A (JA) for 1-9 h was assessed vis flow cytometry using DCFH₂-DA probe. The accumulation of intracellular ROS level was significantly noticed after 6 h of JA treatment. Data represent means \pm SD of three independent experiments. * $p < 0.05$ versus non-treated control.

3.2 The pro-oxidative effect of jorunnamycin A on tumor-initiating cells in lung cancer H460 cells

To clarify the role of pro-oxidant activity in lung cancer H460 cells cultured with jorunnamycin A, the link between alteration of cellular ROS and tumor-initiating capacity was further investigated. Human lung cancer cells were pretreated with N-acetyl cysteine (NAC), a general antioxidant, for 30 min prior to treatment with jorunnamycin. LDA was used to explore colony formation. Figure 4.14 indicates spheroid-forming ability in human lung cancer H460 cells at day 14. NAC treatment did not alter tumor-initiating capability in H460 cells compared with control cells (Figure 4.14A). It should be noted that there was no difference of formed colony number between cotreatment of NAC and jorunnamycin A and treated only jorunnamycin A (Figure 4.14B). These results suggest that the suppressive effect of jorunnamycin A on cancer spheroid-initiating cells in lung cancer H460 cells does not involve with the pro-oxidant activity of jorunnamycin A.

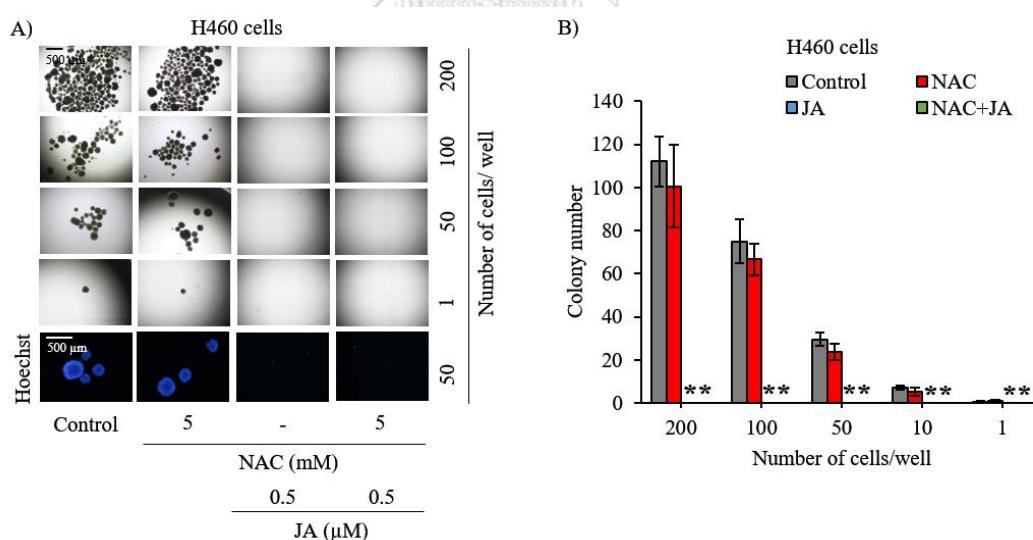


Figure 4.14 ROS effect in spheroid-initiating capability of jorunnamycin A observed in human lung cancer H460 cells. (A) Pretreatment with 5 mM N-acetyl cysteine (NAC) did not reverse inhibitory effect jorunnamycin A (JA) on tumor-initiating activity in lung cancer H460 cells determined by limiting dilution assay (LDA) for 14 days. Optical microscopy (4x) was used to take spheroid images, while fluorescence microscopy

(10×) was used to capture blue fluorescence of Hoechst 33342. (B) The significant decreased colony number was detected in both groups of JA (0.5 μ M) and pre-treated group with NAC (5 mM) then followed by JA (0.5 μ M). The colony number (B) was analyzed from cancer colonies (A). Data represent means \pm SD of three independent experiments. * $p < 0.05$ versus non-treated control.

3.3 The effect of ROS generated by jorunnamycin A in CSC-enriched H460 spheroids

The intracellular ROS has been recognized as essential elements for CSC fate [163]. The relation between the alteration of cellular ROS and CSCs was further observed in secondary H460 spheroids after co-culture with 5 mM NAC and 0.5 μ M jorunnamycin A for 7 days. The ROS-modulating effect of jorunnamycin A in colony size is depicts in Figure 4.15. Although there was no significant difference in the relative size of NAC compared with untreated control (Figure 4.15A), pretreatment with NAC obviously restrained the suppressive effect of jorunnamycin A in CSC-enriched spheroids (Figure 4.15B). This evidence indicates the pro-oxidant effect of jorunnamycin A influences on self-renewal capacity of CSC subpopulation in lung cancer H460 cells.

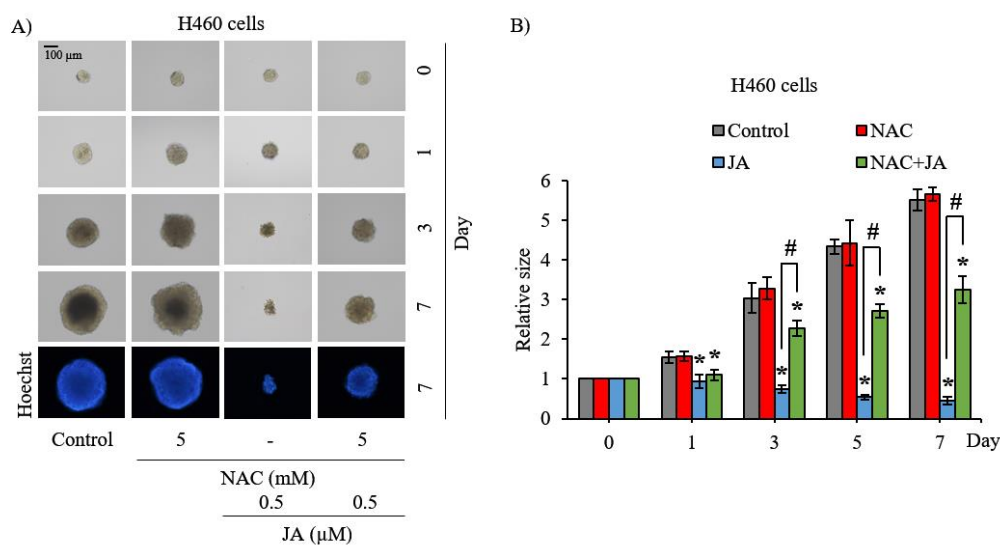


Figure 4.15 ROS modulating effect of jorunnamycin A in CSC-enriched H460 spheroid. Single three-dimensional (3D) CSC spheroid formation was used to determine the effect of ROS-modulated by jorunnamycin A in CSC-enriched lung cancer cells. **(A)** CSC-enriched spheroids were pre-incubation with nontoxic concentration (5 mM) of N-acetyl cysteine (NAC) for 30 min followed by 0.5 μM jorunnamycin A (JA) for 7 days. All single 3D CSCs were visualized by optical microscopy (10x), and images depicting bright blue fluorescence of Hoechst 33342 were taken by fluorescence microscopy (10x). **(B)** The enlargement of spheroid size relative to JA-cultured spheroids was significantly observed at day 3-7 in the cotreatment of NAC (5 mM) and JA (0.5 μM). The relative size **(B)** was analyzed in CSC-enriched spheroids **(A)**. Data represent means ± SD of three independent experiments. * $p < 0.05$ versus non-treated control. # $p < 0.05$ versus only JA-treated group.

4. Investigation on the relationship between autophagy modulating activity and suppressing activity of JA on CSCs in H460 lung cancer cells

4.1 Jorunnamycin A mediates autophagy in CSC-enriched lung cancer cells

Self-consumption known as autophagy has been played attention in chemotherapeutic resistance and cancer therapy [164]. Herein, the autophagic response mediated by jorunnamycin was investigated. The alteration of autophagy marker proteins including p62, Beclin-1, LC3-I and LC3-II was evaluated in CSC-enriched H460 spheroids cultured with 0.5 μM jorunnamycin at various time points (0-12 h). Figure 4.16A reveals the expression levels of regulating autophagy proteins. Beclin-1 and LC3-I/LC3-II conversion levels significantly increased after 6 h of incubation time. Interestingly, the protein level of autophagy substrate, p62 was noticeably reduced at 3 h of jorunnamycin A treatment (Figure 4.16B). These results suggest that jorunnamycin A induced autophagic response in CSC-enriched lung cancer cells.

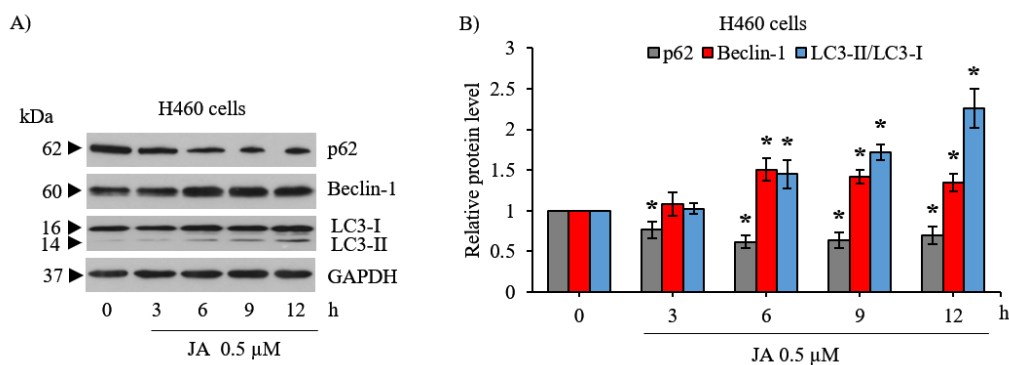


Figure 4.16 The alteration of autophagy-related proteins in jorunnamycin A-treated CSC-enriched spheroid. **(A)** Expression protein levels of the autophagic markers, p62, Beclin-1, LC3-I and LC3-II in H460 cells after culture with 0.5 μM jorunnamycin (JA) for 0-12 h, as evaluated by western blot analysis. **(B)** Densitometry analysis indicated that jorunnamycin A up-regulated Beclin-1 and LC3-II/LC3-I conversion and diminished p62 in a time-dependent manner. The relative protein level **(B)** was analyzed from the chemiluminescent signal detected in Western blotting, as presented in **(A)**. Data represent means \pm SD of three independent experiments. * $p < 0.05$ versus non-treated control.

4.2 The effect of autophagic response of jorunnamycin A on tumor-initiating cells in lung cancer H460 cells

Because jorunnamycin A induced autophagy activity in CSC-enriched H460 cells, the connection between autophagic response and tumor-initiating capacity was further observed by limiting dilution assay (LDA). Human lung cancer H460 cells were pretreated with autophagy inhibitor, wortmannin at non-toxic concentration (0.5 μM) for 30 min before cultured with 0.5 μM jorunnamycin A. As indicates in Figure 4.17A and B, wortmannin alone did not significantly alter spheroid-forming capability of detached cell over 14 days compared with untreated control. Meanwhile pretreatment with this autophagy preventing agents followed by jorunnamycin A resulted in lessening formed colony, which was similarly observed in only jorunnamycin A treated group. These finding demonstrated that the inhibitory effect of JA on tumor-initiating cells in lung cancer H460 cells does not associate with jorunnamycin A-inducing autophagic response.

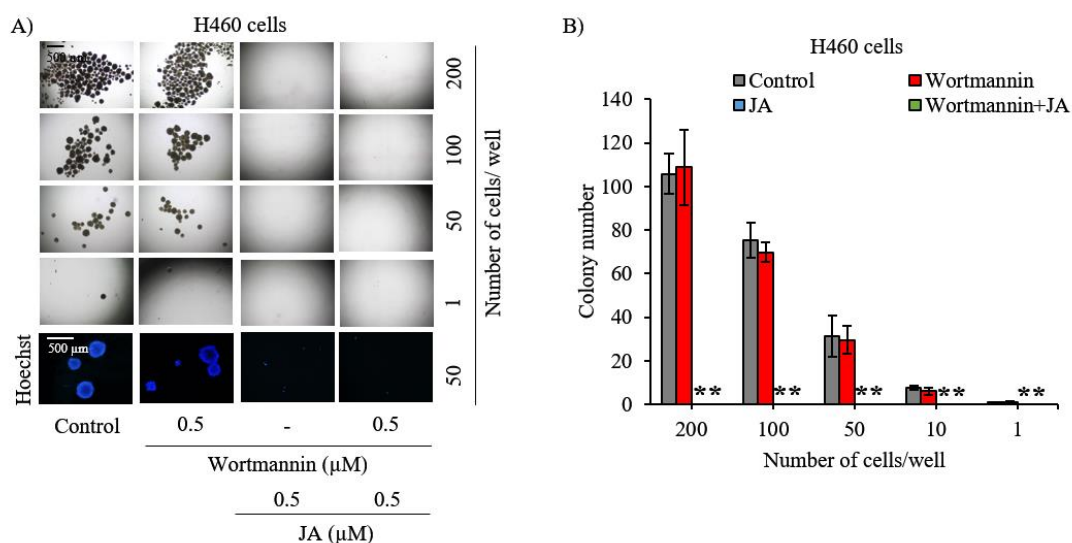


Figure 4.17 Autophagic effect of jorunnamycin A on tumor-initiating cell observed in human lung cancer H460 cells. **(A)** Limiting dilution assay (LDA) reveals the inhibitory effect of jorunnamycin A (JA) on tumor-initiating activity in lung cancer H460 cells was not restrained by pretreatment with 0.5 μM wortmannin. **(B)** JA (0.5 μM) alone and pretreatment with wortmannin (0.5 μM) then followed by JA (0.5 μM) significantly decreased the number of forming colony. The colony number **(B)** was analyzed from cancer colonies **(A)**. Data represent means \pm SD of three independent experiments. * $p < 0.05$ versus nontreated control.

4.3 The effect of autophagy induced by jorunnamycin A in CSC-enriched H460 spheroids

To elucidate the relation of autophagy and stemness traits of self-renewal, single three-dimensional (3D) spheroid formation was performed. Secondary H460 spheroids were co-treated with 0.5 μM wortmannin and 0.5 μM jorunnamycin A for 7 days. Figure 4.18 illustrates the autophagy inducing effect of jorunnamycin A on the size of CSC-enriched spheroids. No significant differences of the relative size were found in between wortmannin treatment and untreated control (Figure 4.18A) while the suppressive effect of jorunnamycin A in CSC-enriched spheroids was reduced by pretreatment with wortmannin (Figure 4.18B). The obtained results demonstrate that

the autophagy inducing effect of jorunnamycin A contributes the regulation on self-renewal capacity of CSC-enriched H460 spheroids.

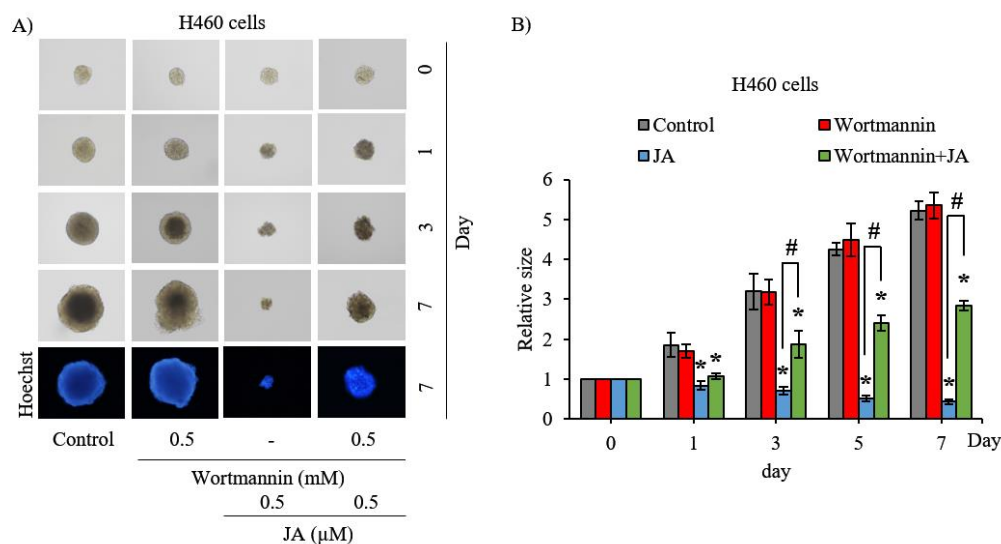


Figure 4.18 Autophagy inducing effect of jorunnamycin A in CSC-enriched H460 spheroids. (A) CSC-enriched spheroids obtained from H460 cancer cells were precultured with nontoxic concentration (0.5 μM) of wortmannin for 30 min prior to treatment with 0.5 μM jorunnamycin A (JA) for 7 days. All single three-dimensional (3D) CSC spheroids were photographed by optical microscopy (10 \times), and spheroid images depicting bright blue fluorescence of Hoechst33342 were obtained by fluorescence microscopy (10 \times) at day 7 of treatment. (B) Pre-incubation with 0.5 μM wortmannin followed by 0.5 μM JA significantly regulated relative CSC-enriched H460 spheroids size at day 3-7, compared with JA treatment. The relative spheroid size (B) was analyzed from CSC-enriched spheroids (A). Data represent means \pm SD of three independent experiments. * $p < 0.05$ versus non-treated control. # $p < 0.05$ versus only JA-treated group.

5. The effect of JA in sensitization of cisplatin-induced cell death in human lung cancer H460 cells

5.1 Jorunnamycin A promotes apoptosis in cisplatin-treated human lung cancer H460 cells

Although platinum-based chemotherapy is widely regarded as a primary option for lung cancer treatment, cisplatin resistance is a major problem that causes poor clinical outcomes [165]. To improve this adverse event, the effect of jorunnamycin A in sensitization of cisplatin-induced apoptosis was initially investigated in attached lung cancer cells. Figure 4.19A shows that treatment lung cancer H460 cells for 24 h with jorunnamycin A at 0.5 μM does not cause significantly decrease cell viability meanwhile pretreatment with jorunnamycin A (0.5 μM) for 24 h caused lower cell viability in cisplatin-treated H460 cells. Measurement of % apoptosis was conducted by Hoechst33342 and PI costaining (Figure 4.19C). Interestingly, combination treatment of 0.5 μM jorunnamycin A and 25 μM cisplatin significantly increased %apoptosis as compared to only cisplatin treatment (Figure 4.19B). These results provide evidence that jorunnamycin A facilitated to the chemosensitizing effect in cisplatin-treated human lung cancer H460 cells.

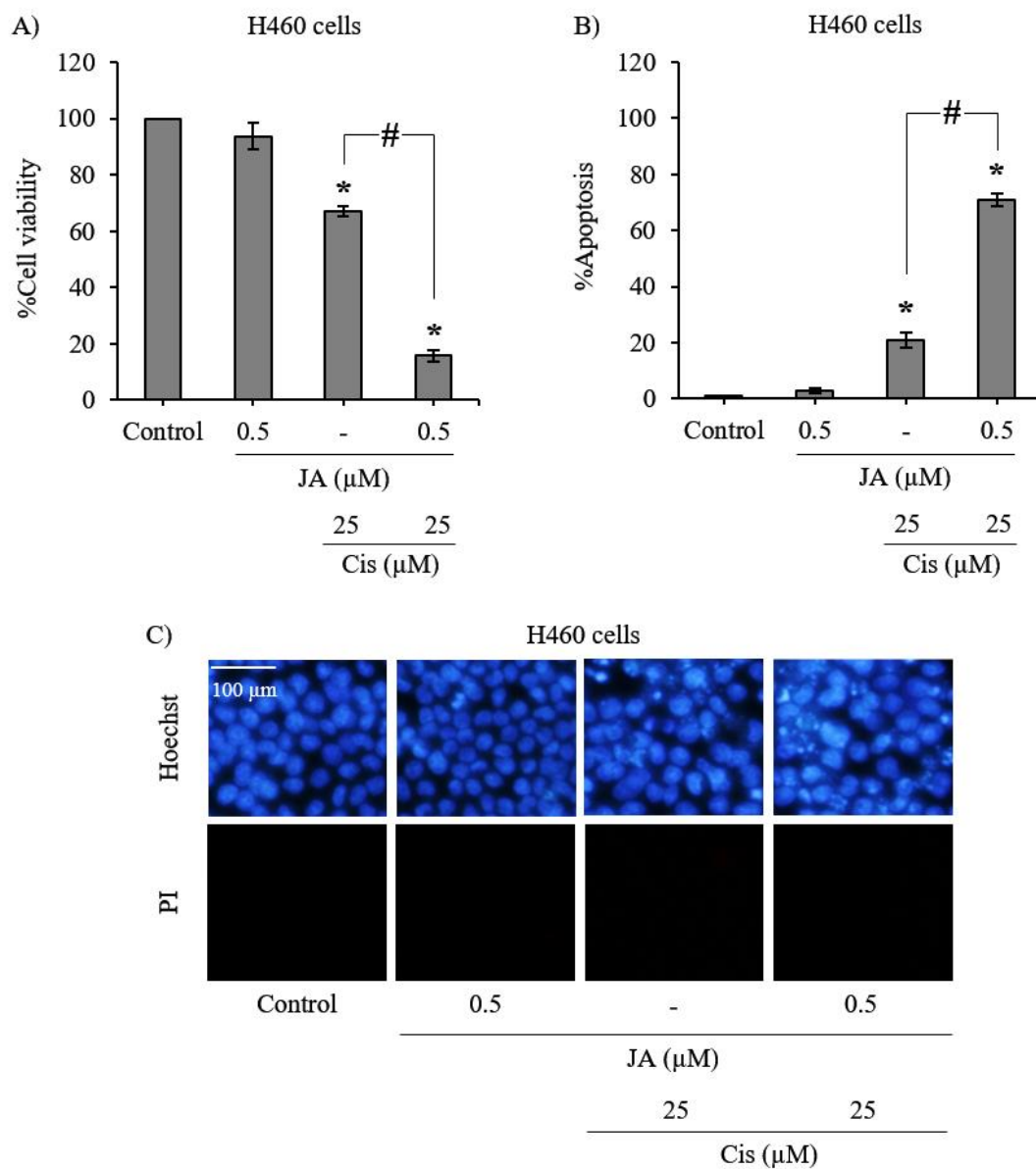


Figure 4.19 The sensitizing effect of jorunnamycin A in cisplatin-induced apoptosis in lung cancer H460 cells. **(A)** Cell viability of H460 cells treated with 0.5 μM jorunnamycin A (JA) for 24 h and 25 μM cisplatin for 24 h was significantly observed as compared to cisplatin treatment group. **(B)** Pretreatment with JA significantly raised %apoptosis induced by cisplatin in comparison to cisplatin treatment alone. **(C)** Visualization of attached H460 cells co-stained with Hoechst33342/PI was used to detected apoptosis cells induced by respective treatment. The %apoptosis **(B)** was analyzed in H460 cells co-stained with Hoechst33342/PI **(C)**. Data represent means \pm SD of three independent

experiments. * $p < 0.05$ versus non-treated control. # $p < 0.05$ versus only cisplatin-treated group.

5.2 Jorunnamycin A sensitizes cisplatin-induced apoptosis in CSC-enriched spheroids

To address the issues of drug resistance and eventual tumor recurrence [17], the co-administration of a natural product with the standard therapy of cisplatin has been regarded as a plausible option for achieving synergy [166]. CSCs are resistant to traditional chemotherapeutic agents [167] and the sensitization of chemo-resistant cells to cisplatin was evaluated after co-administration of jorunnamycin A and cisplatin to CSC-enriched spheroids. The suppressive effect of cisplatin (25 μM) on CSC-enriched spheroids is indicated in Figure 4.20A. Pretreatment with 0.5 μM jorunnamycin A for 24 h obviously sensitized H460 spheroids to cisplatin cytotoxicity. CSC-enriched H460 spheroids treated with cisplatin were evidently diminished in size by day 3 and nearly absent by day 5 in response to pre-incubation with 0.5 μM jorunnamycin A. Furthermore, there was a significant difference in the relative size of the spheroids subjected to cisplatin-only treatment versus the cisplatin-treated spheroids precultured with jorunnamycin A, which was evident within 3–7 days of incubation (Figure 4.20B).

Resistance to chemotherapy has been attributed to lung CSCs [8]. Thus, the CSC-targeted effect of cisplatin was also elucidated through the detection of the CD133^{high} population in CSC-enriched spheroids. CSC-enriched spheroids were pretreated with jorunnamycin A (0.5 μM) for 24 h and further incubated with 25 μM cisplatin for 3 days, then were subjected to flow cytometry analysis. Treatment with either cisplatin (25 μM) or jorunnamycin A (0.5 μM) was able to reduce the %CD133-overexpressing cells in CSC-enriched H460 spheroids (Figure 4.20C). In comparison, a higher reduction of CD133^{high} population was found in cisplatin-treated spheroids that were pre-incubated with jorunnamycin A, compared with the cisplatin-treated only group (Figure 4.20D), which points to a synergistic effect.

To confirm the chemosensitizing activity of jorunnamycin A in CSCs of human lung cancer cells, annexin V-FITC/propidium iodide (PI) staining and subsequent flow cytometry was performed to characterize mode of cell death [168]. Flow cytometry revealed that the untreated, jorunnamycin A-treated and cisplatin-treated CSC populations displayed similar distribution patterns of living cells (annexin V⁻/PI⁻) and early apoptosis (annexin V⁺/PI⁻) (Figure 4.20E). In contrast with the spheroids that received either cisplatin or jorunnamycin A treatment alone, an increased level of early apoptosis cells was found in CSC enriched spheroids that were pretreated with jorunnamycin A (0.5 μ M) for 24 h and further incubated with 25 μ M cisplatin for another 24 h (Figure 4.20F). On the other hand, there was no modification of the %necrosis (annexin V⁻/PI⁺) in any of the treatments. These results strongly indicate that jorunnamycin A sensitized the CSCs of H460 spheroids to cisplatin-induced apoptosis. Indeed, the chemosensitizing effect of jorunnamycin A was also observed in CSCs spheroids obtained from lung cancer H23 (Figure 4.21A, B) and A549 cells (Figure 4.21C, D), which strongly indicate the anticancer activity of jorunnamycin A targeting of various lung CSCs.

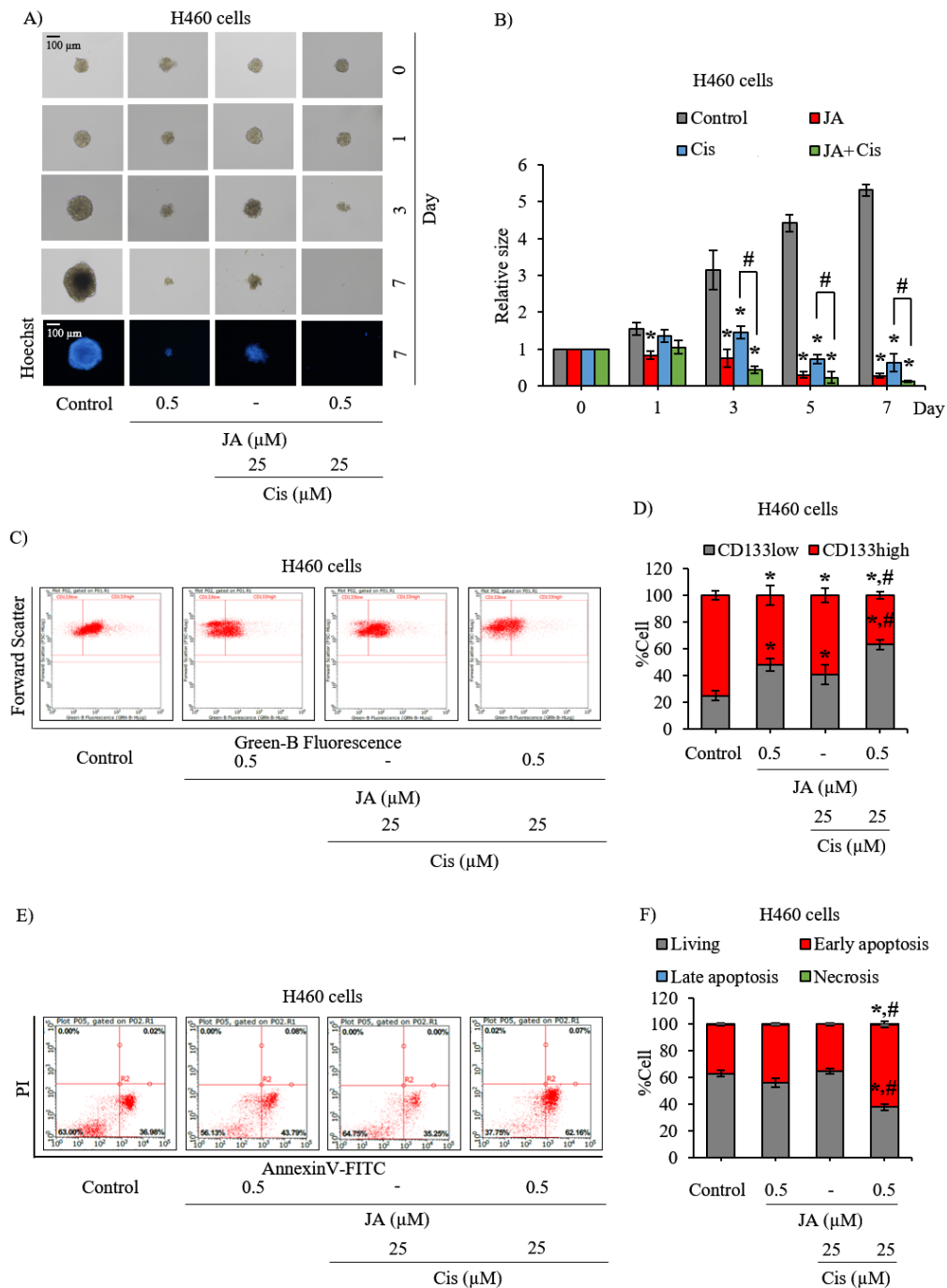


Figure 4.20 Sensitization of CSC-enriched lung cancer cells to cisplatin-induced apoptosis by jorunnamycin A. **(A)** Pre-incubation with jorunnamycin A (JA) followed by cisplatin (Cis) treatment dramatically suppressed CSC-enriched H460 spheroids cultured for 7 days. All single three-dimensional (3D) CSC spheroids were photographed by optical microscopy (10x), and spheroid images depicting bright blue fluorescence of Hoechst33342 were obtained by fluorescence microscopy (10x) at day

7 of treatment. (B) A greater decrease in the spheroid size relative to culture with cisplatin only was observed at days 3–7 in the combination treatment of 0.5 μ M JA and 25 μ M cisplatin. (C) Flow cytometry analysis reveals the decrease of CD133^{high} population in JA-pretreated CSCs after incubation with cisplatin for 3 days. (D) The reduction of %CD133^{high} population of CSC-enriched spheroids treated with cisplatin was evidenced in 24 h pretreatment with JA followed by 72 h cisplatin treatment. (E) Flow cytometry plots of CSC-enriched H460 spheroids co-stained with annexin V-FITC and propidium iodide (PI) indicate the increase of early apoptosis after the incubation with JA for 24 h prior to 24 h of cisplatin treatment. (F) A reduction of %living cells was significantly observed following cotreatment with JA and cisplatin in CSC-enriched population. The relative size indicated in (B) was analyzed from the morphology of CSC-enriched spheroids, as presented in (A). The %cell demonstrated in (D, F) was calculated from dot plots, as presented in (C, E), respectively. Data represent means \pm SD of three independent experiments. * p < 0.05 versus non-treated control. # p < 0.05 versus only cisplatin-treated group.

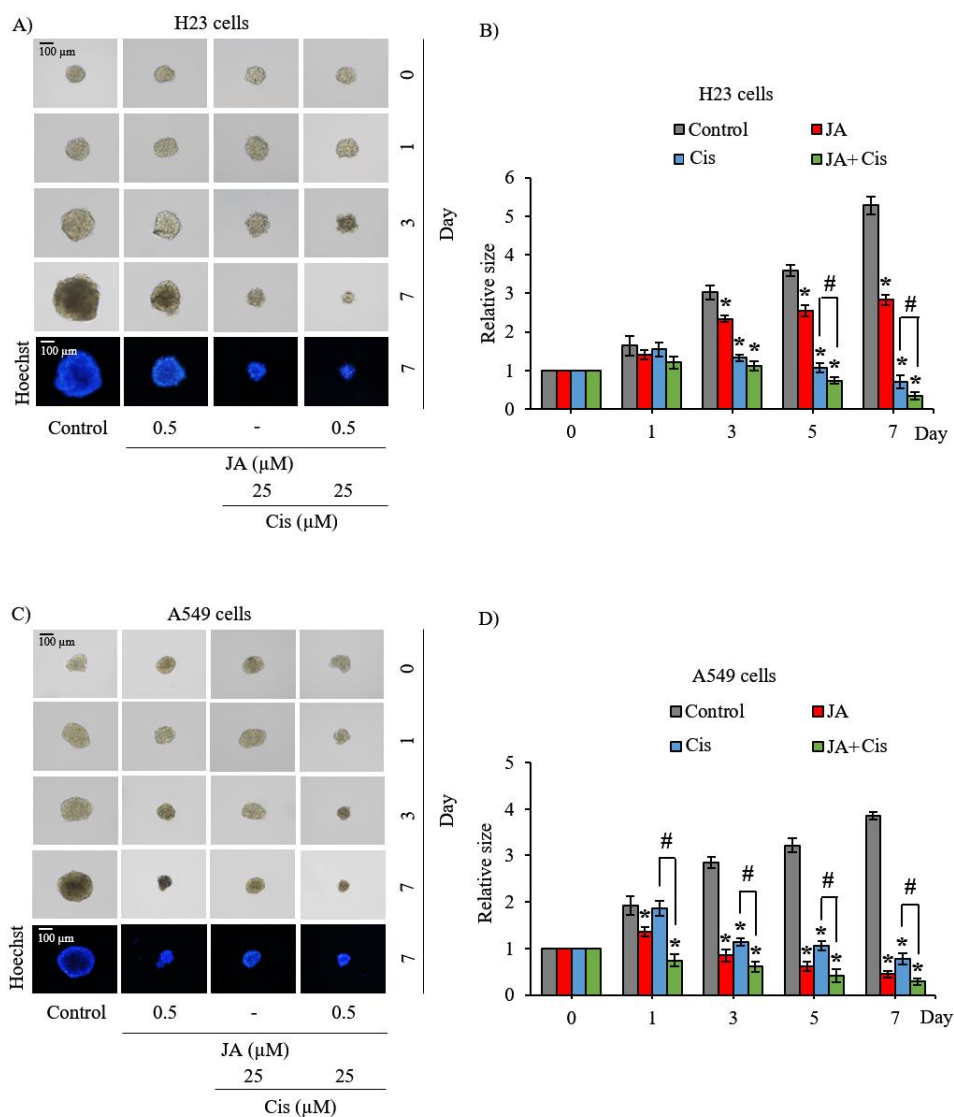


Figure 4.21 Cisplatin sensitizing effect of jorunnamycin A in various lung CSCs. CSC-enriched spheroids obtained from (A) H23 and (C) A549 lung cancer cells were precultured with nontoxic concentration (0.5 μM) of jorunnamycin A (JA) prior to treatment with 25 μM cisplatin (Cis) for 7 days. All single three-dimensional (3D) CSC spheroids were photographed by optical microscopy (10 \times), and spheroid images depicting bright blue fluorescence of Hoechst33342 were obtained by fluorescence microscopy (10 \times) at day 7 of treatment. Pretreatment with JA significantly diminished relative size of (B) H23 and (D) A549 CSC-enriched spheroids cultured with cisplatin. The relative size indicated in (B, D) was analyzed from the morphology of CSC-enriched spheroids, as presented in (A, C), respectively. Data represent means \pm SD of three

independent experiments. * $p < 0.05$ versus non-treated control. # $p < 0.05$ versus only cisplatin-treated group.

5.3 Modulation of p53 and Bcl-2 family proteins in CSC-enriched spheroids mediated by jorunnamycin A

To investigate the underlying mechanisms involved in the chemosensitizing activity of jorunnamycin A in CSCs of human lung cancer cells, Western blot analysis was performed in the CSC-enriched H460 spheroids after culture with jorunnamycin A (0.05–0.5 μM) for 24 h. Figure 4.22A presents the expression levels of tumor suppressor p53 protein and related apoptosis-modulating proteins. Remarkably, p53 was upregulated in CSC-enriched spheroids treated with jorunnamycin A for 24 h in a dose-dependent manner. In addition, jorunnamycin A (0.05–0.5 μM) significantly reduced the level of Bcl-2, an antiapoptotic protein, while the expression of Mcl-1 (myeloid cell leukemia 1) and BAX (Bcl-2-associated X) was not altered in response to the treatment with jorunnamycin A (Figure 4.22B). This information further confirms the apoptosis regulating capacity of jorunnamycin A in CSCs of human lung cancer cells.

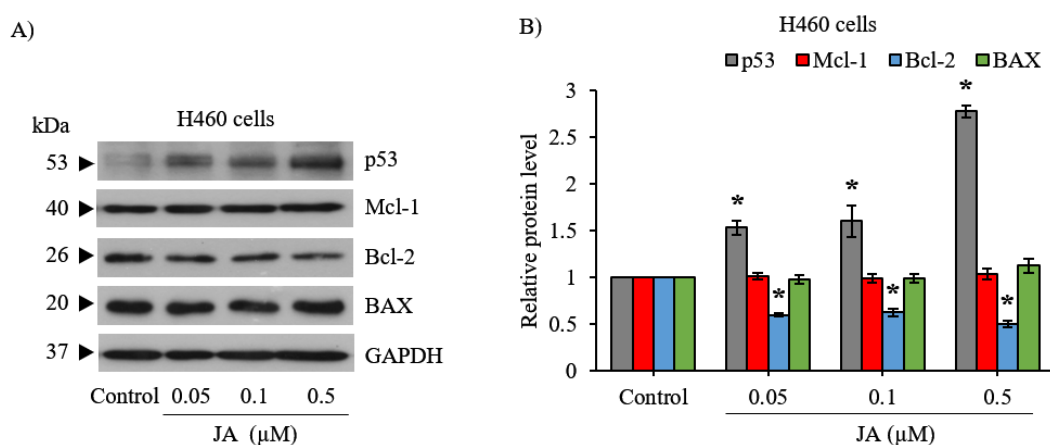


Figure 4.22 Alteration of apoptosis-related proteins in jorunnamycin A-treated lung CSCs. **(A)** Western blot analysis reveals the decline of anti-apoptosis Bcl-2 protein in CSC-enriched H460 spheroids incubated with 0.05–0.5 μM of jorunnamycin A (JA) for 24 h. **(B)** The relative protein levels were analyzed from the chemiluminescent signal detected in Western blotting, as presented in **(A)**. JA obviously upregulated the

expression level of p53, a tumor suppressor protein in CSC-enriched H460 cells, in a dose-dependent manner. Data represent means \pm SD of three independent experiments. * $p < 0.05$ versus non-treated control.



CHAPTER V DISCUSSION AND CONCLUSION

The search for new strategies for improving therapeutic outcomes in lung cancer patients has led to great research interest in CSCs, a unique subpopulation in tumor tissue [7, 67, 91, 169, 170]. CSCs display self-renewal capacity to generate identical daughter cells, accounting for heterogeneity, therapeutic resistance, and other malignancies [85, 171]. Cumulative evidence indicates that the modulating self-renewal pathways of CSCs are a promising strategy for cancer therapy [85, 172, 173] since these self-renewing and extremely tumorigenic CD133-overexpressing subpopulations have been clinically observed to produce poor clinical outcomes [174]. The outstanding anticancer potential of jorunnamycin A was indicated by the suppressive effect and chemosensitizing activity in CSCs derived from various human lung cancer cells, including H460 (p53 and KRas wild type), H23 (p53 and KRas mutant), and A549 (KRas mutant). The composition of the subpopulation that overexpresses CSC protein markers and exhibits self-renewal activity has been demonstrated in these lung cancer cells [16, 156]. The tumor-initiating activity of CSCs isolated from H460 and A549 cells has been reported in an *in vivo* experiment [156]. Additionally, the selective suppression on CSCs of jorunnamycin A was supported with no alteration of stemness traits in normal lung epithelial BEAS-2B cells cultured with jorunnamycin A (Figure 4.12). The selective cancer activity of jorunnamycin A might results from overactivation of survival signaling Akt and GSK3 pathway in uncontrolled cell growth or cancer cells [175, 176].

As an improvement in preclinical testing, 3D spheroids that mimic *in vivo* conditions and contain important tumor features, particularly drug resistance and stem-like phenotype, serve as a more robust and valuable model for *in vitro* screening for lung cancer treatments [44, 167]. Culture under detachment condition used in 3D spheroid assays has been used to successfully stimulate and maintain the self-renewal capability of the CSC subpopulation in cancer cells [77-79, 177]. This coincides with the disclosed results revealing that secondary spheroids from various human lung cancer cells obtained from 3D anchorage-independent culture were found to comprise approximately 80% CSCs that highly express CD133, a CSC protein marker [44, 173]

(Figures 4.4B, 4.9F and 4.10F). Moreover, the overexpression of Sox2, Nanog and Oct-4, the transcription factors mediating self-renewal and proliferation in CSCs [85], are notably expressed in the untreated spheroids. Collectively, the present results suggest that the 3D spheroids are enriched with CSCs. It is worth noting that the number of CSCs characterized as CD133^{high} cancer cells was only 1–5% of total human lung cancer populations maintained under attachment culture (data not shown). Therefore, the reduction of both the relative size (Figures 4.2B, 4.9B and 4.10B) and the %highCD133 cells of CSC-enriched spheroids (Figures 4.4B, 4.9F and 4.10F) distinctly demonstrated the suppressive effect of jorunnamycin A on self-renewal in CSCs of human lung cancer cells. It is also noted that the dot plots of highCD133 cells in cisplatin-treated group were raised in the range of very high green-B fluorescence intensity ($\log_{10}^3\text{-}10^5$) corresponding with the enlargement of CSC population in lung cancer cells after cisplatin treated reported by various studies [12, 17]. Therefore, re-analysis in sub-dividing group of highCD133 cells in cisplatin-treated group might be benefit for emphasizing cisplatin-enriched CSCs in lung cancer cells.

Self-renewal activity is modulated through the collaboration of Oct-4 and Sox2 and the consequent transcription of the Nanog stemness gene [22, 83]. Specifically, abnormal expression of Nanog accounts for CSC self-renewal and proliferation, while Oct-4 is highly expressed and more upregulated in response to cisplatin treatment in lung CSCs [85]. The role of Sox2 in regulating tumor development and maintenance of pluripotency in lung cancer has also been documented [84]. Moreover, co-expression of Oct-4 and Nanog is required for the induction of CSC properties and the enhancement of malignancy in lung adenocarcinoma [86]. On the contrary, the depletion of these stemness transcription factors decreases self-renewal activity and tumor formation in lung cancer [19, 79, 87]. Remarkably, downregulated mRNA levels of Nanog, Oct-4, and Sox2 transcription factor (Figures 4.5A, 4.11A and 4.11B) in jorunnamycin A-treated CSC-enriched spheroids evidently confirmed the inhibitory effect on self-renewal in lung CSCs.

In lung CSCs, the Akt molecule not only promotes survival but also regulates the expression of self-renewal transcription factors [19, 21, 23, 178, 179]. The downregulation of stemness transcription factors is mediated through the Akt/GSK-

$3\beta/\beta$ -catenin cascade [91], which correlates with the suppressive effect of jorunnamycin A on these key proteins in the CSC-enriched spheroids obtained from H460 cells (Figure 4.5D). Although jorunnamycin A-mediated downregulation of Akt signaling has been previously reported in various human lung cancer cells [45], the investigation of CSC-related mechanisms demonstrated the suppression of p-Akt/Akt level only in CSC-enriched H460 spheroids but not in CSC subpopulations derived from H23 (Figure 4.11C,D) and A549 cells (Figure 4.11E,F). The low correlation between Akt signal and down-stream molecules presented in H23 and A549 spheroids might result from the fact that the alteration of an up-stream mediator should be detected at an earlier time point. Moreover, KRAS mutation has been reported to resist to AKT inhibitors [180-182]. The effect of jorunnamycin A on Akt signaling in H460 cells over H23 and A549 cells might result from the inhibition on KRAS wild type subsequent with Akt inhibition while effect of Akt signaling was not clearly observed in H23 and A549 cells which are KRAS mutation cells. However, the suppressive effect on the CSC phenotype (Figures 4.2, 4.3, 4.4, 4.9 and 4.10) and diminution of related stemness transcription factors (Figures 4.5A, 4.11A and 4.11B) indicates the inhibitory role of jorunnamycin A in the GSK-3 β / β -catenin pathway. Therefore, the present study reveals that jorunnamycin A downregulation of Nanog, Oct-4, and Sox2 might be mediated through the GSK-3 β / β -catenin signal, although the direct targets of jorunnamycin A have not been thoroughly elucidated. Nevertheless, the role of Akt as well as its downstream signaling molecules, GSK-3 β and β -catenin in suppressing CSC-phenotype as observed in jorunnamycin A-treated cells should be further evaluated.

CSCs are also known as tumor-initiating cells since these cells are responsible for maintaining primary tumors as well as initiating secondary ones [183]. The restraint on this defining trait of CSCs was suggested with the marked diminution of cancer spheroid initiating cells assessed via LDA in jorunnamycin A-treated lung cancer cell populations (Figures 4.2B, 4.9B and 4.10B). Tumor initiation capacity has been found to be facilitated by EMT, a dynamic process of converting epithelial cells into a mesenchymal phenotype [184, 185]. The molecular link between EMT and CSC traits of self-renewal and tumor initiation has garnered much interest. Indeed, manipulating EMT is regarded as a potential strategy for targeting CSCs [186]. A previous study

proposed that jorunnamycin A at nontoxic concentration (0.05–0.5 μM) stimulates detachment-induced cell death and suppresses anchorage-independent growth in human lung cancer cells by inhibiting EMT [45]. The barely detected level of cancer spheroid initiation in response to treatment with jorunnamycin A at a low concentration of 0.05 μM (Figures 4.2A, 4.9A and 4.10A) might result from the combined activity of sensitizing detached cell death, inhibiting EMT, and suppressing of the CSC phenotype. In this study, the suppressive effect of jorunnamycin A was demonstrated only on cancer spheroid-initiating and self-renewal capabilities of CSC-enriched lung cancer cells however the effect of this marine compound on differentiation activity in CSCs should be additionally investigated. Nevertheless, the efficacy of jorunnamycin A at lower concentration (<0.05 μM) on tumor initiation in both in vitro and in vivo models should be further elucidated.

ROS have been considered as the reactive molecules regulating various cell functions [187]. It has been showed that lowering ROS levels were found in CSCs compared with non-CSCs because their raised antioxidant capacity to prevent oxidative damage [34, 35, 37]. Thus, excessive ROS level could be a potential *strategy* for eliminating CSCs through lessen clonogenicity and mediate CSC death [188]. In the present study, jorunnamycin A was also shown to induce ROS generation in CSC-enriched lung cancer cells (Figure 4.13). Although jorunnamycin A reveals a pro-oxidant activity, the investigation of cellular ROS alteration and tumor-initiating capacity illustrated that pro-oxidant event of jorunnamycin A does not associate with suppressive effect on cancer spheroid-initiating cells in lung cancer cells (Figure 4.14). Meanwhile pre-incubation with NAC, antioxidant agent, prior jorunnamycin A treatment moderated suppressive effect of jorunnamycin A on self-renewal capacity of CSC subpopulation (Figure 4.15). These results correspond with previous data that ROS modulation inhibited tumor development with ability to eliminate CSC phenotypes in NSCLC by suppression of Oct-4, Nanog and Sox2 mRNA levels [37]. However, the link between jorunnamycin A-mediated ROS and the alteration of related stemness transcription factors should be further clarified.

Another point investigated in this study is the effect of autophagy modulating activity on CSC suppression mediated by jorunnamycin. Autophagy is an individual-

degraded process which preserves cellular homeostasis. Autophagy not only maintains energy balance under nutrition deficiency but also acts as a housekeeper to eradicate misfolded-proteins, damaged-organelles and intracellular pathogens [189]. The induction of autophagy level in suppressing CSC-phenotype has been evaluated [190]. Herein, the autophagy modulating effect of jorunnamycin A was demonstrated by upregulation of autophagy-related proteins in CSC-enriched spheroids (Figure 4.16) however, its enhancement of autophagic response dose not relate with inhibitory effect on tumor-initiating cells in lung cancer cells (Figure 4.17). Interestingly, the regulation on self-renewal capacity of CSC-enriched H460 spheroids was facilitated by the autophagy inducing effect of jorunnamycin A (Figure 4.18). These results correspond with recent evidence demonstrating that suppressing effect in CSC-enriched spheroids was mediated by autophagy induction which involved with inhibition of Akt pathway and diminution of Oct-4, stemness-related protein marker [191]. Moreover, the autophagy modulated self-renewal inhibition in CSCs might result from the modulation of the interaction between the autophagic protein, Beclin-1 and anti-apoptosis protein, Bcl-2 [192]. Bcl-2 reportedly showed as a Beclin-1 interacting protein inhibitor resulting in autophagy disruption [193]. Jorunnamycin A down-regulated Bcl-2 protein consequently autophagic response was increased. Further studies are required to determine the regulation of autophagy on stemness transcription factors and the association of jorunnamycin A-induced ROS and autophagy induction in CSC-subpopulation.

Although cisplatin or cis-diamminedichloroplatinum (II) has been widely used as a first-line platinum based-chemotherapy for lung cancer patients [194], eventual drug resistance and cancer relapse severely limit clinical benefit [195, 196]. The subpopulation of CSCs in tumors are recognized contributors to cisplatin resistance in lung cancer [197-199]. The promising CSC-targeting activity of jorunnamycin A was demonstrated by its enhancement of cisplatin-induced apoptosis in CSC-enriched spheroids (Figure 4.20C and D). Pre-incubation for 24 h with jorunnamycin A (0.05–0.5 μ M) activated p53 and subsequently downregulated anti-apoptosis Bcl-2 protein in CSC-enriched lung cancer cells (Figure 4.22). These results correspond with previous data showing that p53 is a key modulator for drug sensitization in CSCs [200] and a

promoter of apoptosis through direct inhibition on Bcl-2 family proteins, including anti-apoptosis Bcl-2 [201]. Furthermore, Bcl-2 downregulation mediates apoptosis induction in chemo-resistant lung CSCs [202]. It should be noted that jorunnamycin A at nontoxic concentrations (0.05–0.5 μM) was previously reported to augment the level of BAX, a pro-apoptosis protein in human lung cancer cells [45]; however, the overexpression of BAX was not indicated in CSC-enriched spheroids treated with jorunnamycin A (Figure 4.22). Although sole treatment with either jorunnamycin A (0.5 μM) or cisplatin (25 μM) did not alter the %living cells, preincubation with jorunnamycin A prior to cisplatin treatment greatly triggered apoptosis (Figure 4.20E and F) and abolished the CD133high population in CSCs-enriched H460 spheroids (Figure 4.20C and D). Taken together, this study provides the potential benefits of jorunnamycin A in cancer treatment by inhibition of self-renewal and drug resistance in CSCs (Figure 5.1).

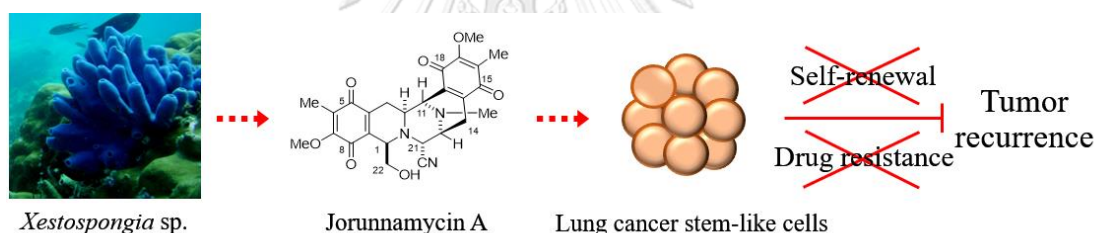


Figure 5.1 Jorunnamycin A potential benefits in cancer treatment

It is a fact that the inactivation of p53 and the consequent upregulation of downstream Bcl-2 protein contributes to chemotherapeutic resistance in both normal cancer and the CSC subpopulation. Although Bcl-2 inhibition has an established apoptosis-inducing effect in normal cancer cells, targeted Bcl-2 inhibition alone may insufficiently trigger apoptosis in CSCs [203]. Not only is the stem-like phenotype regulated by Nanog, a stemness transcription factor, but the apoptosis signal is also regulated by Nanog. It has been revealed that Nanog diminishes p53 expression [16, 80, 140]. Moreover, downregulation of Nanog and activation of p53 were found to efficiently improve chemotherapeutic response, especially in lung CSCs [141]. Corresponding with the results obtained in this study, the chemosensitizing effect of

lorunnamycin A may result from the modulation on apoptosis-regulating proteins, including p53 and Bcl-2 mediated by stemness transcription factors.

By conclusion, this study reveals that lorunnamycin A selectively suppresses stem-like phenotypes in lung CSC-enriched spheroids through the inhibition of GSK-3 β / β -catenin signal mediating downregulation of Nanog, Oct-4 and Sox2 transcription factors. Furthermore, the anticancer activity of lorunnamycin A targeting on CSCs is evidenced by the sensitizing effect on cisplatin-induced apoptosis in CSC-enriched lung cancer cells via upregulation of p53 tumor suppressor protein and decreased expression of anti-apoptosis Bcl-2 (Figure 5.2). These data support the further development of lorunnamycin A as an effective chemosensitizer for overcoming drug resistance and eradicating CSCs in lung cancer treatment.

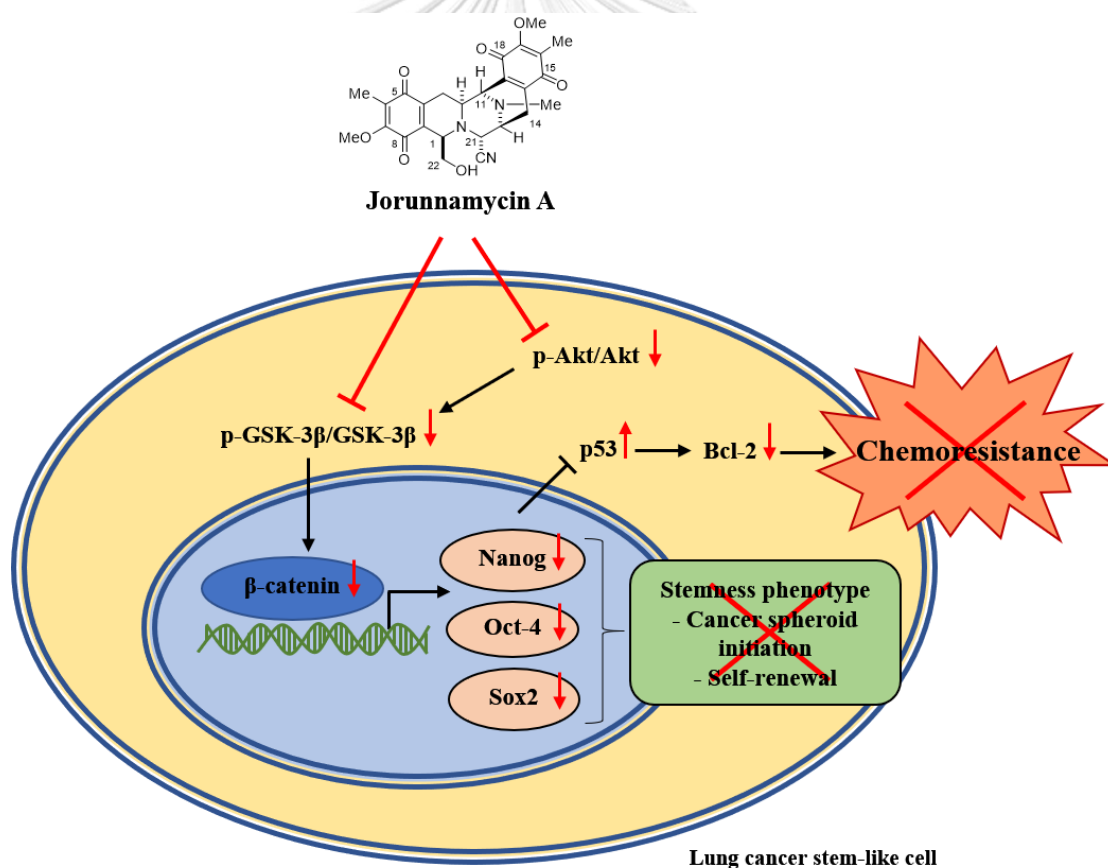


Figure 5.2 Schematic representation of lorunnamycin A-mediated suppression of CSC phenotype and sensitization of CSC-enriched lung cancer cells to cisplatin-induced apoptosis. The symbols and arrows in red color depict the effect of lorunnamycin A in CSCs of human lung cancer cells.

REFERENCES

1. Sung, H., et al., *Global cancer statistics 2020: GLOBOCAN estimates of incidence and mortality worldwide for 36 cancers in 185 countries*. CA Cancer J Clin, 2021.
2. Siegel, R.L., K.D. Miller, and A. Jemal, *Cancer statistics, 2019*. CA Cancer J Clin, 2019. **69**(1): p. 7-34.
3. Zhang, J., et al., *Intratumor heterogeneity in localized lung adenocarcinomas delineated by multiregion sequencing*. Science, 2014. **346**(6206): p. 256-9.
4. Dagogo-Jack, I. and A.T. Shaw, *Tumour heterogeneity and resistance to cancer therapies*. Nat Rev Clin Oncol, 2018. **15**(2): p. 81-94.
5. Tang, D.G., *Understanding cancer stem cell heterogeneity and plasticity*. Cell Res, 2012. **22**(3): p. 457-472.
6. Abdullah, L.N. and E.K. Chow, *Mechanisms of chemoresistance in cancer stem cells*. Clin Transl Med, 2013. **2**(1): p. 3.
7. Prabavathy, D., Y. Swarnalatha, and N. Ramadoss, *Lung cancer stem cells-origin, characteristics and therapy*. Stem Cell Investig, 2018. **5**: p. 6.
8. Suresh, R., et al., *The Role of Cancer Stem Cells in Recurrent and Drug-Resistant Lung Cancer*. Adv Exp Med Biol, 2016. **890**: p. 57-74.
9. Zakaria, N., et al., *Targeting Lung Cancer Stem Cells: Research and Clinical Impacts*. Front Oncol, 2017. **7**: p. 80.
10. Chen, S.F., et al., *Pulmonary Adenocarcinoma in Malignant Pleural Effusion Enriches Cancer Stem Cell Properties during Metastatic Cascade*. PLoS One, 2013. **8**(5): p. e54659.
11. Chen, Y.C., et al., *Oct-4 expression maintained cancer stem-like properties in lung cancer-derived CD133-positive cells*. PLoS One, 2008. **3**(7): p. e2637.
12. Bertolini, G., et al., *Highly tumorigenic lung cancer CD133+ cells display stem-like features and are spared by cisplatin treatment*. Proc Natl Acad Sci U S A, 2009. **106**(38): p. 16281-16286.
13. Chen, E., et al., *The prognostic value of CSCs biomarker CD133 in NSCLC: a meta-analysis*. Oncotarget, 2016. **7**(35): p. 56526-56539.

14. Slawek, S., et al., *Pluripotency transcription factors in lung cancer-a review*. *Tumour Biol*, 2016. **37**(4): p. 4241-9.
15. Amini, S., et al., *The expressions of stem cell markers: Oct4, Nanog, Sox2, nucleostemin, Bmi, Zfx, Tcl1, Tbx3, Dppa4, and Esrrb in bladder, colon, and prostate cancer, and certain cancer cell lines*. *Anat Cell Biol*, 2014. **47**(1): p. 1-11.
16. Wang, Y., et al., *Utilization of lung cancer cell lines for the study of lung cancer stem cells*. *Oncol Lett*, 2018. **15**(5): p. 6791-6798.
17. Wang, L., et al., *Cisplatin-enriching cancer stem cells confer multidrug resistance in non-small cell lung cancer via enhancing TRIB1/HDAC activity*. *Cell Death Dis*, 2017. **8**(4): p. e2746.
18. Zhao, Q.W., et al., *Aktmediated phosphorylation of Oct4 is associated with the proliferation of stemlike cancer cells*. *Oncol Rep*, 2015. **33**(4): p. 1621-9.
19. Srinual, S., P. Chanvorachote, and V. Pongrakhananon, *Suppression of cancer stem-like phenotypes in NCI-H460 lung cancer cells by vanillin through an Akt-dependent pathway*. *Int J Oncol*, 2017. **50**(4): p. 1341-1351.
20. Liu, W., et al., *Dioscin inhibits stem-cell-like properties and tumor growth of osteosarcoma through Akt/GSK3/beta-catenin signaling pathway*. *Cell Death Dis*, 2018. **9**(3): p. 343.
21. Cheng, H., et al., *Targeting the PI3K/AKT/mTOR pathway: potential for lung cancer treatment*. *Lung Cancer Manag*, 2014. **3**(1): p. 67-75.
22. Lin, Y., et al., *Reciprocal regulation of Akt and Oct4 promotes the self-renewal and survival of embryonal carcinoma cells*. *Mol Cell*, 2012. **48**(4): p. 627-640.
23. Li, W., et al., *Dual inhibiting OCT4 and AKT potently suppresses the propagation of human cancer cells*. *Sci Rep*, 2017. **7**: p. 46246.
24. Xia, P. and X.Y. Xu, *PI3K/Akt/mTOR signaling pathway in cancer stem cells: from basic research to clinical application*. *Am J Cancer Res*, 2015. **5**(5): p. 1602-9.
25. Sun, R., et al., *Nanoparticle-facilitated autophagy inhibition promotes the efficacy of chemotherapeutics against breast cancer stem cells*. *Biomaterials*, 2016. **103**: p. 44-55.

26. Galavotti, S., et al., *The autophagy-associated factors DRAM1 and p62 regulate cell migration and invasion in glioblastoma stem cells*. *Oncogene*, 2013. **32**(6): p. 699-712.
27. Kantara, C., et al., *Curcumin promotes autophagic survival of a subset of colon cancer stem cells, which are ablated by DCLK1-siRNA*. *Cancer Res*, 2014. **74**(9): p. 2487-98.
28. Kaur, J. and J. Debnath, *Autophagy at the crossroads of catabolism and anabolism*. *Nat Rev Mol Cell Biol*, 2015. **16**(8): p. 461-72.
29. Schmitz, K.J., et al., *Prognostic relevance of autophagy-related markers LC3, p62/sequestosome 1, Beclin-1 and ULK1 in colorectal cancer patients with respect to KRAS mutational status*. *World J Surg Oncol*, 2016. **14**(1): p. 189.
30. Wang, R.C., et al., *Akt-mediated regulation of autophagy and tumorigenesis through Beclin 1 phosphorylation*. *Science*, 2012. **338**(6109): p. 956-9.
31. Lu, R., et al., *Inhibition of CD133 Overcomes Cisplatin Resistance Through Inhibiting PI3K/AKT/mTOR Signaling Pathway and Autophagy in CD133-Positive Gastric Cancer Cells*. *Technol Cancer Res Treat*, 2019. **18**: p. 1533033819864311.
32. Ojha, R., S. Bhattacharyya, and S.K. Singh, *Autophagy in Cancer Stem Cells: A Potential Link Between Chemoresistance, Recurrence, and Metastasis*. *Biores Open Access*, 2015. **4**(1): p. 97-108.
33. Hao, C., G. Liu, and G. Tian, *Autophagy inhibition of cancer stem cells promotes the efficacy of cisplatin against non-small cell lung carcinoma*. *Ther Adv Respir Dis*, 2019. **13**: p. 1753466619866097.
34. Diehn, M., et al., *Association of reactive oxygen species levels and radioresistance in cancer stem cells*. *Nature*, 2009. **458**(7239): p. 780-3.
35. Dando, I., et al., *Antioxidant Mechanisms and ROS-Related MicroRNAs in Cancer Stem Cells*. *Oxid Med Cell Longev*, 2015. **2015**: p. 425708.
36. Kumari, S., et al., *Reactive Oxygen Species: A Key Constituent in Cancer Survival*. *Biomark Insights*, 2018. **13**: p. 1177271918755391.
37. Wang, J., et al., *Inhibition of cancer growth in vitro and in vivo by a novel ROS-modulating agent with ability to eliminate stem-like cancer cells*. *Cell Death Dis*, 2017. **8**(6): p. e2887.

38. Petpiroon, N., et al., *TiO₂ Nanosheets Inhibit Lung Cancer Stem Cells by Inducing Production of Superoxide Anion*. *Mol Pharmacol*, 2019. **95**(4): p. 418-432.
39. Chanvorachote, P. and S. Luanpitpong, *Iron induces cancer stem cells and aggressive phenotypes in human lung cancer cells*. *Am J Physiol Cell Physiol*, 2016. **310**(9): p. C728-39.
40. Charupant, K., et al., *Jorunnamycins A-C, new stabilized renieramycin-type bistetrahydroisoquinolines isolated from the Thai nudibranch Jorunna funebris*. *Chem Pharm Bull (Tokyo)*, 2007. **55**(1): p. 81-86.
41. Charupant, K., et al., *Chemistry of renieramycins. Part 8: synthesis and cytotoxicity evaluation of renieramycin M-jorunnamycin A analogues*. *Bioorg Med Chem*, 2009. **17**(13): p. 4548-58.
42. Chamni, S., et al., *Chemistry of Renieramycins. 17. A New Generation of Renieramycins: Hydroquinone 5-O-Monoester Analogues of Renieramycin M as Potential Cytotoxic Agents against Non-Small-Cell Lung Cancer Cells*. *J Nat Prod*, 2017. **80**(5): p. 1541-1547.
43. Halim, H., et al., *Anticancer and antimetastatic activities of Renieramycin M, a marine tetrahydroisoquinoline alkaloid, in human non-small cell lung cancer cells*. *Anticancer Res*, 2011. **31**(1): p. 193-201.
44. Sirimangkalakitti, N., et al., *Renieramycin M Attenuates Cancer Stem Cell-like Phenotypes in H460 Lung Cancer Cells*. *Anticancer Res*, 2017. **37**(2): p. 615-621.
45. Ecoy, G.A.U., et al., *Jorunnamycin A from Xestospongia sp. Suppresses Epithelial to Mesenchymal Transition and Sensitizes Anoikis in Human Lung Cancer Cells*. *J Nat Prod*, 2019. **82**(7): p. 1861-1873.
46. Bray, F., et al., *Global cancer statistics 2018: GLOBOCAN estimates of incidence and mortality worldwide for 36 cancers in 185 countries*. *CA Cancer J Clin*, 2018. **68**(6): p. 394-424.
47. Siegel, R.L., K.D. Miller, and A. Jemal, *Cancer statistics, 2020*. *CA Cancer J Clin*, 2020. **70**(1): p. 7-30.
48. de Groot, P.M., et al., *The epidemiology of lung cancer*. *Transl Lung Cancer Res*, 2018. **7**(3): p. 220-233.

49. Inamura, K., *Lung Cancer: Understanding Its Molecular Pathology and the 2015 WHO Classification*. Front Oncol, 2017. **7**: p. 193.
50. Song, H., et al., *Functional characterization of pulmonary neuroendocrine cells in lung development, injury, and tumorigenesis*. Proc Natl Acad Sci U S A, 2012. **109**(43): p. 17531-6.
51. Lemjabbar-Alaoui, H., et al., *Lung cancer: Biology and treatment options*. Biochim Biophys Acta, 2015. **1856**(2): p. 189-210.
52. Pietanza, M.C., et al., *Small cell lung cancer: will recent progress lead to improved outcomes?* Clin Cancer Res, 2015. **21**(10): p. 2244-55.
53. Zappa, C. and S.A. Mousa, *Non-small cell lung cancer: current treatment and future advances*. Transl Lung Cancer Res, 2016. **5**(3): p. 288-300.
54. Bender, E., *Epidemiology: The dominant malignancy*. Nature, 2014. **513**(7517): p. S2-3.
55. Shepherd, F.A., et al., *The International Association for the Study of Lung Cancer lung cancer staging project: proposals regarding the clinical staging of small cell lung cancer in the forthcoming (seventh) edition of the tumor, node, metastasis classification for lung cancer*. J Thorac Oncol, 2007. **2**(12): p. 1067-77.
56. Goldstraw, P., et al., *The IASLC Lung Cancer Staging Project: Proposals for Revision of the TNM Stage Groupings in the Forthcoming (Eighth) Edition of the TNM Classification for Lung Cancer*. J Thorac Oncol, 2016. **11**(1): p. 39-51.
57. Tsvetkova, E. and G.D. Goss, *Drug resistance and its significance for treatment decisions in non-small-cell lung cancer*. Curr Oncol, 2012. **19**(Suppl 1): p. S45-51.
58. Lackey, A. and J.S. Donington, *Surgical management of lung cancer*. Semin Intervent Radiol, 2013. **30**(2): p. 133-40.
59. Tanoue, L.T. and F.C. Detterbeck, *New TNM classification for non-small-cell lung cancer*. Expert Rev Anticancer Ther, 2009. **9**(4): p. 413-23.
60. Kim, C.S. and M.D. Jeter, *Radiation Therapy, Early Stage Non-Small Cell Lung Cancer*, in *StatPearls*. 2020: Treasure Island (FL).
61. Masters, G.A., et al., *Systemic Therapy for Stage IV Non-Small-Cell Lung Cancer: American Society of Clinical Oncology Clinical Practice Guideline Update*. J Clin Oncol, 2015. **33**(30): p. 3488-515.

62. Kelly, K., et al., *Randomized phase III trial of paclitaxel plus carboplatin versus vinorelbine plus cisplatin in the treatment of patients with advanced non-small-cell lung cancer: a Southwest Oncology Group trial*. J Clin Oncol, 2001. **19**(13): p. 3210-8.
63. Scagliotti, G.V., et al., *Phase III randomized trial comparing three platinum-based doublets in advanced non-small-cell lung cancer*. J Clin Oncol, 2002. **20**(21): p. 4285-91.
64. Fossella, F., et al., *Randomized, multinational, phase III study of docetaxel plus platinum combinations versus vinorelbine plus cisplatin for advanced non-small-cell lung cancer: the TAX 326 study group*. J Clin Oncol, 2003. **21**(16): p. 3016-24.
65. Nurgali, K., R.T. Jagoe, and R. Abalo, *Editorial: Adverse Effects of Cancer Chemotherapy: Anything New to Improve Tolerance and Reduce Sequelae?* Front Pharmacol, 2018. **9**: p. 245.
66. Joo, W.D., I. Visintin, and G. Mor, *Targeted cancer therapy--are the days of systemic chemotherapy numbered?* Maturitas, 2013. **76**(4): p. 308-14.
67. Yuan, M., et al., *The emerging treatment landscape of targeted therapy in non-small-cell lung cancer*. Signal Transduct Target Ther, 2019. **4**: p. 61.
68. Kanwal, B., et al., *Immunotherapy in Advanced Non-small Cell Lung Cancer Patients: Ushering Chemotherapy Through the Checkpoint Inhibitors?* Cureus, 2018. **10**(9): p. e3254.
69. Reck, M., et al., *Pembrolizumab versus Chemotherapy for PD-L1-Positive Non-Small-Cell Lung Cancer*. N Engl J Med, 2016. **375**(19): p. 1823-1833.
70. Christofi, T., et al., *Current Perspectives in Cancer Immunotherapy*. Cancers (Basel), 2019. **11**(10).
71. Berghmans, T., et al., *Immunotherapy: From Advanced NSCLC to Early Stages, an Evolving Concept*. Front Med (Lausanne), 2020. **7**: p. 90.
72. Amin, M.B., et al., *The Eighth Edition AJCC Cancer Staging Manual: Continuing to build a bridge from a population-based to a more "personalized" approach to cancer staging*. CA Cancer J Clin, 2017. **67**(2): p. 93-99.

73. Herreros-Pomares, A., et al., *Lung tumorspheres reveal cancer stem cell-like properties and a score with prognostic impact in resected non-small-cell lung cancer*. *Cell Death & Disease*, 2019. **10**(9): p. 660.
74. Yadav, A.K. and N.S. Desai, *Cancer Stem Cells: Acquisition, Characteristics, Therapeutic Implications, Targeting Strategies and Future Prospects*. *Stem Cell Rev Rep*, 2019. **15**(3): p. 331-355.
75. Tirino, V., et al., *Cancer stem cells in solid tumors: an overview and new approaches for their isolation and characterization*. *FASEB J*, 2013. **27**(1): p. 13-24.
76. Agro, L. and C. O'Brien, *In vitro and in vivo Limiting Dilution Assay for Colorectal Cancer*. *Bio Protoc*, 2015. **5**(22): p. 1-11.
77. Bahmad, H.F., et al., *Sphere-Formation Assay: Three-Dimensional in vitro Culturing of Prostate Cancer Stem/Progenitor Sphere-Forming Cells*. *Front Oncol*, 2018. **8**: p. 347.
78. Phiboonchaiyanan, P.P. and P. Chanvorachote, *Suppression of a cancer stem-like phenotype mediated by alpha-lipoic acid in human lung cancer cells through down-regulation of beta-catenin and Oct-4*. *Cell Oncol (Dordr)*, 2017. **40**(5): p. 497-510.
79. Bhummaphan, N. and P. Chanvorachote, *Gigantol Suppresses Cancer Stem Cell-Like Phenotypes in Lung Cancer Cells*. *Evid Based Complement Alternat Med*, 2015. **2015**: p. 836564.
80. Sarvi, S., et al., *CD133+ cancer stem-like cells in small cell lung cancer are highly tumorigenic and chemoresistant but sensitive to a novel neuropeptide antagonist*. *Cancer Res*, 2014. **74**(5): p. 1554-1565.
81. Ma, Z., et al., *Characterisation of a subpopulation of CD133(+) cancer stem cells from Chinese patients with oral squamous cell carcinoma*. *Sci Rep*, 2020. **10**(1): p. 8875.
82. Hepburn, A.C., et al., *The induction of core pluripotency master regulators in cancers defines poor clinical outcomes and treatment resistance*. *Oncogene*, 2019. **38**(22): p. 4412-4424.

83. Seymour, T., A.J. Twigger, and F. Kakulas, *Pluripotency Genes and Their Functions in the Normal and Aberrant Breast and Brain*. *Int J Mol Sci*, 2015. **16**(11): p. 27288-27301.
84. Karachaliou, N., R. Rosell, and S. Viteri, *The role of SOX2 in small cell lung cancer, lung adenocarcinoma and squamous cell carcinoma of the lung*. *Transl Lung Cancer Res*, 2013. **2**(3): p. 172-179.
85. Yang, L., et al., *Targeting cancer stem cell pathways for cancer therapy*. *Signal Transduct Target Ther*, 2020. **5**(1): p. 8.
86. Chiou, S.H., et al., *Coexpression of Oct4 and Nanog enhances malignancy in lung adenocarcinoma by inducing cancer stem cell-like properties and epithelial-mesenchymal transdifferentiation*. *Cancer Res*, 2010. **70**(24): p. 10433-10444.
87. Choe, C., et al., *SOX2, a stemness gene, induces progression of NSCLC A549 cells toward anchorage-independent growth and chemoresistance to vinblastine*. *Onco Targets Ther*, 2018. **11**: p. 6197-6207.
88. Wuebben, E.L. and A. Rizzino, *The dark side of SOX2: cancer - a comprehensive overview*. *Oncotarget*, 2017. **8**(27): p. 44917-44943.
89. You, L., X. Guo, and Y. Huang, *Correlation of Cancer Stem-Cell Markers OCT4, SOX2, and NANOG with Clinicopathological Features and Prognosis in Operative Patients with Rectal Cancer*. *Yonsei Med J*, 2018. **59**(1): p. 35-42.
90. Piva, M., et al., *Sox2 promotes tamoxifen resistance in breast cancer cells*. *EMBO Mol Med*, 2014. **6**(1): p. 66-79.
91. Korkaya, H., et al., *Regulation of mammary stem/progenitor cells by PTEN/Akt/beta-catenin signaling*. *PLoS Biol*, 2009. **7**(6): p. e1000121.
92. Yong, X., et al., *Helicobacter pylori upregulates Nanog and Oct4 via Wnt/beta-catenin signaling pathway to promote cancer stem cell-like properties in human gastric cancer*. *Cancer Lett*, 2016. **374**(2): p. 292-303.
93. Pizzino, G., et al., *Oxidative Stress: Harms and Benefits for Human Health*. *Oxid Med Cell Longev*, 2017. **2017**: p. 8416763.
94. Cao, S.S. and R.J. Kaufman, *Endoplasmic reticulum stress and oxidative stress in cell fate decision and human disease*. *Antioxid Redox Signal*, 2014. **21**(3): p. 396-413.

95. Trachootham, D., J. Alexandre, and P. Huang, *Targeting cancer cells by ROS-mediated mechanisms: a radical therapeutic approach?* Nat Rev Drug Discov, 2009. **8**(7): p. 579-91.
96. Martinez-Reyes, I. and J.M. Cuezva, *The H(+)-ATP synthase: a gate to ROS-mediated cell death or cell survival.* Biochim Biophys Acta, 2014. **1837**(7): p. 1099-112.
97. Liou, G.Y. and P. Storz, *Reactive oxygen species in cancer.* Free Radic Res, 2010. **44**(5): p. 479-96.
98. Shi, X., et al., *Reactive oxygen species in cancer stem cells.* Antioxid Redox Signal, 2012. **16**(11): p. 1215-28.
99. Ishimoto, T., et al., *CD44 variant regulates redox status in cancer cells by stabilizing the xCT subunit of system xc(-) and thereby promotes tumor growth.* Cancer Cell, 2011. **19**(3): p. 387-400.
100. Zhou, D., L. Shao, and D.R. Spitz, *Reactive oxygen species in normal and tumor stem cells.* Adv Cancer Res, 2014. **122**: p. 1-67.
101. Filomeni, G., D. De Zio, and F. Cecconi, *Oxidative stress and autophagy: the clash between damage and metabolic needs.* Cell Death Differ, 2015. **22**(3): p. 377-88.
102. Kimmelman, A.C. and E. White, *Autophagy and Tumor Metabolism.* Cell Metab, 2017. **25**(5): p. 1037-1043.
103. Yang, R., et al., *Chaperone-Mediated Autophagy and Mitochondrial Homeostasis in Parkinson's Disease.* Parkinsons Dis, 2016. **2016**: p. 2613401.
104. Kroemer, G., G. Marino, and B. Levine, *Autophagy and the integrated stress response.* Mol Cell, 2010. **40**(2): p. 280-93.
105. Cuervo, A.M. and E. Wong, *Chaperone-mediated autophagy: roles in disease and aging.* Cell Res, 2014. **24**(1): p. 92-104.
106. Chen, Y., et al., *The crosstalk between autophagy and apoptosis was mediated by phosphorylation of Bcl-2 and beclin1 in benzene-induced hematotoxicity.* Cell Death Dis, 2019. **10**(10): p. 772.
107. Schlafli, A.M., et al., *Prognostic value of the autophagy markers LC3 and p62/SQSTM1 in early-stage non-small cell lung cancer.* Oncotarget, 2016. **7**(26): p. 39544-39555.

108. Wang, X., et al., *Beclin 1 and p62 expression in non-small cell lung cancer: relation with malignant behaviors and clinical outcome*. Int J Clin Exp Pathol, 2015. **8**(9): p. 10644-52.
109. Yun, C.W. and S.H. Lee, *The Roles of Autophagy in Cancer*. Int J Mol Sci, 2018. **19**(11).
110. Maiuri, M.C., et al., *Control of autophagy by oncogenes and tumor suppressor genes*. Cell Death Differ, 2009. **16**(1): p. 87-93.
111. Botti, J., et al., *Autophagy signaling and the cogwheels of cancer*. Autophagy, 2006. **2**(2): p. 67-73.
112. Lim, K.H. and L.M. Staudt, *Toll-like receptor signaling*. Cold Spring Harb Perspect Biol, 2013. **5**(1): p. a011247.
113. Salminen, A., K. Kaarniranta, and A. Kauppinen, *Beclin 1 interactome controls the crosstalk between apoptosis, autophagy and inflammasome activation: impact on the aging process*. Ageing Res Rev, 2013. **12**(2): p. 520-34.
114. Rosenfeldt, M.T. and K.M. Ryan, *The multiple roles of autophagy in cancer*. Carcinogenesis, 2011. **32**(7): p. 955-63.
115. Gewirtz, D.A., *The four faces of autophagy: implications for cancer therapy*. Cancer Res, 2014. **74**(3): p. 647-51.
116. Kaminsky, V.O., et al., *Suppression of basal autophagy reduces lung cancer cell proliferation and enhances caspase-dependent and -independent apoptosis by stimulating ROS formation*. Autophagy, 2012. **8**(7): p. 1032-44.
117. Nazio, F., et al., *Autophagy and cancer stem cells: molecular mechanisms and therapeutic applications*. Cell Death Differ, 2019. **26**(4): p. 690-702.
118. Song, Y.J., et al., *Autophagy contributes to the survival of CD133+ liver cancer stem cells in the hypoxic and nutrient-deprived tumor microenvironment*. Cancer Lett, 2013. **339**(1): p. 70-81.
119. Wolf, J., et al., *A mammosphere formation RNAi screen reveals that ATG4A promotes a breast cancer stem-like phenotype*. Breast Cancer Res, 2013. **15**(6): p. R109.

120. Mao, X., et al., *Curcumin suppresses LGR5(+) colorectal cancer stem cells by inducing autophagy and via repressing TFAP2A-mediated ECM pathway*. J Nat Med, 2021. **75**(3): p. 590-601.
121. Krysko, D.V., et al., *Apoptosis and necrosis: detection, discrimination and phagocytosis*. Methods, 2008. **44**(3): p. 205-21.
122. Chaabane, W., et al., *Autophagy, apoptosis, mitoptosis and necrosis: interdependence between those pathways and effects on cancer*. Arch Immunol Ther Exp (Warsz), 2013. **61**(1): p. 43-58.
123. Pfeffer, C.M. and A.T.K. Singh, *Apoptosis: A Target for Anticancer Therapy*. Int J Mol Sci, 2018. **19**(2).
124. Elmore, S., *Apoptosis: a review of programmed cell death*. Toxicol Pathol, 2007. **35**(4): p. 495-516.
125. Favaloro, B., et al., *Role of apoptosis in disease*. Aging (Albany NY), 2012. **4**(5): p. 330-49.
126. Ichim, G. and S.W. Tait, *A fate worse than death: apoptosis as an oncogenic process*. Nat Rev Cancer, 2016. **16**(8): p. 539-48.
127. D'Aguzzo, S. and D. Del Bufalo, *Inhibition of Anti-Apoptotic Bcl-2 Proteins in Preclinical and Clinical Studies: Current Overview in Cancer*. Cells, 2020. **9**(5).
128. Matsumoto, M., et al., *Cisplatin-induced apoptosis in non-small-cell lung cancer cells is dependent on Bax- and Bak-induction pathway and synergistically activated by BH3-mimetic ABT-263 in p53 wild-type and mutant cells*. Biochem Biophys Res Commun, 2016. **473**(2): p. 490-6.
129. Xu, H. and G.W. Krystal, *Actinomycin D decreases Mcl-1 expression and acts synergistically with ABT-737 against small cell lung cancer cell lines*. Clin Cancer Res, 2010. **16**(17): p. 4392-400.
130. Baritaki, S., et al., *Chemotherapeutic drugs sensitize cancer cells to TRAIL-mediated apoptosis: up-regulation of DR5 and inhibition of Yin Yang 1*. Mol Cancer Ther, 2007. **6**(4): p. 1387-99.
131. Safa, A.R., *Roles of c-FLIP in Apoptosis, Necroptosis, and Autophagy*. J Carcinog Mutagen, 2013. **Suppl 6**.

132. Morizot, A., et al., *Chemotherapy overcomes TRAIL-R4-mediated TRAIL resistance at the DISC level*. Cell Death Differ, 2011. **18**(4): p. 700-11.
133. Jia, Y., et al., *Aberrantly elevated redox sensing factor Nrf2 promotes cancer stem cell survival via enhanced transcriptional regulation of ABCG2 and Bcl-2/Bmi-1 genes*. Oncol Rep, 2015. **34**(5): p. 2296-304.
134. Wu, M.S., et al., *Smac mimetics in combination with TRAIL selectively target cancer stem cells in nasopharyngeal carcinoma*. Mol Cancer Ther, 2013. **12**(9): p. 1728-37.
135. Hu, Y., et al., *Sabutoclax, pan-active BCL-2 protein family antagonist, overcomes drug resistance and eliminates cancer stem cells in breast cancer*. Cancer Lett, 2018. **423**: p. 47-59.
136. Sun, Q., Y. Wang, and J.S. Desgrosellier, *Combined Bcl-2/Src inhibition synergize to deplete stem-like breast cancer cells*. Cancer Lett, 2019. **457**: p. 40-46.
137. Xu, Y., et al., *Mutated p53 Promotes the Symmetric Self-Renewal of Cisplatin-Resistant Lung Cancer Stem-Like Cells and Inhibits the Recruitment of Macrophages*. J Immunol Res, 2019. **2019**: p. 7478538.
138. Mantovani, F., L. Collavin, and G. Del Sal, *Mutant p53 as a guardian of the cancer cell*. Cell Death Differ, 2019. **26**(2): p. 199-212.
139. Shetzer, Y., et al., *The paradigm of mutant p53-expressing cancer stem cells and drug resistance*. Carcinogenesis, 2014. **35**(6): p. 1196-208.
140. Golubovskaya, V.M., *FAK and Nanog cross talk with p53 in cancer stem cells*. Anticancer Agents Med Chem, 2013. **13**(4): p. 576-580.
141. Chantarawong, W., et al., *5-O-Acetyl-Renieramycin T from Blue Sponge Xestospongia sp. Induces Lung Cancer Stem Cell Apoptosis*. Mar Drugs, 2019. **17**(2): p. 109.
142. Dasari, S. and P.B. Tchounwou, *Cisplatin in cancer therapy: molecular mechanisms of action*. Eur J Pharmacol, 2014. **740**: p. 364-78.
143. Besse, B., et al., *2nd ESMO Consensus Conference on Lung Cancer: non-small-cell lung cancer first-line/second and further lines of treatment in advanced disease*. Ann Oncol, 2014. **25**(8): p. 1475-84.

144. Rocha, C.R.R., et al., *DNA repair pathways and cisplatin resistance: an intimate relationship*. Clinics (Sao Paulo), 2018. **73**(suppl 1): p. e478s.
145. Michels, J., et al., *MCL-1 dependency of cisplatin-resistant cancer cells*. Biochem Pharmacol, 2014. **92**(1): p. 55-61.
146. Garcia-Aranda, M., E. Perez-Ruiz, and M. Redondo, *Bcl-2 Inhibition to Overcome Resistance to Chemo- and Immunotherapy*. Int J Mol Sci, 2018. **19**(12).
147. Cui, Y., et al., *Increased MALAT1 expression contributes to cisplatin resistance in non-small cell lung cancer*. Oncol Lett, 2018. **16**(4): p. 4821-4828.
148. Cetintas, V.B., et al., *Cisplatin resistance induced by decreased apoptotic activity in non-small-cell lung cancer cell lines*. Cell Biol Int, 2012. **36**(3): p. 261-265.
149. Liu, Y.P., et al., *Cisplatin selects for multidrug-resistant CD133+ cells in lung adenocarcinoma by activating Notch signaling*. Cancer Res, 2013. **73**(1): p. 406-16.
150. Scott, J.D. and R.M. Williams, *Chemistry and biology of the tetrahydroisoquinoline antitumor antibiotics*. Chem Rev, 2002. **102**(5): p. 1669-730.
151. Schoffski, P., et al., *Trabectedin (ET-743): evaluation of its use in advanced soft-tissue sarcoma*. Future Oncol, 2007. **3**(4): p. 381-92.
152. Perez-Ruixo, J.J., et al., *Population pharmacokinetic meta-analysis of trabectedin (ET-743, Yondelis) in cancer patients*. Clin Pharmacokinet, 2007. **46**(10): p. 867-84.
153. Sirimangkalakitti, N., et al., *Chemistry of Renieramycins. 15. Synthesis of 22-O-Ester Derivatives of Jorunnamycin A and Their Cytotoxicity against Non-Small-Cell Lung Cancer Cells*. J Nat Prod, 2016. **79**(8): p. 2089-2093.
154. Chamni, S., et al., *Chemistry of Renieramycins. Part 19: Semi-Syntheses of 22-O-Amino Ester and Hydroquinone 5-O-Amino Ester Derivatives of Renieramycin M and Their Cytotoxicity against Non-Small-Cell Lung Cancer Cell Lines*. Mar Drugs, 2020. **18**(8): p. 418.
155. Wen, H., et al., *Inhibiting of self-renewal, migration and invasion of ovarian cancer stem cells by blocking TGF-beta pathway*. PLoS One, 2020. **15**(3): p. e0230230.
156. Ho, M.M., et al., *Side population in human lung cancer cell lines and tumors is enriched with stem-like cancer cells*. Cancer Res, 2007. **67**(10): p. 4827-33.

157. Rycaj, K. and D.G. Tang, *Cell-of-Origin of Cancer versus Cancer Stem Cells: Assays and Interpretations*. *Cancer Res*, 2015. **75**(19): p. 4003-4011.
158. Han, X., et al., *Human lung epithelial BEAS-2B cells exhibit characteristics of mesenchymal stem cells*. *PLoS One*, 2020. **15**(1): p. e0227174.
159. Leeman, K.T., C.M. Fillmore, and C.F. Kim, *Lung stem and progenitor cells in tissue homeostasis and disease*. *Curr Top Dev Biol*, 2014. **107**: p. 207-233.
160. Barzegar Behrooz, A., A. Syahir, and S. Ahmad, *CD133: beyond a cancer stem cell biomarker*. *J Drug Target*, 2019. **27**(3): p. 257-269.
161. Tan, Y., et al., *Clinicopathological significance of CD133 in lung cancer: A meta-analysis*. *Mol Clin Oncol*, 2014. **2**(1): p. 111-115.
162. Wu, H., et al., *Is CD133 expression a prognostic biomarker of non-small-cell lung cancer? A systematic review and meta-analysis*. *PLoS One*, 2014. **9**(6): p. e100168.
163. Lee, B.W.L., P. Ghode, and D.S.T. Ong, *Redox regulation of cell state and fate*. *Redox Biol*, 2019. **25**: p. 101056.
164. Chang, H. and Z. Zou, *Targeting autophagy to overcome drug resistance: further developments*. *J Hematol Oncol*, 2020. **13**(1): p. 159.
165. Tan, L.M., et al., *Genetic Polymorphisms and Platinum-based Chemotherapy Treatment Outcomes in Patients with Non-Small Cell Lung Cancer: A Genetic Epidemiology Study Based Meta-analysis*. *Sci Rep*, 2017. **7**(1): p. 5593.
166. El-Senduny, F.F., et al., *Approach for chemosensitization of cisplatin-resistant ovarian cancer by cucurbitacin B*. *Tumour Biol*, 2016. **37**(1): p. 685-98.
167. Zaroni, M., et al., *3D tumor spheroid models for in vitro therapeutic screening: a systematic approach to enhance the biological relevance of data obtained*. *Sci Rep*, 2016. **6**: p. 19103.
168. Rieger, A.M., et al., *Modified annexin V/propidium iodide apoptosis assay for accurate assessment of cell death*. *J Vis Exp*, 2011. **50**(50): p. 2597.
169. Huang, T.H., et al., *In silico identification of thiostrepton as an inhibitor of cancer stem cell growth and an enhancer for chemotherapy in non-small-cell lung cancer*. *J Cell Mol Med*, 2019. **23**(12): p. 8184-8195.

170. Zhang, Y., et al., *NOTCH1 Signaling Regulates Self-Renewal and Platinum Chemoresistance of Cancer Stem-like Cells in Human Non-Small Cell Lung Cancer*. *Cancer Res*, 2017. **77**(11): p. 3082-3091.
171. Aponte, P.M. and A. Caicedo, *Stemness in Cancer: Stem Cells, Cancer Stem Cells, and Their Microenvironment*. *Stem Cells Int*, 2017. **2017**: p. 5619472.
172. Hu, J., et al., *Cancer stem cell self-renewal as a therapeutic target in human oral cancer*. *Oncogene*, 2019. **38**(27): p. 5440-5456.
173. Borah, A., et al., *Targeting self-renewal pathways in cancer stem cells: clinical implications for cancer therapy*. *Oncogenesis*, 2015. **4**: p. e177.
174. Pallini, R., et al., *Cancer stem cell analysis and clinical outcome in patients with glioblastoma multiforme*. *Clin Cancer Res*, 2008. **14**(24): p. 8205-8212.
175. Song, M., et al., *AKT as a Therapeutic Target for Cancer*. *Cancer Res*, 2019. **79**(6): p. 1019-1031.
176. Duda, P., et al., *Targeting GSK3 and Associated Signaling Pathways Involved in Cancer*. *Cells*, 2020. **9**(5).
177. Shaheen, S., et al., *Spheroid-Formation (Colonosphere) Assay for in Vitro Assessment and Expansion of Stem Cells in Colon Cancer*. *Stem Cell Rev Rep*, 2016. **12**(4): p. 492-9.
178. Pettit, G.R., et al., *Antineoplastic agents. 485. Isolation and structure of cribrostatin 6, a dark blue cancer cell growth inhibitor from the marine sponge *Cribrochalina* sp.* *J Nat Prod*, 2003. **66**(4): p. 544-547.
179. Luongo, F., et al., *PTEN Tumor-Suppressor: The Dam of Stemness in Cancer*. *Cancers (Basel)*, 2019. **11**(8): p. 1076.
180. Zhu, Z., H.G. Golay, and D.A. Barbie, *Targeting pathways downstream of KRAS in lung adenocarcinoma*. *Pharmacogenomics*, 2014. **15**(11): p. 1507-18.
181. Mazumdar, T., et al., *A comprehensive evaluation of biomarkers predictive of response to PI3K inhibitors and of resistance mechanisms in head and neck squamous cell carcinoma*. *Mol Cancer Ther*, 2014. **13**(11): p. 2738-50.
182. Kim, M.J., et al., *Combination of KRAS gene silencing and PI3K inhibition for ovarian cancer treatment*. *J Control Release*, 2020. **318**: p. 98-108.
183. Visvader, J.E., *Cells of origin in cancer*. *Nature*, 2011. **469**(7330): p. 314-322.

184. Roche, J., *The Epithelial-to-Mesenchymal Transition in Cancer*. *Cancers (Basel)*, 2018. **10**(2): p. 52.
185. Fantozzi, A., et al., *VEGF-mediated angiogenesis links EMT-induced cancer stemness to tumor initiation*. *Cancer Res*, 2014. **74**(5): p. 1566-1575.
186. Singh, A. and J. Settleman, *EMT, cancer stem cells and drug resistance: an emerging axis of evil in the war on cancer*. *Oncogene*, 2010. **29**(34): p. 4741-4751.
187. Milkovic, L., et al., *Short Overview of ROS as Cell Function Regulators and Their Implications in Therapy Concepts*. *Cells*, 2019. **8**(8).
188. Trachootham, D., et al., *Selective killing of oncogenically transformed cells through a ROS-mediated mechanism by beta-phenylethyl isothiocyanate*. *Cancer Cell*, 2006. **10**(3): p. 241-52.
189. Glick, D., S. Barth, and K.F. Macleod, *Autophagy: cellular and molecular mechanisms*. *J Pathol*, 2010. **221**(1): p. 3-12.
190. Shi, H., et al., *Rapamycin may inhibit murine S180 sarcoma growth by regulating the pathways associated with autophagy and cancer stem cells*. *J Cancer Res Ther*, 2019. **15**(2): p. 398-403.
191. Moon, H.J., et al., *Nonsteroidal Anti-inflammatory Drugs Sensitize CD44-Overexpressing Cancer Cells to Hsp90 Inhibitor Through Autophagy Activation*. *Oncol Res*, 2019. **27**(7): p. 835-847.
192. Marquez, R.T. and L. Xu, *Bcl-2:Beclin 1 complex: multiple, mechanisms regulating autophagy/apoptosis toggle switch*. *Am J Cancer Res*, 2012. **2**(2): p. 214-21.
193. Strappazzon, F., et al., *Mitochondrial BCL-2 inhibits AMBRA1-induced autophagy*. *EMBO J*, 2011. **30**(7): p. 1195-208.
194. Barlesi, F., et al., *Pemetrexed and cisplatin as first-line chemotherapy for advanced non-small-cell lung cancer (NSCLC) with asymptomatic inoperable brain metastases: a multicenter phase II trial (GFPC 07-01)*. *Ann Oncol*, 2011. **22**(11): p. 2466-2470.
195. Florea, A.M. and D. Busselberg, *Cisplatin as an anti-tumor drug: cellular mechanisms of activity, drug resistance and induced side effects*. *Cancers (Basel)*, 2011. **3**(1): p. 1351-71.

196. Duan, Z., et al., *Cisplatin-induced renal toxicity in elderly people*. Ther Adv Med Oncol, 2020. **12**: p. 1758835920923430.
197. Zhu, Y., et al., *Overexpression of CD133 enhances chemoresistance to 5-fluorouracil by activating the PI3K/Akt/p70S6K pathway in gastric cancer cells*. Oncol Rep, 2014. **32**(6): p. 2437-2444.
198. MacDonagh, L., et al., *Targeting the cancer stem cell marker, aldehyde dehydrogenase 1, to circumvent cisplatin resistance in NSCLC*. Oncotarget, 2017. **8**(42): p. 72544-72563.
199. Zhao, J., et al., *Epigenetic activation of FOXF1 confers cancer stem cell properties to cisplatinresistant nonsmall cell lung cancer*. Int J Oncol, 2020. **56**(5): p. 1083-1092.
200. Miao, W., et al., *p53 upregulated modulator of apoptosis sensitizes drug-resistant U251 glioblastoma stem cells to temozolomide through enhanced apoptosis*. Mol Med Rep, 2015. **11**(6): p. 4165-4173.
201. Hemann, M.T. and S.W. Lowe, *The p53-Bcl-2 connection*. Cell Death Differ, 2006. **13**(8): p. 1256-9.
202. Yeh, C.T., et al., *Trifluoperazine, an antipsychotic agent, inhibits cancer stem cell growth and overcomes drug resistance of lung cancer*. Am J Respir Crit Care Med, 2012. **186**(11): p. 1180-1188.
203. Tagscherer, K.E., et al., *Apoptosis-based treatment of glioblastomas with ABT-737, a novel small molecule inhibitor of Bcl-2 family proteins*. Oncogene, 2008. **27**(52): p. 6646-56.

APPENDICES

TABLES AND FIGURES OF EXPERIMENTAL RESULTS

Table 2 Cell viability of human lung cancer H460 cells after treatment with jorunnamycin A (JA) for 24 h

JA (μM)	Cell viability (%)
Control	100 \pm 0.00
0.05	98.52 \pm 2.87
0.1	96.35 \pm 3.73
0.5	90.19 \pm 5.32
1	73.91 \pm 3.42*
5	55.78 \pm 1.26*

Data represent means \pm SD of three independent experiments.

* $p < 0.05$ versus non-treated control.

Table 3 Percent apoptosis of attached H460 cells after 24 h jorunnamycin A (JA) treatment

JA (μM)	Apoptosis (%)
Control	1.12 \pm 0.28
0.05	1.37 \pm 0.43
0.1	2.18 \pm 0.41
0.5	2.76 \pm 0.49
1	10.27 \pm 2.22*
5	18.30 \pm 1.59*

Data represent means \pm SD of three independent experiments.

* $p < 0.05$ versus non-treated control.

Table 4 Percent growth inhibition of human lung cancer H460 cells over 24-72 h of jorunnamycin A (JA) treatment

Time (h)	Growth inhibition (%)			
	Control	JA 0.05 μ M	JA 0.1 μ M	JA 0.5 μ M
24	0.00 \pm 0.00	1.63 \pm 0.96	0.70 \pm 9.16	9.09 \pm 8.60
48	0.00 \pm 0.00	8.46 \pm 5.71	15.00 \pm 6.45	42.41 \pm 2.10*
72	0.00 \pm 0.00	9.19 \pm 5.70	24.89 \pm 8.25*	49.12 \pm 5.90*

Data represent means \pm SD of three independent experiments.

* $p < 0.05$ versus non-treated control at the same timepoint.

Table 5 Colony number of jorunnamycin A (JA)-treated human lung cancer H460 cells evaluated through limiting dilution assay (LDA) for 14 days

Treatment	Number of cells/well				
	200	100	50	10	1
Control	106.67 ±19.88	71.33 ±21.01	27.22 ±10.08	7.22 ±1.35	1.11 ±0.51
JA 0.05 µM	0.78±0.70*	0.00±0.00*	0.00±0.00*	0.00±0.00*	0.00±0.00*
JA 0.1 µM	0.00±0.00*	0.00±0.00*	0.00±0.00*	0.00±0.00*	0.00±0.00*
JA 0.5 µM	0.00±0.00*	0.00±0.00*	0.00±0.00*	0.00±0.00*	0.00±0.00*
Cisplatin 25 µM	0.00±0.00*	0.00±0.00*	0.00±0.00*	0.00±0.00*	0.00±0.00*

Data represent means ± SD of three independent experiments.

* $p < 0.05$ versus non-treated control at the same number of cells/well.

Table 6 Relative colony size of jorunnamycin A (JA)-treated CSC-enriched H460 spheroids evaluated by single 3D spheroid formation

Day	Control	JA 0.05 μM	JA 0.1 μM	JA 0.5 μM	Cisplatin 25 μM
0	1.00 \pm 0.00	1.00 \pm 0.00	1.00 \pm 0.00	1.00 \pm 0.00	1.00 \pm 0.00
1	1.45 \pm 0.07	1.24 \pm 0.07	1.13 \pm 0.14*	0.63 \pm 0.17*	1.25 \pm 0.14
3	2.46 \pm 0.33	1.50 \pm 0.15*	1.27 \pm 0.21*	0.44 \pm 0.24*	0.74 \pm 0.16*
5	3.42 \pm 0.44	2.53 \pm 0.13*	1.59 \pm 0.26*	0.45 \pm 0.13*	0.51 \pm 0.18*
7	4.15 \pm 0.25	2.96 \pm 0.24*	2.20 \pm 0.22*	0.34 \pm 0.16*	0.43 \pm 0.14*

Data represent means \pm SD of three independent experiments.

* $p < 0.05$ versus non-treated control at the same timepoint.

Table 7 Percent CD133-overexpressing cells detected in jorunnamycin A (JA)-treated CSC-enriched spheroids of H460 cells for 3 days via flow cytometry

Treatment	CD133low population (%)	CD133high population (%)
Control	11.68 ± 3.33	88.32 ± 4.14
JA 0.1 µM	26.05 ± 5.43*	73.95 ± 3.22*
JA 0.5 µM	42.51 ± 4.44*	57.49 ± 2.43*
Cisplatin 25 µM	35.35 ± 6.8*	64.06 ± 5.23*

Data represent means ± SD of three independent experiments.

* $p < 0.05$ versus non-treated control.

Table 8 Relative mRNA level of stemness transcription factors in CSC-enriched lung cancer H460 cells treated with jorunnamycin A (JA) for 24 h

JA (μM)	Relative mRNA level		
	Oct-4	Nanog	Sox-2
Control	1.00 \pm 0.00	1.00 \pm 0.00	1.00 \pm 0.00
0.05	0.92 \pm 0.39	0.55 \pm 0.19	0.74 \pm 0.36
0.1	0.45 \pm 0.13*	0.20 \pm 0.09*	0.28 \pm 0.06*
0.5	0.21 \pm 0.02*	0.16 \pm 0.08*	0.24 \pm 0.02*

Data represent means \pm SD of three independent experiments.

* $p < 0.05$ versus non-treated control.

Table 9 Relative protein level of CSC self-renewal markers in CSC-enriched lung cancer H460 cells treated with jorunnamycin A (JA) for 24 h

JA (μM)	Relative protein level		
	Oct-4	Nanog	Sox-2
Control	1.00 \pm 0.00	1.00 \pm 0.00	1.00 \pm 0.00
0.05	1.02 \pm 0.07	0.94 \pm 0.05	0.84 \pm 0.11
0.1	0.44 \pm 0.04*	0.72 \pm 0.05*	1.06 \pm 0.11
0.5	0.22 \pm 0.04*	0.55 \pm 0.03*	0.49 \pm 0.06*

Data represent means \pm SD of three independent experiments.

* $p < 0.05$ versus non-treated control.

Table 10 Relative protein level of related up-stream proteins in CSC population of lung cancer H460 cells treated with jorunnamycin A (JA) for 24 h

JA (μM)	Relative protein level		
	β -catenin	p-Akt/Akt	p-GSK-3 β /GSK-3 β
Control	1.00 \pm 0.00	1.00 \pm 0.00	1.00 \pm 0.00
0.05	0.65 \pm 0.06*	0.58 \pm 0.03*	0.67 \pm 0.10*
0.1	0.35 \pm 0.04*	0.52 \pm 0.06*	0.71 \pm 0.05*
0.5	0.55 \pm 0.01*	0.55 \pm 0.02*	0.64 \pm 0.03*

Data represent means \pm SD of three independent experiments.

* $p < 0.05$ versus non-treated control.



Table 11 Cell viability of human lung cancer H23 cells after treatment with jorunnamycin A (JA) for 24 h

JA (μM)	Cell viability (%)
Control	100 \pm 0.00
0.05	94.76 \pm 1.82
0.1	92.18 \pm 3.11
0.5	89.74 \pm 3.44
1	62.83 \pm 7.50*
5	36.85 \pm 4.72*

Data represent means \pm SD of three independent experiments.

* $p < 0.05$ versus non-treated control.

Table 12 Percent apoptosis of attached H23 cells after 24 h jorunnamycin A (JA) treatment

JA (μM)	Apoptosis (%)
Control	1.04 \pm 0.29
0.05	1.63 \pm 0.63
0.1	2.21 \pm 0.56
0.5	2.73 \pm 0.78
1	13.88 \pm 1.72*
5	23.53 \pm 2.32*

Data represent means \pm SD of three independent experiments.

* $p < 0.05$ versus non-treated control.

Table 13 Percent growth inhibition of human lung cancer H23 cells over 24-72 h of jorunnamycin A (JA) treatment

Time (h)	Growth inhibition (%)			
	Control	JA 0.05 μ M	JA 0.1 μ M	JA 0.5 μ M
24	0.00 \pm 0.00	4.03 \pm 0.76	7.31 \pm 2.81	8.99 \pm 2.35
48	0.00 \pm 0.00	24.57 \pm 2.78	39.89 \pm 2.01*	60.59 \pm 1.18*
72	0.00 \pm 0.00	34.59 \pm 2.78	49.75 \pm 3.23*	89.24 \pm 0.38*

Data represent means \pm SD of three independent experiments.

* $p < 0.05$ versus non-treated control at the same timepoint.

Table 14 Cell viability of human lung cancer A549 cells after treatment with jorunnamycin A (JA) for 24 h

JA (μM)	Cell viability (%)
Control	100 \pm 0.00
0.05	97.44 \pm 1.74
0.1	95.44 \pm 3.79
0.5	89.46 \pm 5.01
1	60.45 \pm 3.86*
5	50.99 \pm 3.09*

Data represent means \pm SD of three independent experiments.

* $p < 0.05$ versus non-treated control.

Table 15 Percent apoptosis of attached A549 cells after 24 h jorunnamycin A (JA) treatment

JA (μM)	Apoptosis (%)
Control	1.10 \pm 0.16
0.05	1.55 \pm 0.29
0.1	2.24 \pm 0.47
0.5	2.99 \pm 0.57
1	13.23 \pm 3.38*
5	21.53 \pm 4.02*

Data represent means \pm SD of three independent experiments.

* $p < 0.05$ versus non-treated control.

Table 16 Percent growth inhibition of human lung cancer A549 cells over 24-72 h of jorunnamycin A (JA) treatment

Time (h)	Growth inhibition (%)			
	Control	JA 0.05 μ M	JA 0.1 μ M	JA 0.5 μ M
24	0.00 \pm 0.00	1.95 \pm 1.63	3.39 \pm 4.11	9.32 \pm 5.86
48	0.00 \pm 0.00	8.30 \pm 2.53	20.07 \pm 3.37	40.88 \pm 10.37*
72	0.00 \pm 0.00	17.50 \pm 8.97	24.66 \pm 12.52	69.16 \pm 7.75*

Data represent means \pm SD of three independent experiments.

* $p < 0.05$ versus non-treated control at the same timepoint.

Table 17 Cell viability of human lung epithelial BEAS-2B cells after treatment with jorunnamycin A (JA) for 24 h

JA (μM)	Cell viability (%)
Control	100 \pm 0.00
0.05	99.32 \pm 1.96
0.1	97.15 \pm 1.75
0.5	92.92 \pm 3.68
1	78.94 \pm 3.50*
5	63.52 \pm 5.29*

Data represent means \pm SD of three independent experiments.

* $p < 0.05$ versus non-treated control.

Table 18 Percent apoptosis of attached BEAS-2B cells after 24 h jorunnamycin A (JA) treatment

JA (μM)	Apoptosis (%)
Control	1.05 \pm 0.25
0.05	1.31 \pm 0.35
0.1	1.40 \pm 0.32
0.5	2.09 \pm 0.55
1	4.56 \pm 2.29
5	12.53 \pm 2.47*

Data represent means \pm SD of three independent experiments.

* $p < 0.05$ versus non-treated control.

Table 19 Percent growth inhibition of human lung epithelial BEAS-2B cells over 24-72 h of jorunnamycin A (JA) treatment

Time (h)	Growth inhibition (%)			
	Control	JA 0.05 μ M	JA 0.1 μ M	JA 0.5 μ M
24	0.00 \pm 0.00	1.91 \pm 0.65	2.85 \pm 1.75	6.08 \pm 4.51
48	0.00 \pm 0.00	2.60 \pm 0.55	5.31 \pm 0.93	22.53 \pm 4.89*
72	0.00 \pm 0.00	3.10 \pm 2.79	8.18 \pm 5.08	36.11 \pm 3.05*

Data represent means \pm SD of three independent experiments.

* $p < 0.05$ versus non-treated control at the same timepoint.

Table 20 Colony number of jorunnamycin A (JA)-treated human lung cancer H23 cells evaluated through limiting dilution assay (LDA) for 14 days

Treatment	Number of cells/well				
	200	100	50	10	1
Control	71.00±3.61	42.00±2.65	23.67±1.53	6.00±1.00	1.00±1.00
JA 0.05 μ M	0.00±0.00*	0.00±0.00*	0.00±0.00*	0.00±0.00*	0.00±0.00*
JA 0.1 μ M	0.00±0.00*	0.00±0.00*	0.00±0.00*	0.00±0.00*	0.00±0.00*
JA 0.5 μ M	0.00±0.00*	0.00±0.00*	0.00±0.00*	0.00±0.00*	0.00±0.00*
Cisplatin 25 μ M	0.00±0.00*	0.00±0.00*	0.00±0.00*	0.00±0.00*	0.00±0.00*

Data represent means \pm SD of three independent experiments.

* $p < 0.05$ versus non-treated control at the same number of cells/well.

Table 21 Relative colony size of jorunnamycin A (JA)-treated CSC-enriched H23 spheroids evaluated by single 3D spheroid formation

Day	Control	JA 0.05 μ M	JA 0.1 μ M	JA 0.5 μ M	Cisplatin 25 μ M
0	1.00 \pm 0.00	1.00 \pm 0.00	1.00 \pm 0.00	1.00 \pm 0.00	1.00 \pm 0.00
1	1.28 \pm 0.09	1.11 \pm 0.21	1.01 \pm 0.19	0.79 \pm 0.09*	1.25 \pm 0.09
3	2.73 \pm 0.61	2.52 \pm 0.45	2.45 \pm 0.30	1.12 \pm 0.23*	0.68 \pm 0.05*
5	3.39 \pm 0.28	3.53 \pm 0.35	3.26 \pm 0.29	1.22 \pm 0.23*	0.55 \pm 0.17*
7	4.42 \pm 0.29	3.87 \pm 0.23	3.55 \pm 0.19	1.56 \pm 0.17*	0.46 \pm 0.29*

Data represent means \pm SD of three independent experiments.

* $p < 0.05$ versus non-treated control at the same timepoint.

Table 22 Percent CD133-overexpressing cells detected in jorunnamycin A (JA)-treated CSC-enriched spheroids of H23 cells for 3 days via flow cytometry

Treatment	CD133low population (%)	CD133high population (%)
Control	12.36 ± 3.09	87.64 ± 4.21
JA 0.1 µM	21.21 ± 4.17	78.76 ± 5.57
JA 0.5 µM	30.54 ± 2.27*	69.46 ± 3.22*
Cisplatin 25 µM	29.25 ± 3.70*	70.62 ± 3.78*

Data represent means ± SD of three independent experiments.

* $p < 0.05$ versus non-treated control.

Table 23 Colony number of jorunnamycin A (JA)-treated human lung cancer A549 cells evaluated through limiting dilution assay (LDA) for 14 days

Treatment	Number of cells/well				
	200	100	50	10	1
Control	36.00±8.72	17.00±2.65	9.00±2.65	3.00±1.00	1.33±0.58
JA 0.05 μ M	0.00±0.00*	0.00±0.00*	0.00±0.00*	0.00±0.00*	0.00±0.00*
JA 0.1 μ M	0.00±0.00*	0.00±0.00*	0.00±0.00*	0.00±0.00*	0.00±0.00*
JA 0.5 μ M	0.00±0.00*	0.00±0.00*	0.00±0.00*	0.00±0.00*	0.00±0.00*
Cisplatin 25 μ M	0.00±0.00*	0.00±0.00*	0.00±0.00*	0.00±0.00*	0.00±0.00*

Data represent means \pm SD of three independent experiments.

* $p < 0.05$ versus non-treated control at the same number of cells/well.

Table 24 Relative colony size of jorunnamycin A (JA)-treated CSC-enriched A549 spheroids evaluated by single 3D spheroid formation

Day	Control	JA 0.05 μ M	JA 0.1 μ M	JA 0.5 μ M	Cisplatin 25 μ M
0	1.00 \pm 0.00	1.00 \pm 0.00	1.00 \pm 0.00	1.00 \pm 0.00	1.00 \pm 0.00
1	1.58 \pm 0.12	1.32 \pm 0.17	1.10 \pm 0.14*	1.06 \pm 0.10*	1.30 \pm 0.14
3	2.44 \pm 0.25	2.09 \pm 0.30	1.71 \pm 0.07*	0.96 \pm 0.13*	1.14 \pm 0.25*
5	3.08 \pm 0.18	2.44 \pm 0.17*	2.20 \pm 0.15*	0.77 \pm 0.11*	1.01 \pm 0.35*
7	3.75 \pm 0.31	2.81 \pm 0.23*	2.21 \pm 0.23*	0.74 \pm 0.15*	1.09 \pm 0.15*

Data represent means \pm SD of three independent experiments.

* $p < 0.05$ versus non-treated control at the same timepoint.

Table 25 Percent CD133-overexpressing cells detected in jorunnamycin A (JA)-treated CSC-enriched spheroids of A549 cells for 3 days via flow cytometry

Treatment	CD133low population (%)	CD133high population (%)
Control	27.61 ± 6.12	71.94 ± 5.75
JA 0.1 µM	37.74 ± 5.25*	61.71 ± 5.07*
JA 0.5 µM	51.28 ± 3.60*	48.13 ± 2.68*
Cisplatin 25 µM	46.36 ± 2.65*	53.09 ± 4.21*

Data represent means ± SD of three independent experiments.

* $p < 0.05$ versus non-treated control.

Table 26 Relative mRNA level of stemness transcription factors in CSC-enriched lung cancer H23 cells treated with jorunnamycin A (JA) for 24 h

JA (μM)	Relative mRNA level		
	Oct-4	Nanog	Sox-2
Control	1.00 \pm 0.00	1.00 \pm 0.00	1.00 \pm 0.00
0.05	0.85 \pm 0.21	0.72 \pm 0.20	0.72 \pm 0.14
0.1	1.00 \pm 0.38	0.60 \pm 0.17*	0.73 \pm 0.20
0.5	0.51 \pm 0.08*	0.40 \pm 0.14*	0.39 \pm 0.11*

Data represent means \pm SD of three independent experiments.

* $p < 0.05$ versus non-treated control.

Table 27 Relative mRNA level of stemness transcription factors in CSC-enriched lung cancer A549 cells treated with jorunnamycin A (JA) for 24 h

JA (μM)	Relative mRNA level		
	Oct-4	Nanog	Sox-2
Control	1.00 \pm 0.00	1.00 \pm 0.00	1.00 \pm 0.00
0.05	0.19 \pm 0.04*	0.11 \pm 0.01*	0.20 \pm 0.07*
0.1	0.09 \pm 0.02*	0.10 \pm 0.01*	0.11 \pm 0.05*
0.5	0.10 \pm 0.00*	0.04 \pm 0.01*	0.11 \pm 0.05*

Data represent means \pm SD of three independent experiments.

* $p < 0.05$ versus non-treated control.

Table 28 Relative protein level of related up-stream proteins in CSC population of lung cancer H23 cells treated with jorunnamycin A (JA) for 24 h

JA (μM)	Relative protein level		
	β -catenin	p-Akt/Akt	p-GSK-3 β /GSK-3 β
Control	1.00 \pm 0.00	1.00 \pm 0.00	1.00 \pm 0.00
0.05	0.91 \pm 0.08	1.02 \pm 0.05	1.00 \pm 0.10
0.1	0.75 \pm 0.05*	1.09 \pm 0.07	0.83 \pm 0.07
0.5	0.65 \pm 0.03*	0.97 \pm 0.04	0.62 \pm 0.03*

Data represent means \pm SD of three independent experiments.

* $p < 0.05$ versus non-treated control.

Table 29 Relative protein level of related up-stream proteins in CSC population of lung cancer A549 cells treated with jorunnamycin A (JA) for 24 h

JA (μM)	Relative protein level		
	β -catenin	p-Akt/Akt	p-GSK-3 β /GSK-3 β
Control	1.00 \pm 0.00	1.00 \pm 0.00	1.00 \pm 0.00
0.05	1.01 \pm 0.02	1.09 \pm 0.08	1.03 \pm 0.15
0.1	0.78 \pm 0.05*	1.24 \pm 0.06	0.94 \pm 0.07
0.5	0.81 \pm 0.01*	1.03 \pm 0.06	0.52 \pm 0.05*

Data represent means \pm SD of three independent experiments.

* $p < 0.05$ versus non-treated control.

Table 30 Colony number of jorunnamycin A (JA)-treated human lung epithelial BEAS-2B cells evaluated through limiting dilution assay (LDA) for 14 days

Treatment	Number of cells/well				
	200	100	50	10	1
Control	2.67±1.15	1.00±1.00	0.33±0.58	0.00±0.00	0.00±0.00
JA 0.05 μ M	2.00±1.00	0.33±0.58	0.00±0.00	0.00±0.00	0.00±0.00
JA 0.1 μ M	1.67±0.58	0.00±0.00	0.00±0.00	0.00±0.00	0.00±0.00
JA 0.5 μ M	1.33±0.58	0.33±0.58	0.00±0.00	0.00±0.00	0.00±0.00
Cisplatin 25 μ M	1.00±1.00	0.00±0.00	0.00±0.00	0.00±0.00	0.00±0.00

Data represent means \pm SD of three independent experiments.

Table 31 Relative colony size of jorunnamycin A (JA)-treated stem cell-enriched BEAS-2B spheroid evaluated by single 3D spheroid formation

Day	Control	JA 0.05 μ M	JA 0.1 μ M	JA 0.5 μ M	Cisplatin 25 μ M
0	1.00 \pm 0.00	1.00 \pm 0.00	1.00 \pm 0.00	1.00 \pm 0.00	1.00 \pm 0.00
1	1.22 \pm 0.10	1.20 \pm 0.14	1.20 \pm 0.17	1.06 \pm 0.17	1.03 \pm 0.19
3	1.12 \pm 0.20	1.30 \pm 0.09	1.27 \pm 0.02	1.06 \pm 0.11	1.16 \pm 0.13
5	1.24 \pm 0.10	1.35 \pm 0.19	1.40 \pm 0.10	1.11 \pm 0.18	1.25 \pm 0.14
7	1.30 \pm 0.11	1.37 \pm 0.18	1.40 \pm 0.21	1.10 \pm 0.20	1.19 \pm 0.12

Data represent means \pm SD of three independent experiments.

Table 32 Percent CD133-overexpressing cells detected in jorunnamycin A (JA)-treated BEAS-2B spheroids for 3 days via flow cytometry

Treatment	CD133low population (%)	CD133high population (%)
Control	21.83 ± 4.34	77.92 ± 4.26
JA 0.1 µM	19.03 ± 8.75	78.32 ± 11.75
JA 0.5 µM	24.94 ± 7.92	74.29 ± 7.67
Cisplatin 25 µM	16.35 ± 5.47	83.05 ± 5.49

Data represent means ± SD of three independent experiments.

Table 33 Flow cytometry analysis for ROS measurement in jorunnamycin A (JA)-treated CSC-enriched H460 spheroids for 1-9 h

JA (µM)	Relative fluorescence				
	0 h	1 h	3 h	6 h	9 h
0.5	1.00 ± 0.00	1.05 ± 0.09	1.14 ± 0.09	1.36 ± 0.10	1.44 ± 0.11

Data represent means ± SD of three independent experiments.

* $p < 0.05$ versus non-treated control.

Table 34 Colony number of human lung cancer H460 cells after treatment with jorunnamycin A (JA) for 14 days with or without N-acetyl cysteine (NAC) pretreatment

Treatment	Number of cells/well				
	200	100	50	10	1
Control	112.00±11.79	75.00±10.02	29.56±3.15	7.11±1.17	0.67±0.33
NAC 5 mM	100.56±19.06	66.56±7.18	23.78±3.69	5.22±1.71	0.78±0.84
JA 0.5 µM	0.00±0.00*	0.00±0.00*	0.00±0.00*	0.00±0.00*	0.00±0.00*
NAC 5 mM + JA 0.5 µM	0.00±0.00*	0.00±0.00*	0.00±0.00*	0.00±0.00*	0.00±0.00*

Data represent means ± SD of three independent experiments.

* $p < 0.05$ versus non-treated control at the same number of cells/well.

Table 35 Relative colony size of CSC-enriched H460 spheroids after treatment with jorunnamycin A (JA) for 0-7 days with or without N-acetyl cysteine (NAC) pretreatment

Day	Control	NAC 5 mM	JA 0.5 μ M	NAC 5 mM + JA 0.5 μ M
0	1.00 \pm 0.00	1.00 \pm 0.00	1.00 \pm 0.00	1.00 \pm 0.00
1	1.55 \pm 0.14	1.57 \pm 0.12	0.95 \pm 0.17*	1.10 \pm 0.14*#
3	3.03 \pm 0.37	3.27 \pm 0.28	0.75 \pm 0.09*	2.27 \pm 0.19*#
5	4.33 \pm 0.18	4.43 \pm 0.56	0.54 \pm 0.07*	2.70 \pm 0.17*#
7	5.50 \pm 0.27	5.65 \pm 0.17	0.45 \pm 0.10*	3.26 \pm 0.34*#

Data represent means \pm SD of three independent experiments.

* $p < 0.05$ versus non-treated control at the same timepoint.

$p < 0.05$ versus only JA-treated group.

Table 36 Relative protein level of related autophagy proteins in CSC population of lung cancer H460 cells treated with 0.5 μ M jorunnamycin A (JA) for 0-12 h

Time (h)	Relative protein level		
	p62	Beclin-1	LC3-II/LC3-I
0	1.00 \pm 0.00	1.00 \pm 0.00	1.00 \pm 0.00
3	0.75 \pm 0.09*	1.10 \pm 0.12	1.02 \pm 0.17
6	0.60 \pm 0.06*	1.64 \pm 0.09*	1.45 \pm 0.13*
9	0.62 \pm 0.08*	1.52 \pm 0.08*	1.72 \pm 0.18*
12	0.70 \pm 0.11*	1.43 \pm 0.07*	2.26 \pm 0.24*

Data represent means \pm SD of three independent experiments.

* $p < 0.05$ versus non-treated control.

Table 37 Colony number of human lung cancer H460 cells after treatment with jorunnamycin A (JA) for 14 days with or without wortmannin pretreatment

Treatment	Number of cells/well				
	200	100	50	10	1
Control	105.67±9.29	77.02±9.99	31.22±9.58	7.44±0.96	0.89±0.19
Wortmannin 0.5 µM	108.67±17.10	69.78±4.50	29.56±6.41	6.11±1.68	0.78±0.84
JA 0.5 µM	0.00±0.00*	0.00±0.00*	0.00±0.00*	0.00±0.00*	0.00±0.00*
Wortmannin 0.5 µM + JA 0.5 µM	0.00±0.00*	0.00±0.00*	0.00±0.00*	0.00±0.00*	0.00±0.00*

Data represent means ± SD of three independent experiments.

* $p < 0.05$ versus non-treated control at the same number of cells/well.

Table 38 Relative colony size of CSC-enriched H460 spheroids after treatment with jorunnamycin A (JA) for 0-7 days with or without wortmannin pretreatment

Day	Control	Wortmannin 0.5 μ M	JA 0.5 μ M	Wortmannin 0.5 μ M + JA 0.5 μ M
0	1.00 \pm 0.00	1.00 \pm 0.00	1.00 \pm 0.00	1.00 \pm 0.00
1	1.85 \pm 0.31	1.70 \pm 0.17	0.84 \pm 0.10*	1.07 \pm 0.07*
3	3.20 \pm 0.45	3.18 \pm 0.33	0.71 \pm 0.09*	1.87 \pm 0.35*#
5	4.25 \pm 0.15	4.48 \pm 0.40	0.52 \pm 0.08*	2.47 \pm 0.20*#
7	5.22 \pm 0.22	5.35 \pm 0.33	0.44 \pm 0.07*	2.85 \pm 0.11*#

Data represent means \pm SD of three independent experiments.

* $p < 0.05$ versus non-treated control at the same timepoint.

$p < 0.05$ versus only JA-treated group.

Table 39 Cell viability of attached H460 cells after treatment with cisplatin for 24 h with or without pretreatment with jorunnamycin A (JA)

Treatment	Cell viability (%)
Control	100 ± 0.00
JA 0.5 µM	93.60 ± 4.79
Cisplatin 25 µM	66.91 ± 1.70*
JA 0.5 µM + Cisplatin 25 µM	15.70 ± 1.85*#

Table 40 Percent apoptosis of attached H460 cells after treatment with cisplatin for 24 h with or without pretreatment with jorunnamycin A (JA)

Treatment	Apoptosis (%)
Control	1.00 ± 0.20
JA 0.5 µM	2.80 ± 0.79
Cisplatin 25 µM	20.91 ± 2.70*
JA 0.5 µM + Cisplatin 25 µM	70.70 ± 2.25*#

Data represent means ± SD of three independent experiments.

* $p < 0.05$ versus non-treated control.

$p < 0.05$ versus only cisplatin-treated group.

Table 41 Relative colony size of CSC-enriched H460 spheroids after treatment with cisplatin for 0-7 days with or without jorunnamycin A (JA) pretreatment

Day	Control	JA 0.5 μ M	Cisplatin 25 μ M	JA 0.5 μ M + Cisplatin 25 μ M
0	1.00 \pm 0.00	1.00 \pm 0.00	1.00 \pm 0.00	1.00 \pm 0.00
1	1.55 \pm 0.17	0.83 \pm 0.11*	1.36 \pm 0.16	1.05 \pm 0.18
3	3.15 \pm 0.53	0.75 \pm 0.24*	1.45 \pm 0.16*	0.43 \pm 0.09*#
5	4.42 \pm 0.24	0.29 \pm 0.08*	0.72 \pm 0.11*	0.23 \pm 0.15*#
7	5.31 \pm 0.15	0.27 \pm 0.06*	0.63 \pm 0.23*	0.12 \pm 0.02*#

Data represent means \pm SD of three independent experiments.

* $p < 0.05$ versus non-treated control at the same timepoint.

$p < 0.05$ versus only cisplatin-treated group.

Table 42 Percent CD133-overexpressing cells detected in jorunnamycin A (JA)-pretreated CSC-enriched spheroids of H460 cells after incubation with cisplatin for 3 days via flow cytometry

Treatment	CD133low population (%)	CD133high population (%)
Control	25.09 ± 3.64	74.91 ± 3.57
JA 0.5 µM	48.03 ± 4.80*	51.97 ± 7.50*
Cisplatin 25 µM	40.65 ± 7.25*	59.35 ± 5.07*
JA 0.5 µM + Cisplatin 25 µM	63.11 ± 3.60*	36.89 ± 2.68*#

Data represent means ± SD of three independent experiments.

* $p < 0.05$ versus non-treated control.

$p < 0.05$ versus only cisplatin-treated group.

Table 43 Mode of cell death detected in jorunnamycin A (JA)-pretreated CSC-enriched spheroids of H460 cells for 24 h prior to 24 h of cisplatin treatment via flow cytometry

Treatment	Living cell (%)	Early Apoptosis (%)	Late Apoptosis (%)	Necrosis (%)
Control	63.00 ± 2.19	36.98 ± 1.19	0.02 ± 0.00	0.00 ± 0.00
JA 0.5 µM	56.13 ± 3.59	43.79 ± 0.88	0.08 ± 0.01	0.00 ± 0.00
Cisplatin 25 µM	64.75 ± 1.83	35.25 ± 0.83	0.00 ± 0.00	0.00 ± 0.00
JA 0.5 µM + Cisplatin 25 µM	37.75 ± 2.37*#	62.16 ± 2.36*#	0.09 ± 0.01	0.00 ± 0.00

Data represent means ± SD of three independent experiments.

* $p < 0.05$ versus non-treated control.

$p < 0.05$ versus only cisplatin-treated group.

Table 44 Relative colony size of CSC-enriched H23 spheroids after treatment with cisplatin for 0-7 days with or without jorunnamycin A (JA) pretreatment

Day	Control	JA 0.5 μ M	Cisplatin 25 μ M	JA 0.5 μ M + Cisplatin 25 μ M
0	1.00 \pm 0.00	1.00 \pm 0.00	1.00 \pm 0.00	1.00 \pm 0.00
1	1.64 \pm 0.25	1.41 \pm 0.13	1.54 \pm 0.17	1.20 \pm 0.16
3	3.02 \pm 0.17*	2.34 \pm 0.09*	1.32 \pm 0.10*	1.12 \pm 0.13*
5	3.59 \pm 0.15*	2.54 \pm 0.15*	1.07 \pm 0.12*	0.73 \pm 0.08*#
7	5.28 \pm 0.22*	2.83 \pm 0.14*	0.70 \pm 0.16*	0.33 \pm 0.10*#

Data represent means \pm SD of three independent experiments.

* $p < 0.05$ versus non-treated control.

$p < 0.05$ versus only cisplatin-treated group.

Table 45 Relative colony size of CSC-enriched A549 spheroids after treatment with cisplatin for 0-7 days with or without jorunnamycin A (JA) pretreatment

Day	Control	JA 0.5 μ M	Cisplatin 25 μ M	JA 0.5 μ M + Cisplatin 25 μ M
0	1.00 \pm 0.00	1.00 \pm 0.00	1.00 \pm 0.00	1.00 \pm 0.00
1	1.91 \pm 0.20	1.36 \pm 0.11*	1.86 \pm 0.15	0.74 \pm 0.13*#
3	2.84 \pm 0.12	0.85 \pm 0.14*	1.14 \pm 0.08*	0.61 \pm 0.11*#
5	3.22 \pm 0.16	0.62 \pm 0.10*	1.06 \pm 0.10*	0.41 \pm 0.15*#
7	3.85 \pm 0.07	0.45 \pm 0.07*	0.78 \pm 0.12*	0.29 \pm 0.07*#

Data represent means \pm SD of three independent experiments.

* $p < 0.05$ versus non-treated control at the same timepoint.

$p < 0.05$ versus only cisplatin-treated group.

Table 46 Relative protein level of apoptosis-related proteins in CSC-enriched H460 spheroids treated with jorunnamycin A (JA) for 24 h

JA (μM)	Relative protein level			
	p53	Mcl-1	Bcl-2	BAX
Control	1.00 \pm 0.00	1.00 \pm 0.00	1.00 \pm 0.00	1.00 \pm 0.00
0.05	1.53 \pm 0.08*	1.01 \pm 0.03	0.60 \pm 0.02*	0.98 \pm 0.05
0.1	1.60 \pm 0.16*	0.99 \pm 0.05	0.62 \pm 0.05*	0.99 \pm 0.04
0.5	2.78 \pm 0.07*	1.04 \pm 0.06	0.50 \pm 0.03*	1.12 \pm 0.07

Data represent means \pm SD of three independent experiments.

* $p < 0.05$ versus non-treated control.

VITA

NAME Somruethai Sumkhemthong

DATE OF BIRTH 16 May 1987

PLACE OF BIRTH Chainat, Thailand

INSTITUTIONS ATTENDED 2005 - 2009 Bachelor of Pharmacy (B.Pharm), Faculty of Pharmacy, Srinakharinwirot University, Thailand.

HOME ADDRESS 243 Moo 2, Khaotapra District, Muang Chainat, Chainat. 17000

PUBLICATION

1. Sumkhemthong, S., Chamni, S., Ecoy, G. U., Taweecheep, P., Suwanborirux, K., Prompetchara, E., ... & Chaotham, C. (2021). Jorunnamycin A Suppresses Stem-Like Phenotypes and Sensitizes Cisplatin-Induced Apoptosis in Cancer Stem-Like Cell-Enriched Spheroids of Human Lung Cancer Cells. *Marine drugs*, 19(5), 261.
2. Hlosrichok, A., Sumkhemthong, S., Sritularak, B., Chanvorachote, P., & Chaotham, C. (2018). A bibenzyl from *Dendrobium ellipsophyllum* induces apoptosis in human lung cancer cells. *Journal of natural medicines*, 72(3), 615-625.
3. Prateep, A., Sumkhemthong, S., Karnsomwan, W., De-Eknamkul, W., Chamni, S., Chanvorachote, P., & Chaotham, C. (2018). Avicequinone B sensitizes anoikis in human lung cancer cells. *Journal of biomedical science*, 25(1), 32.
4. Prateep, A., Sumkhemthong, S., Suksomtip, M., Chanvorachote, P., & Chaotham, C. (2017). Peptides extracted from edible mushroom: *Lentinus squarrosulus* induces apoptosis in human lung cancer cells. *Pharmaceutical biology*, 55(1), 1792-1799.

AWARD RECEIVED

2020 The 90th Anniversary of Chulalongkorn University
Fund (Ratchadaphiseksomphot Endowment Fund)
2016 - 2019 The 100th Anniversary Chulalongkorn
University for Doctoral Scholarship

